Supplementary Information

Dynamic bond-driven encapsulation of enzymes in metal–organic frameworks beyond pore size constraints

Youcong Li[1†], Meng Qiao[2†], Lei Gao,[1] Yuxiu Zhong,[1] Ying Yang,[1] Jie Zheng,[3] Jing-Lin Zuo,*[,1] Xing Zhang,*[,3] Shuai Yuan*[,1]

[1]State Key Laboratory of Coordination Chemistry, School of Chemistry and Chemical Engineering, Nanjing University, Nanjing, Jiangsu, 210023, China

[2]Research Center of Pharmaceutical and Synthetic Biology/Department of Food Quality and Safety, College of Engineering, China Pharmaceutical University, Nanjing 211198, China

[3]State Key Laboratory of Microbial Technology, School of Food Science and Pharmaceutical Engineering, Nanjing Normal University, Nanjing 210023, China

*To whom correspondence should be addressed. Email: zuojl@nju.edu.cn; zhangxing@njnu.edu.cn; syuan@nju.edu.cn

[+]These authors contributed equally to this work

Experimental Section

Stability Test

The as-synthesized MOFs (30 mg) were placed in 4mL aqueous solutions (pH = 1-13, adjusted by HCl and NaOH) at room temperature for 24 h. Then, the sample was collected by filtration and washed with water for further PXRD investigations. The leaching of metals in the supernatant during the stability test was analyzed by ICP-OES. The leaching of ligands was analyzed by HPLC with an Agilent 1260 Infinity II LC system equipped with an HPLC C18 column (Pursuit 5 C18, 250 × 4.6 mm, Agilent, US) at 40 °C. Eluent A was 0.1% triethylamine (v/v) in water, and eluent B was methanol. A 50% amount of eluent A was flowed (1 mL/min) through the column for 15 min. The column effluent was continuously detected by PDA at 254 nm.

Methods for Fitting and Calculating Parameters of Adsorption Isotherms

The Langmuir isotherm equation is expressed as follows:

$$q_e = \frac{q_m K_L C_e}{1 + K_L C_e}$$

where q_e (mg g^{-1}) is the adsorption capacity of dye at equilibrium, C_e (mg L^{-1}) is the concentration of dye in solution at equilibrium, q_m (mg g^{-1}) is the Langmuir maximum adsorption capacity, K_L(dm^3 mg^{-1}) is the Langmuir constant, K_F ((mg g^{-1}) (L mg^{-1}) $^{1/n}$) is the Freundlich constant, and n indicates the Freundlich exponent.

Measurement of the protein loading content

The loading of Cyt C and HRP in L3-Cr-M (M=Cu, Co, and Ni) was examined by examining the concentration of enzymes in the supernatant at different incubation times after the centrifugation of a mixed solution of enzymes and MOFs. Standard curves of Cyt C and HRP were constructed in the range from 0 to 4 mg/mL (Figures S34a-b). Typically, a 200 μL CytC/HRP sample was added to 96-well plates and detected by a UV-vis spectrophotometer at 550 nm and 403 nm, respectively.

Expression and purification of enzymes

All recombinant strains harboring corresponding genes were cloned and stored in our laboratory (Table S4). Briefly, *Escherichia coli* BL21 (DE3) strains containing the target plasmid were cultured in Luria-Bertani (LB) medium with 100 μg/ mL antibiotic (ampicillin, kanamycin, or carbenicillin) at 37 ℃ under vigorous shaking at 200 rpm. When OD600 reached 0.6-0.8, isopropyl β-D-1-thiogalactopyranoside (IPTG) with a final concentration of 0.1 mM was added and cultured at 16℃ overnight. Cells were harvested by centrifuging at 8000 rpm for 15 min. Protein purification was performed by utilizing Ni-NTA Sepharose affinity resin. The Ni^{2+} column was then washed with buffer A (50 mM Tris-HCl, pH 7.9, 500 mM NaCl, 10 mM imidazole), and the enzyme was eluted with buffer B (50 mM Tris-HCl, pH 7.9, 500 mM NaCl, 300 mM imidazole) in sequence. The purified fraction was desalted by centrifugal filter (Millipore, 10 kDa) to remove imidazole and other components, and protein concentration was determined by bradford protein assay kit.

Fluorescein-Tagged Enzymes

Fluorescein isothiocyanate (FITC, 4 mg) and enzyme (CytC, HRP, NTR, Nark, and GlmU, 20 mg) were dissolved in carbonate-bicarbonate aqueous buffer solution (0.1 M, pH 9.2, 2 mL) and left for 2 h in darkness at room temperature under gentle stirring. The fluorescein-tagged enzyme was dialyzed against dialysis buffer (1 L, 50 mM Tris-HCl containing 500 mM NaCl, pH 7.9) for 72 h at 4 ºC in the dark, and the dialysis buffer was changed every 4 h. Transfer the dialyzed enzyme into a fresh tube and centrifuge it at 10000 rpm for 10 min at 4 ºC to remove precipitate, if any. The supernatant was then concentrated with Amicon® Ultra-15 Centrifugal Filter Unit (30 kDa) to 1 ml by centrifugation (6000 rpm). Similarly, rhodamine B isothiocyanate-labeled GlmU was obtained.

Measurement of the enzymatic activity of immobilized enzyme and free enzyme

The specific activities for Cr-L3-M (M = Cu, Co, Ni, and Pd) immobilized CytC/HRP and free CytC/HRP were measured with 1 mM ABTS, 2 mM H_2O_2, 1 μg enzyme in 200 μL NaOAc/HOAc (50 mM, pH 4) at 25 °C for 10 min. The catalytic efficiency was evaluated by UV-vis measurement at 420 nm. The specific activities for Cr-L3-M immobilized NTR and free NTR were measured with 5 mM *p*-nitrophenyl, 5mM NADH, and 1 μg enzyme in 200 μL Tris-HCl buffer (200 mM, pH 7.4) at 37 °C for 1 h. The catalytic efficiency was evaluated by UV-vis measurement at 340 nm. The specific activities for Cr-L3-Cu/Co/Ni immobilized NahK&GlmU and free NahK&GlmU were measured with 10 mM GlcNAc, 15 mM ATP, 15 mM UTP, 10 mM $MgCl_2$, 0.5 μg NahK, 0.5 μg GlmU in 200 μL Tris-HCl buffer (50 mM, pH 7.9) at 37 °C for 12 h.

HPLC detected formed sugar nucleotides. HPLC analysis was performed on an Agilent 1260 Infinity II LC system. The column YMC-Pack Polyamine II column (250 × 4.6 mm i.d., S-5 μm) was used to monitor UDP-sugar at 35°C. Eluent A was a 20 mM sodium phosphate buffer, pH 5.8, and eluent B was methanol. Eluent (80% A, 20% B) was flowed (1 mL/min) through the column for 30 min. The column effluent was continuously detected by PDA at 262 nm.

Synthesis of Single Crystal X-Ray Crystallography

Single-crystal X-ray diffraction intensity data for Cr-L1-Cu, Fe-L1-Cu, and Cr-L3-Pd were collected on a Bruker D8 Venture diffractometer fitted with a PHOTON-100 CMOS detector, monochromatized microfocus Mo Kα radiation (λ= 0.71073 Å), and a nitrogen flow controlled by a KRYOFLEX II low-temperature attachment operating at 193 K, 253K, and 296K. Raw data collection and reduction were controlled using APEX3 software.[1] The structures were solved by direct methods and refined by full-matrix least squares. Absorption corrections were applied using the SADABS routine. ast-squares on F^2 using the SHELXTL software package.[2]

Single-crystal X-ray diffraction intensity data for Cr-L1-Pd were collected on a Bruker D8 Liquid diffractometer fitted with a PHOTON-100 CMOS detector, monochromatized microfocus Ga Kα radiation (λ= 1.34139 Å), and a nitrogen flow controlled by a KRYOFLEX II low-temperature attachment operating at 223K. Raw data collection and reduction were controlled using APEX3 software.[1] Absorption corrections were applied using the SADABS routine. The structures were solved by direct methods and refined by full-matrix least-squares on F^2 using the SHELXTL software package.[2]

Theoretical calculations

All first-principles calculations were performed with Perdew–Burke–Ernzerhof exchange–correlation functional[3] (PBE) using the PWscf code of *Quantum ESPRESSO*[4-6] (version 7.3.1). Optimized norm-conserving Vanderbilt (ONCV) pseudopotentials[7] from the PseudoDojo library[8] were employed, with a kinetic energy cutoff of 40 Ry for the plane-wave basis set and 160 Ry for the charge density and potential. The semiempirical Grimme's DFT-D3 method[9] is used to account for the van der Waals correction. We found that only Γ point sampling was enough for the total energy to converge within 1 meV/atom in self-consistent calculation with a self-consistency convergence threshold of 1×10^{-8} Ry. All structure models were fully relaxed with a convergence criterion of 1×10^{-3} a.u for forces and 1×10^{-4} a.u for total energy. Initial magnetic moments of the Cr_3O cluster were set in an antiferromagnetic configuration. The start magnization setting for the Cr_3O cluster is antiferromagnetic. The relaxed crystal structure was visualized using the VESTA package.

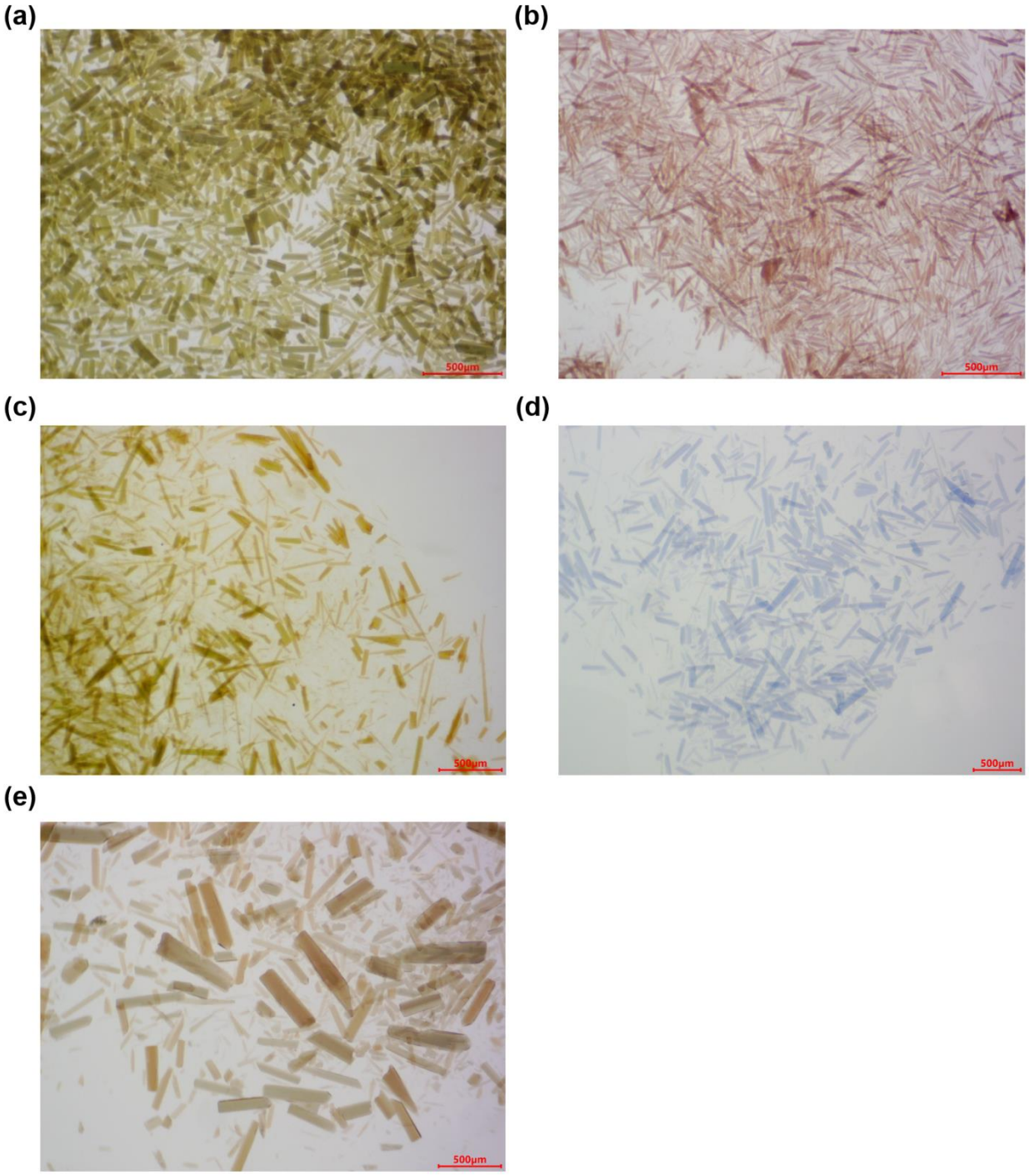

Figure S1. The crystals of Cr-L2-Cu (a), Fe-L1-Cu(b), Fe-L2-Co(c), Al-L2-Cu (d), and Fe-L3-Cu (e) under the optical microscope.

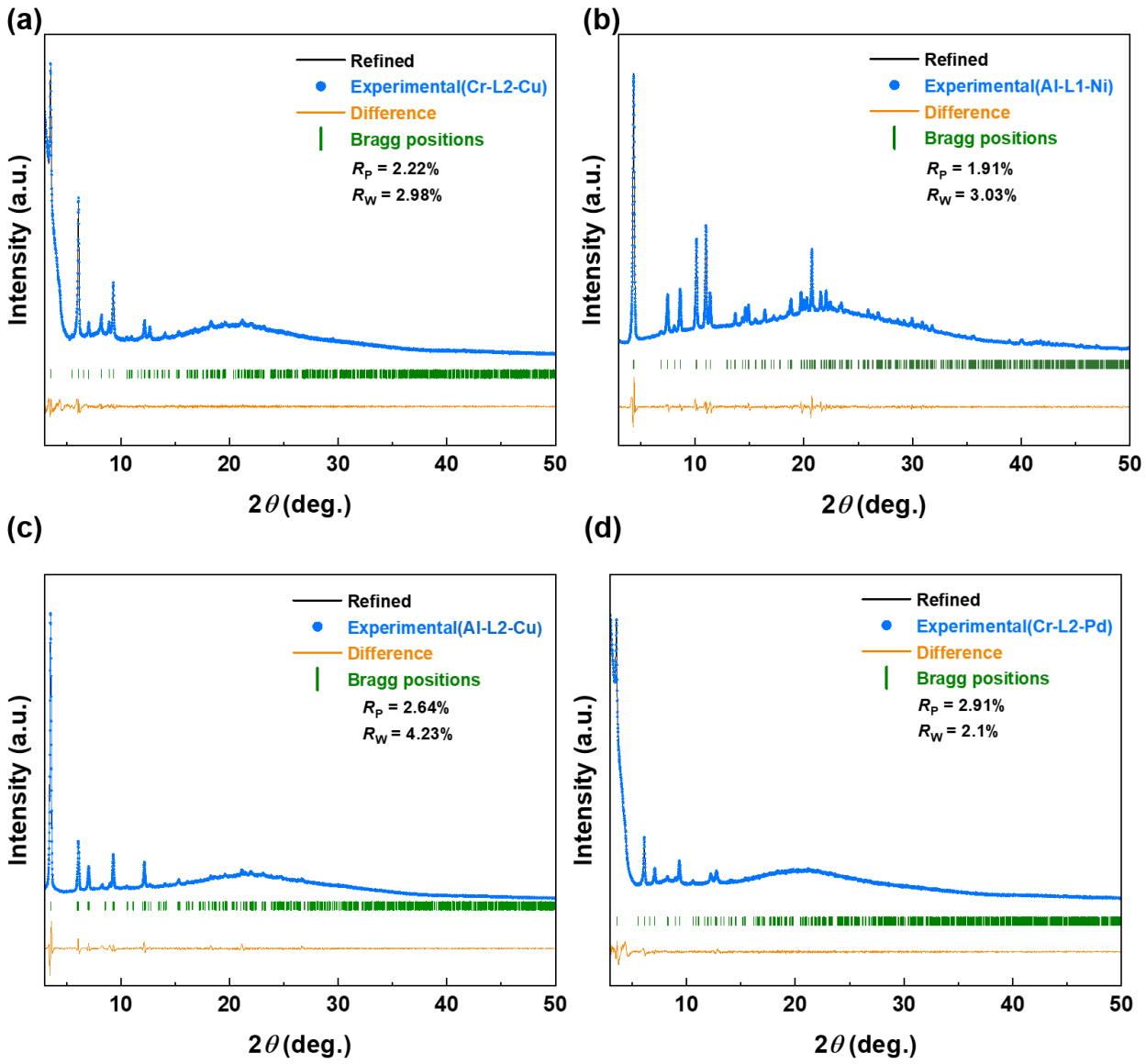

Figure S2. Pawley fit of PXRD patterns (λ = 1.5418 Å) for Cr-L2-Cu (a), Al-L1-Ni (b), Al-L2-Cu (c), and Cr-L2-Pd (d). Black line: calculated; blue line: observed; yellow line: difference. The refined unit cell parameters are shown in Supplementary Table 2.

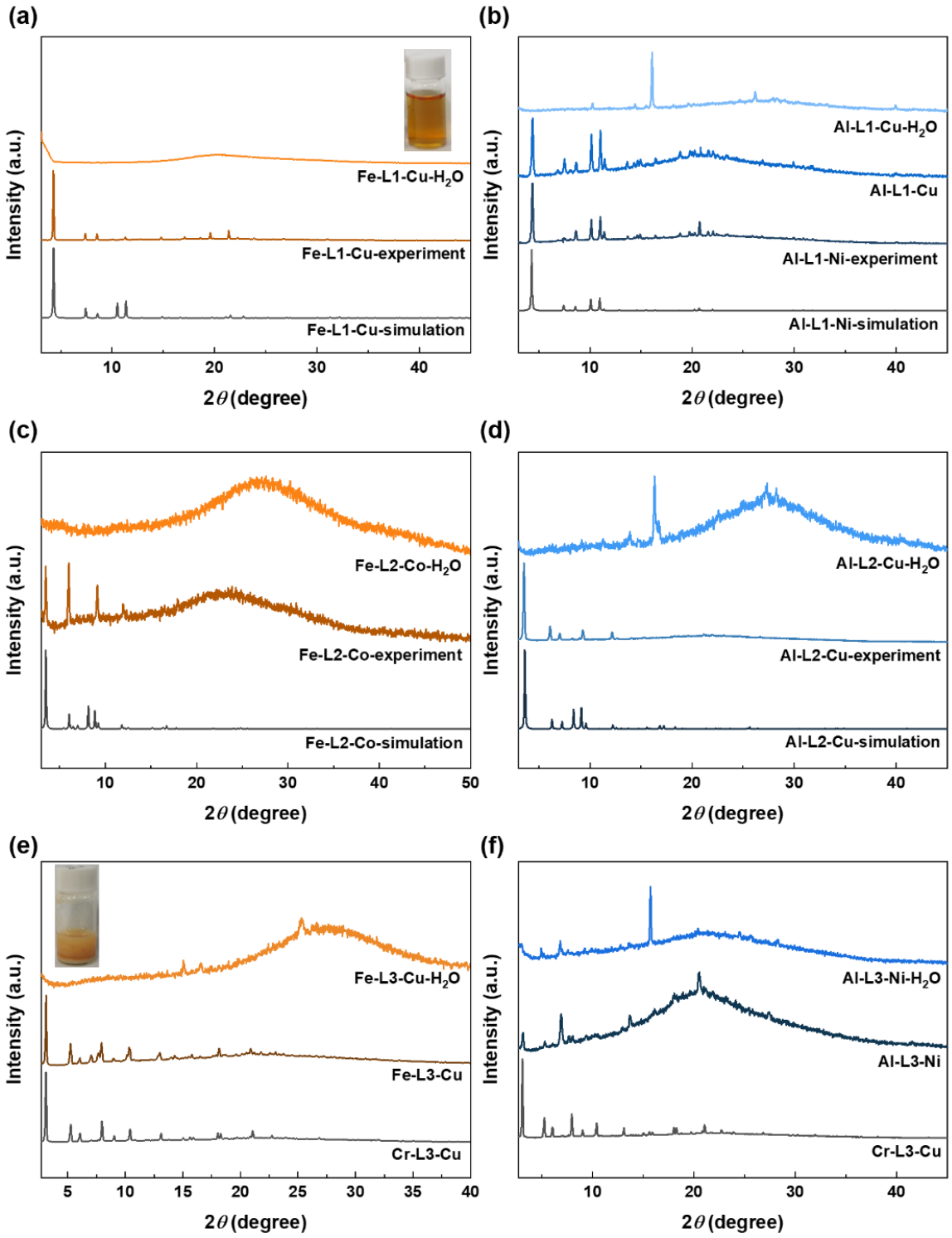

Figure S3. PXRD analysis of M-L-M′ (L = L1, L2, and L3; M′ = Cu^{2+}, Co^{2+}, Ni^{2+}, and Pd^{2+}) MOFs before and after water treatment. (a) Fe-L1-Cu (inset: dissolution yielding an orange-red solution). (b) Al-L1-Ni. (c) Fe-L2-Co. (d) Al-L2-Cu. (e) Fe-L3-Cu (inset: dissolution yielding an orange-red solution and a light-yellow solid). (f) Al-L3-Ni.

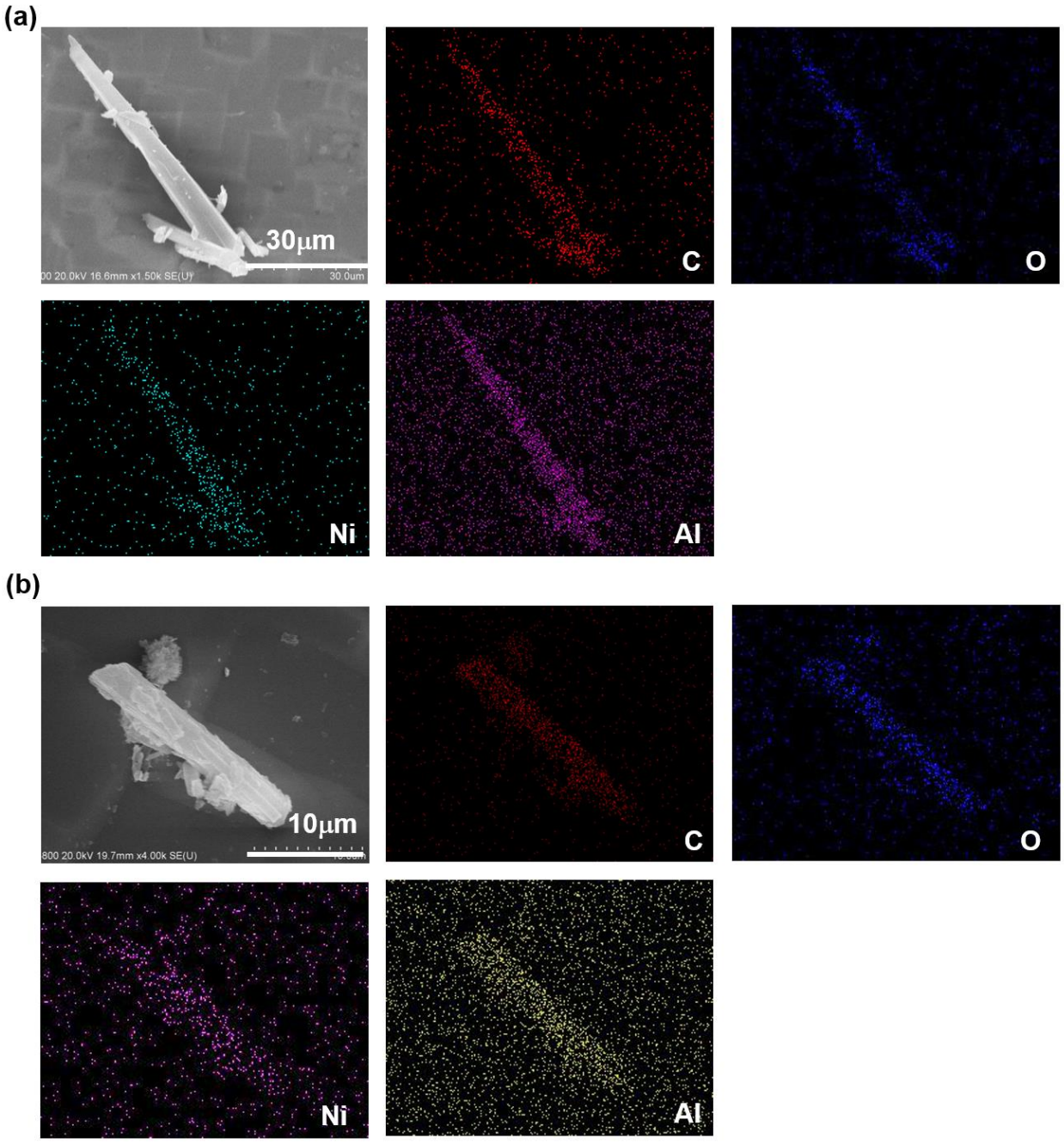

Figure S4. SEM and element mapping of Al-L1-Ni (a) and Al-L3-Ni.

(a)

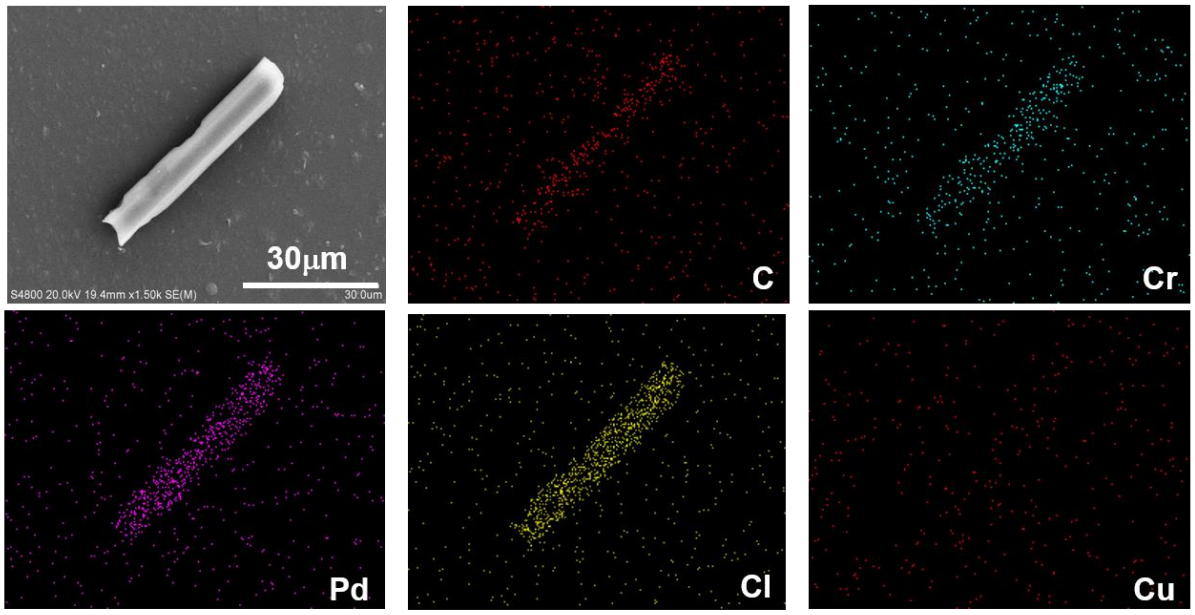

(b)

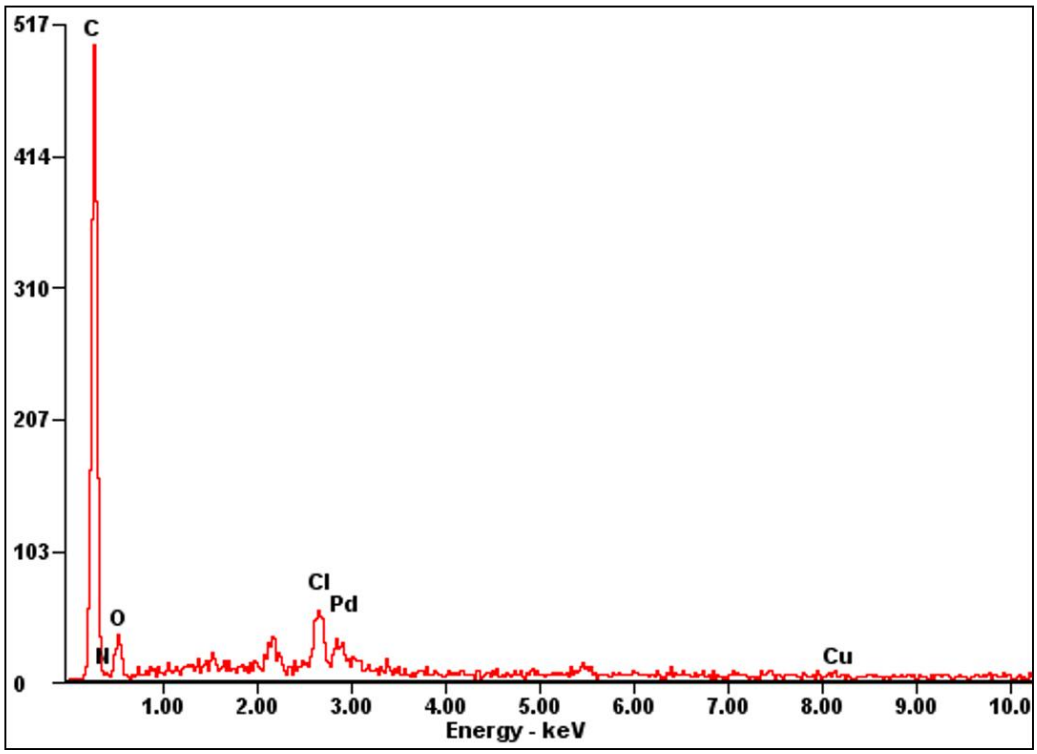

Figure S5. (a) SEM and element mapping of Cr-L1-Pd. (b) Energy-dispersive X-ray spectra (EDX) of Cr-L1-Pd.

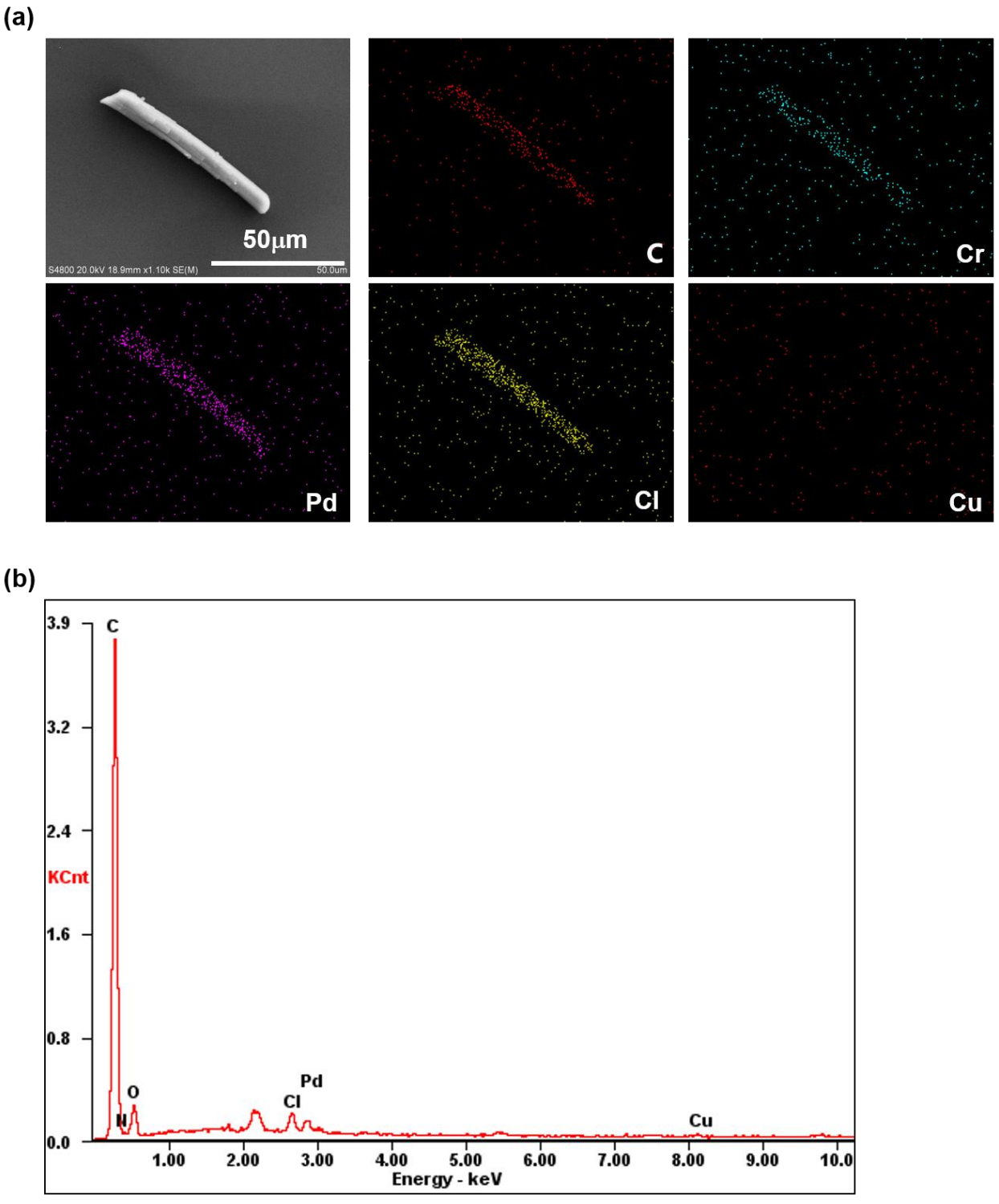

Figure S6. (a) SEM and element mapping of Cr-L2-Pd. (b) Energy-dispersive X-ray spectra (EDX) of Cr-L2-Pd.

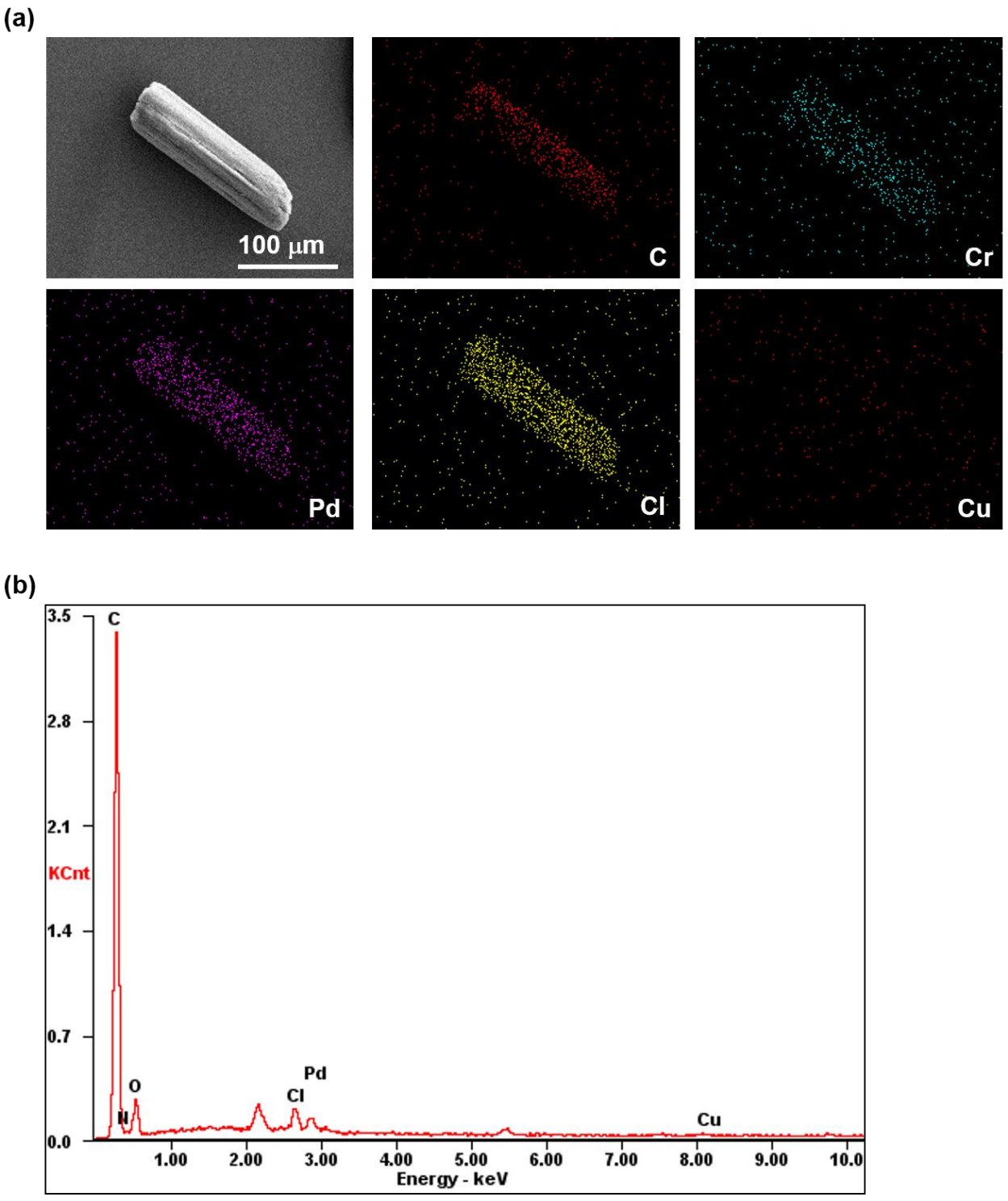

Figure S7. (a) SEM and element mapping of Cr-L3-Pd. (b) Energy-dispersive X-ray spectra (EDX) of Cr-L3-Pd.

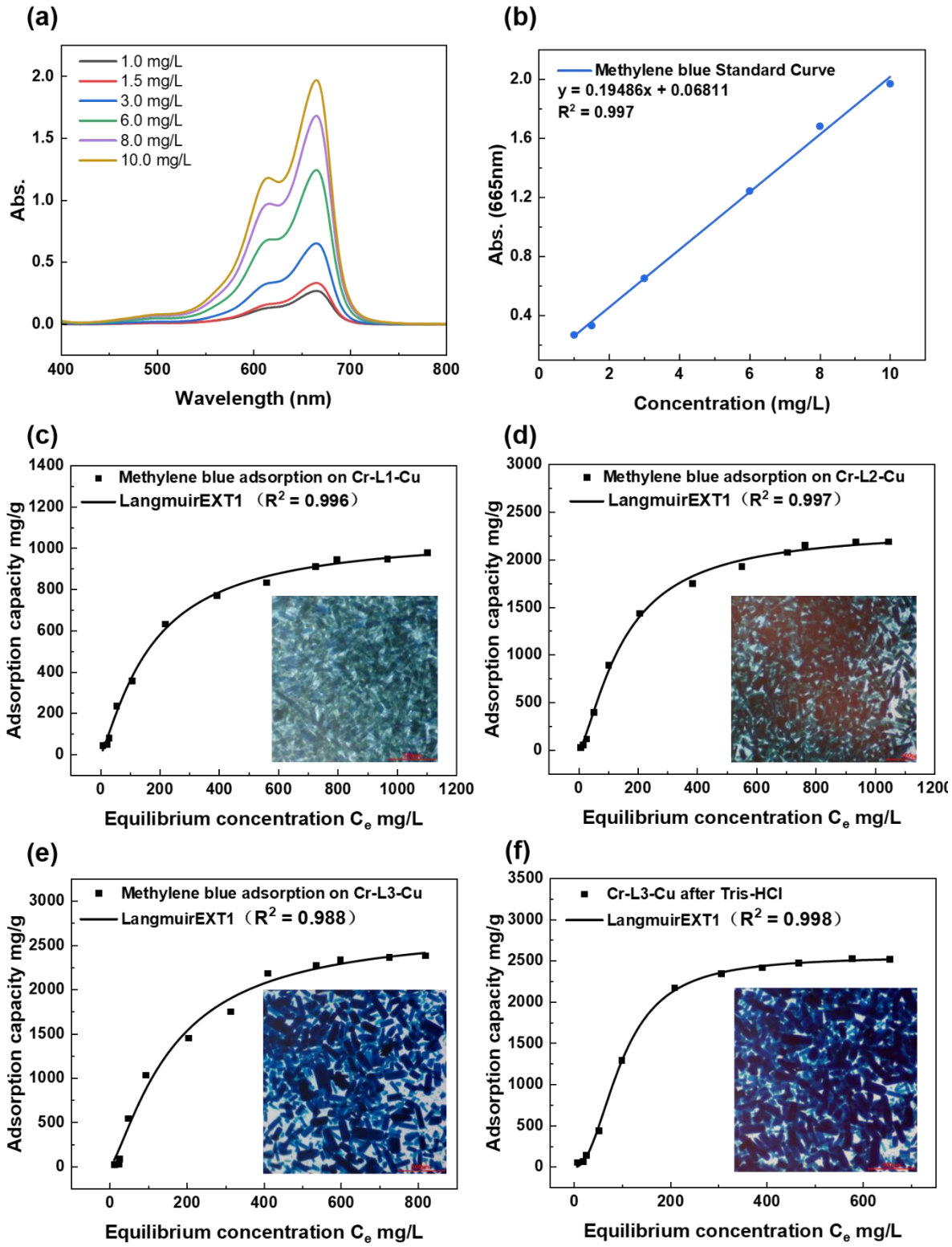

Figure S8. (a) UV-Vis absorption spectra of H_2O solution for MB; (b) Standard curves of MB; Adsorption isotherm plots of Cr-L1-Cu (c), Cr-L2-Cu (d), Cr-L3-Cu (e), and Cr-L3-Cu (f) soaked in Tris-HCl (pH = 7) for two days, fitted with the Langmuir model.

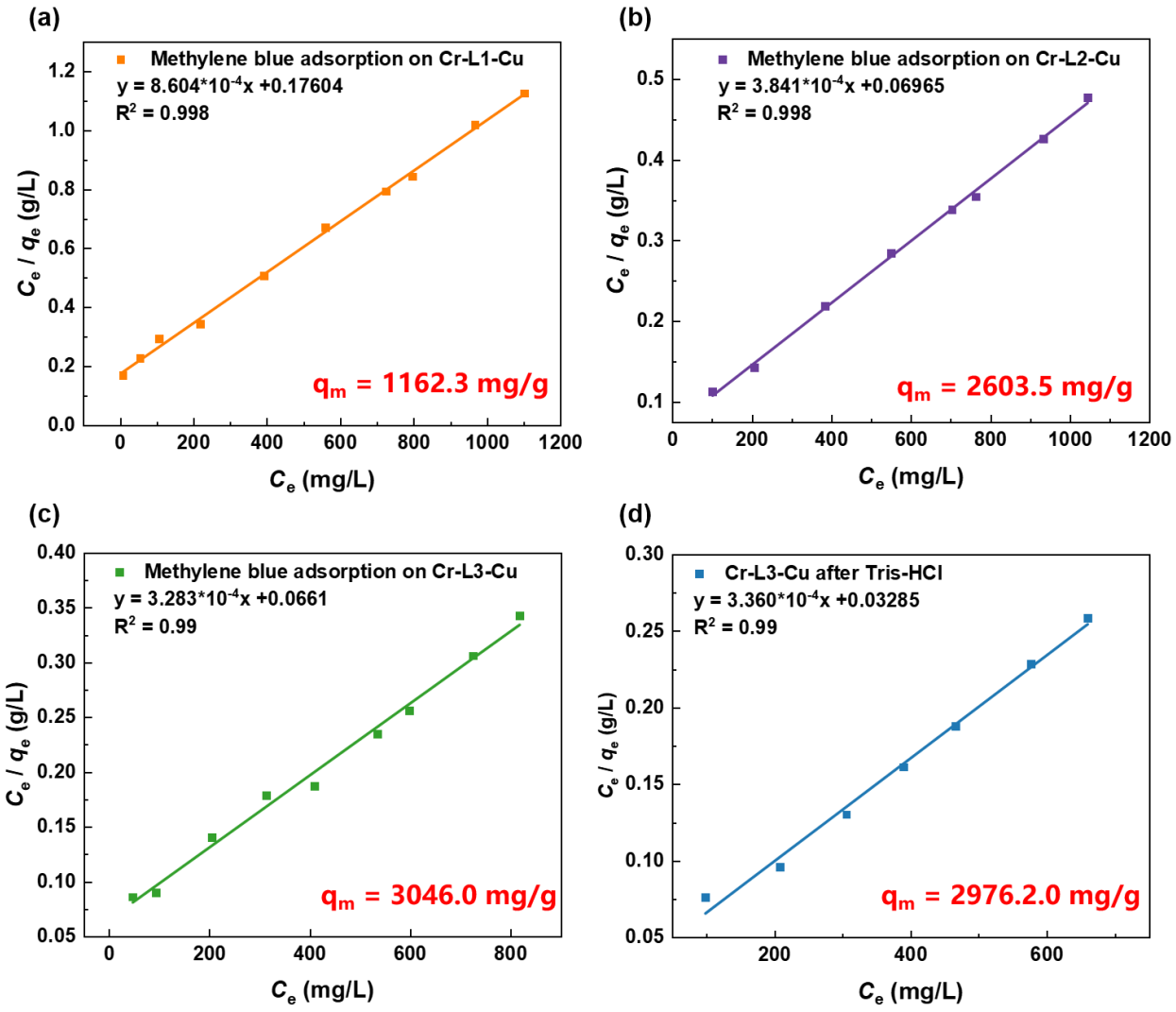

Figure S9. Adsorption isotherm plots of Cr-L1-Cu (a), Cr-L2-Cu (b), Cr-L3-Cu (c), and Cr-L3-Cu (d) soaked in Tris-HCl (pH = 7) for two days, fitted with the Langmuir model.

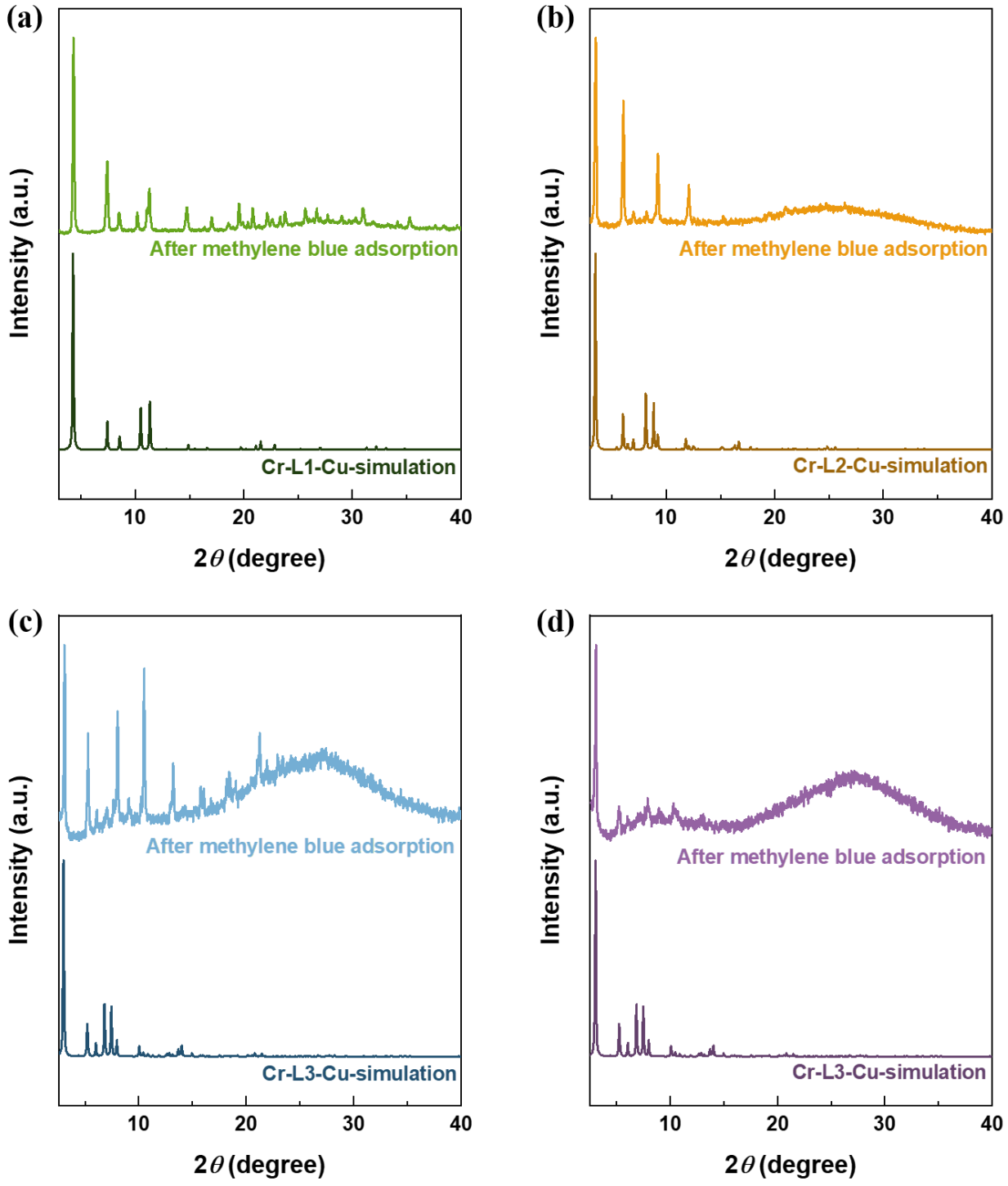

Figure S10. PXRD patterns of MOFs after the adsorption of methylene blue: Cr-L1-Cu (a); Cr-L2-Cu (b); Cr-L3-Cu (c); Cr-L3-Cu soaked in Tris-HCl (pH = 7) for two days (d).

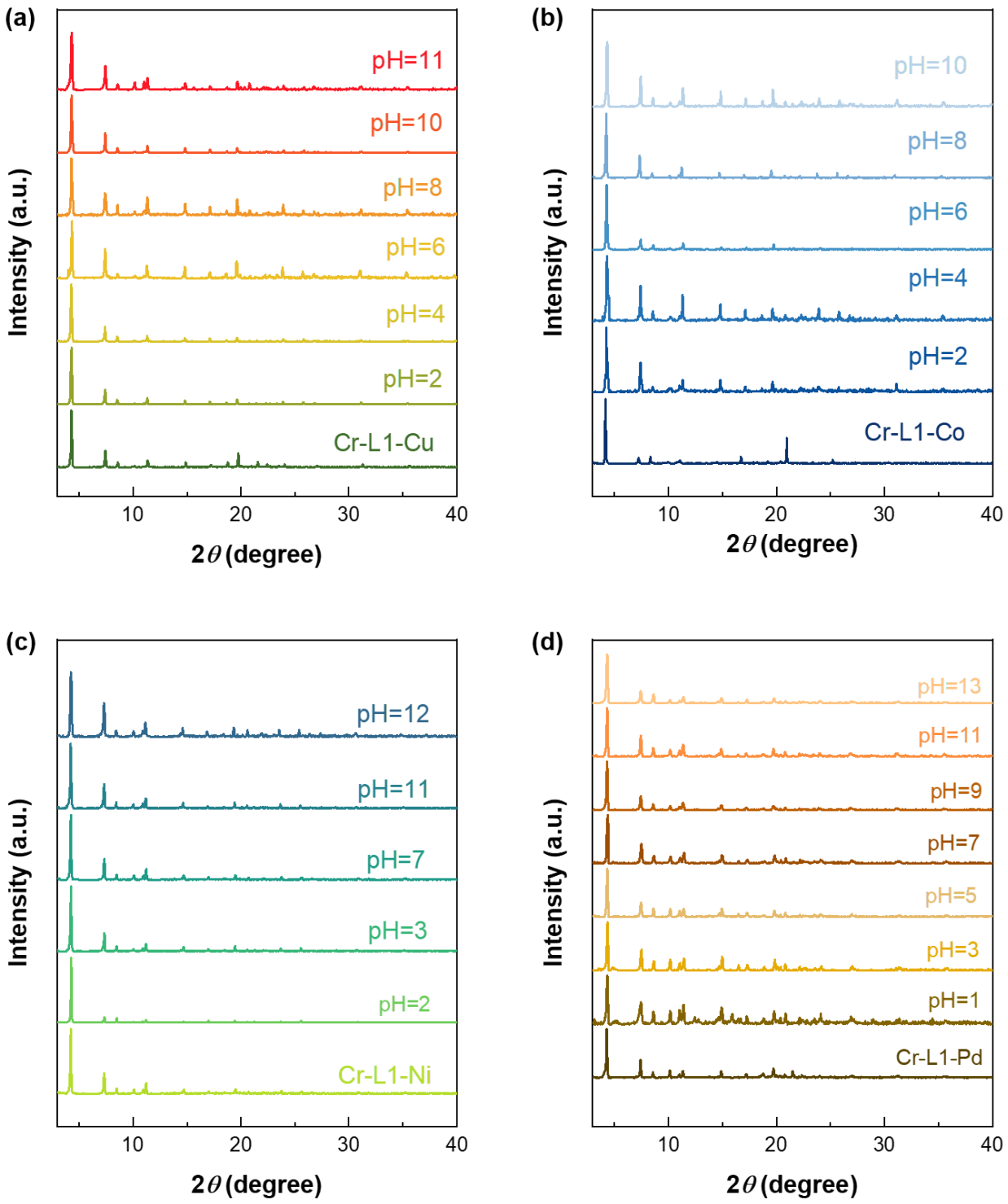

Figure S11. PXRD patterns of Cr-L1-Cu (a), Cr-L1-Co (b), Cr-L1-Ni (c), and Cr-L1-Pd (d) after incubating in aqueous solutions of different pH values for 24 h.

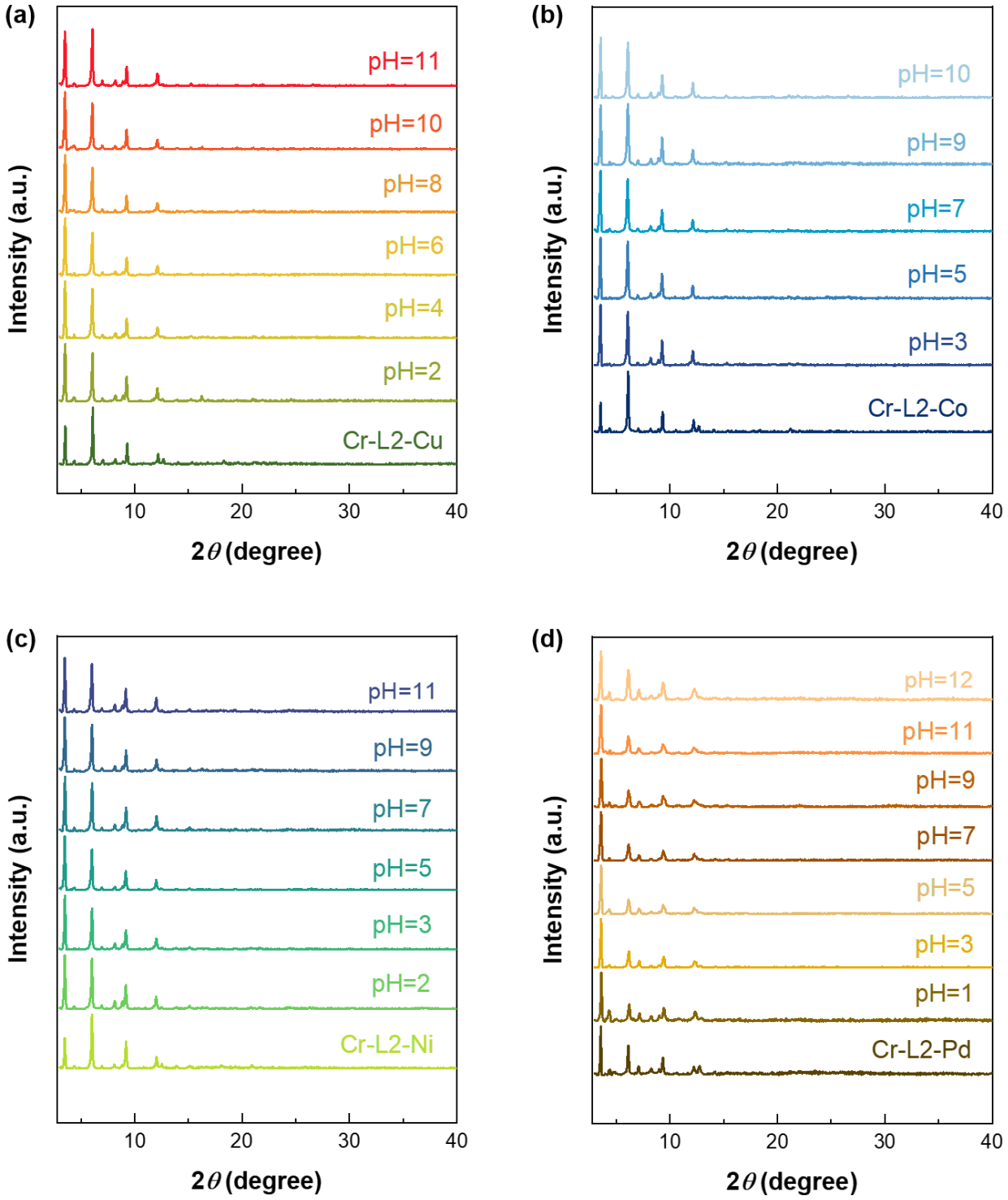

Figure S12. PXRD patterns of Cr-L2-Cu (a), Cr-L2-Co (b), Cr-L2-Ni (c), and Cr-L2-Pd (d) after incubating in aqueous solutions of different pH values for 24 h.

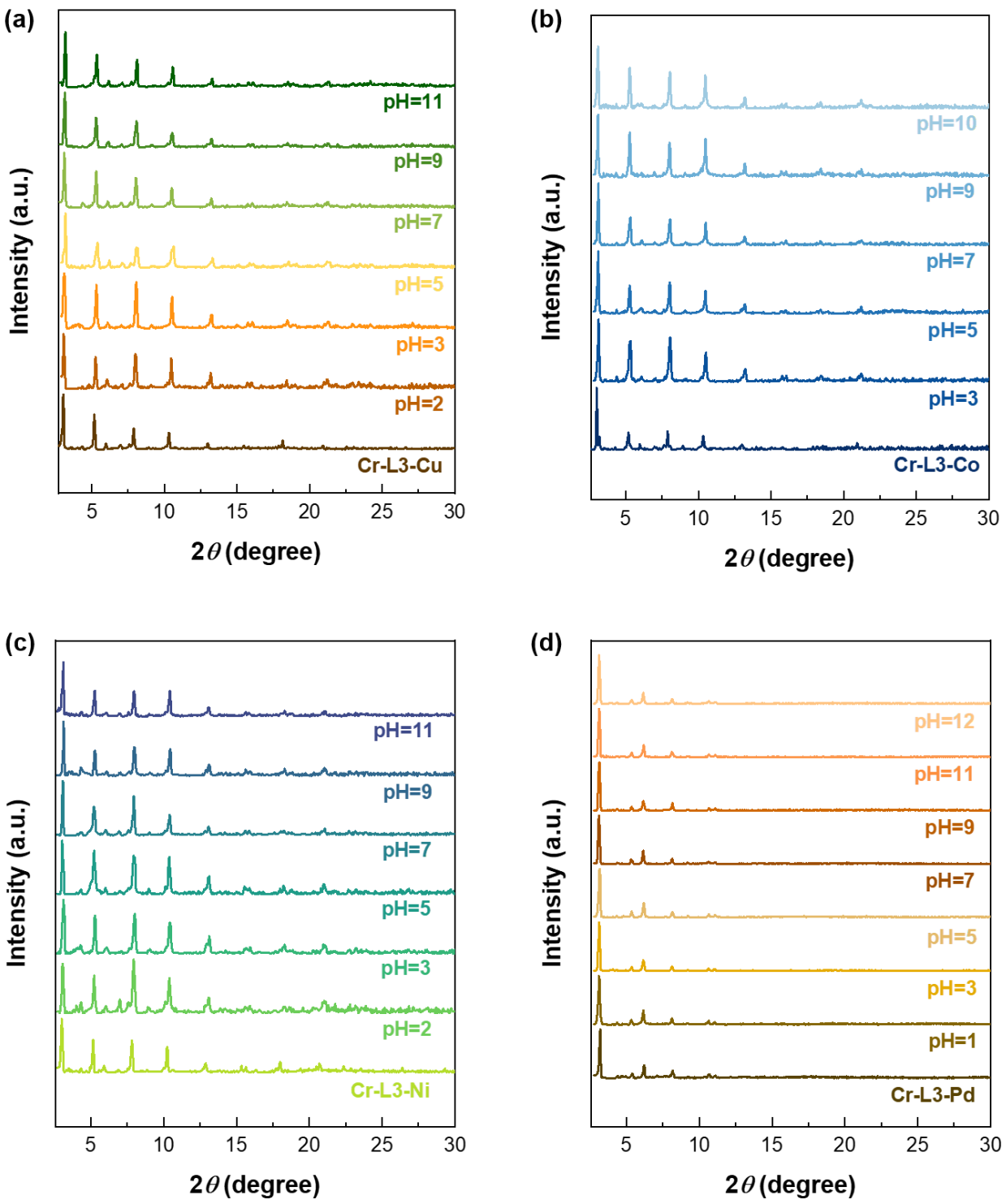

Figure S13. PXRD patterns of Cr-L3-Cu (a), Cr-L3-Co(b), Cr-L3-Ni (c), and Cr-L3-Pd (d) after incubating in aqueous solutions of different pH values for 24 h.

(a)

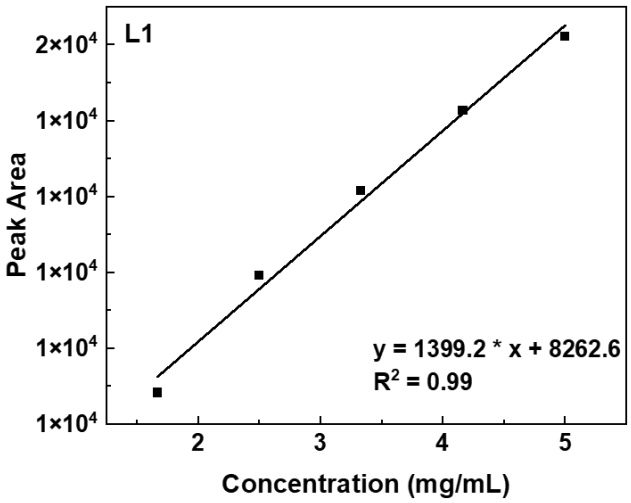
L1
Peak Area
Concentration (mg/mL)
y = 1399.2 * x + 8262.6
R² = 0.99

(b)

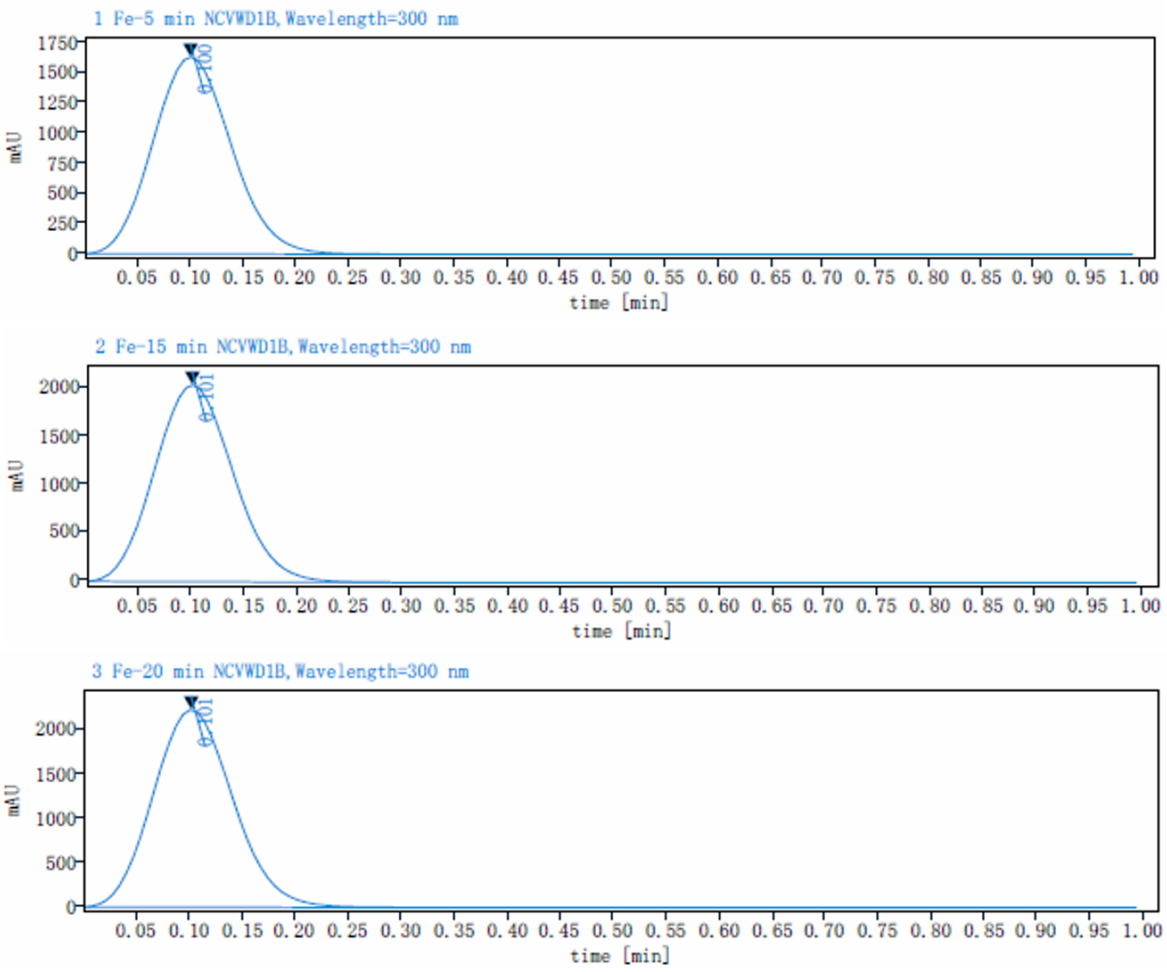
1 Fe-5 min NCVWD1B,Wavelength=300 nm
2 Fe-15 min NCVWD1B,Wavelength=300 nm
3 Fe-20 min NCVWD1B,Wavelength=300 nm
mAU
time [min]

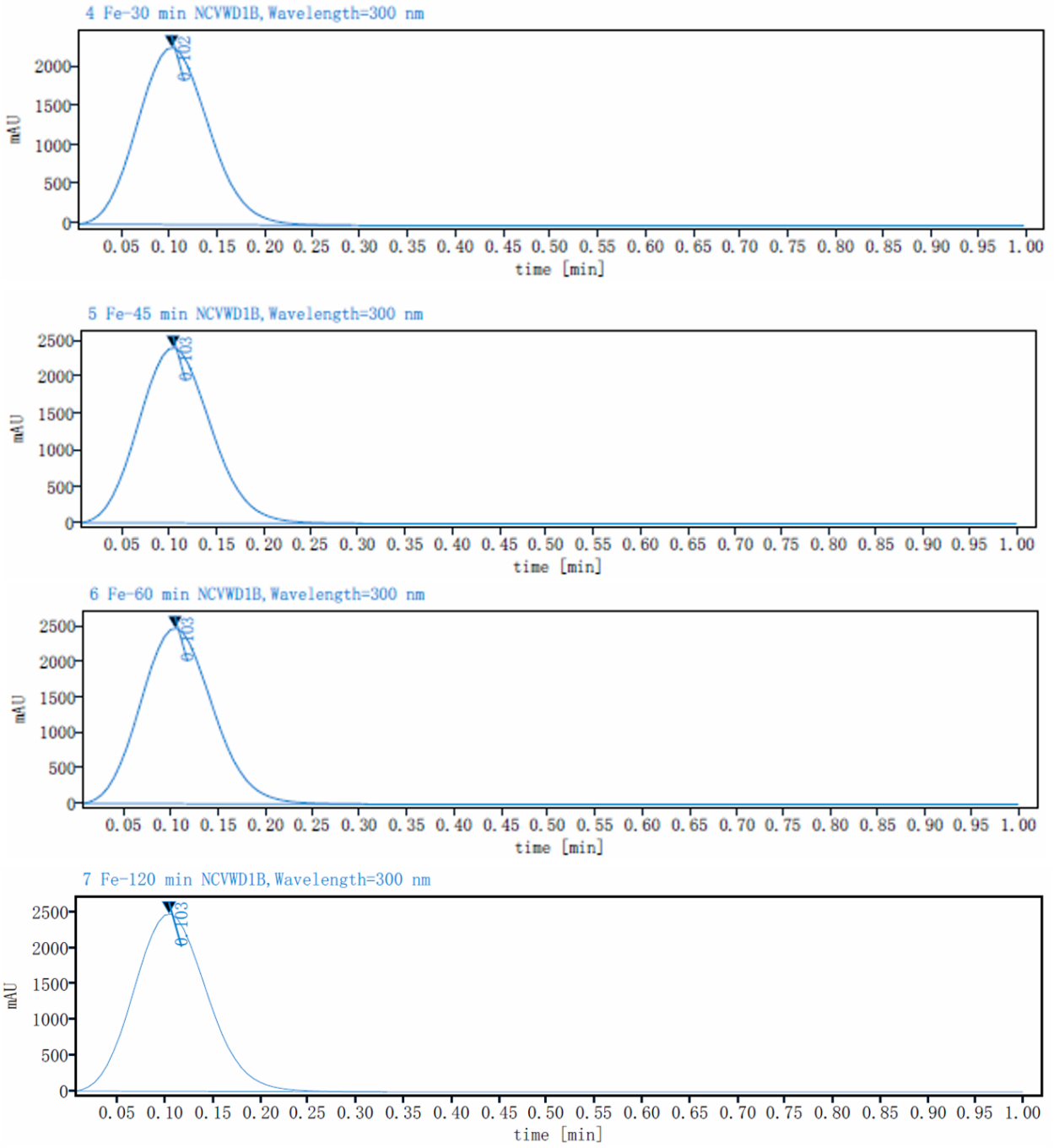

Figure S14. (a) Standard curves for varying concentrations of L1. (b) Plots of L1 quantification by the VWD detector of HPLC.

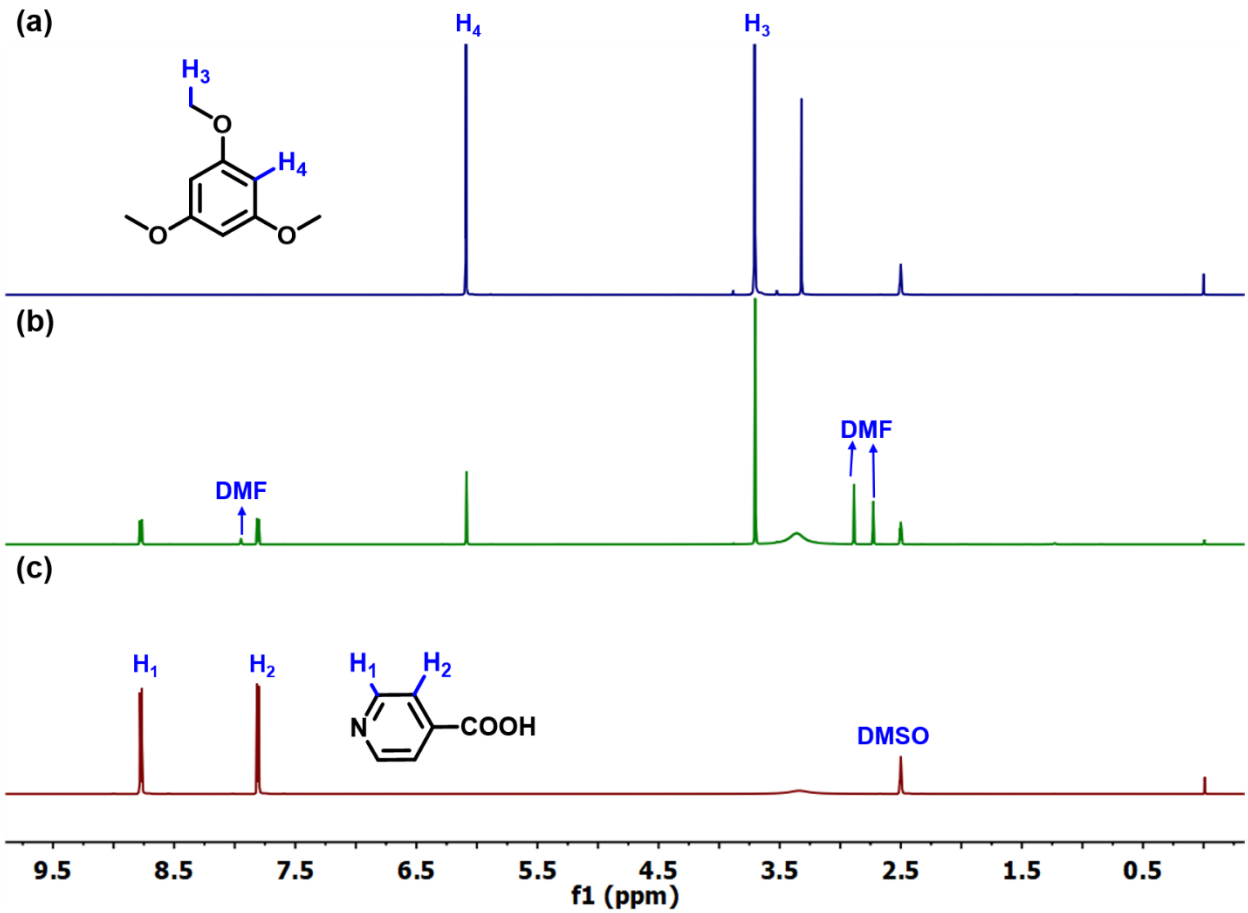

Figure S15. ^{1}H NMR spectra of 1,3,5-Trimethoxybenzene (a), Al-L1-Cu after soaking in Tris-HCl Buffer at room temperature for 24 h (b), and L1 (c).

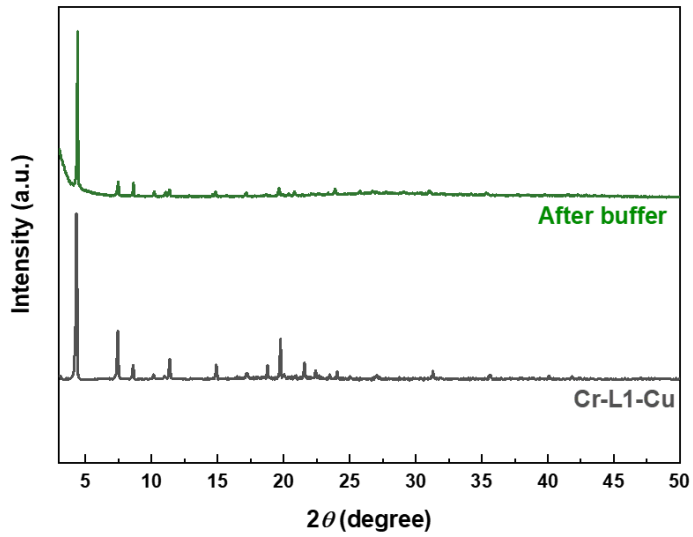

Figure S16. PXRD patterns for Cr-L1-Cu and Cr-L1-Cu after soaking in Tris-HCl buffer for 36 h.

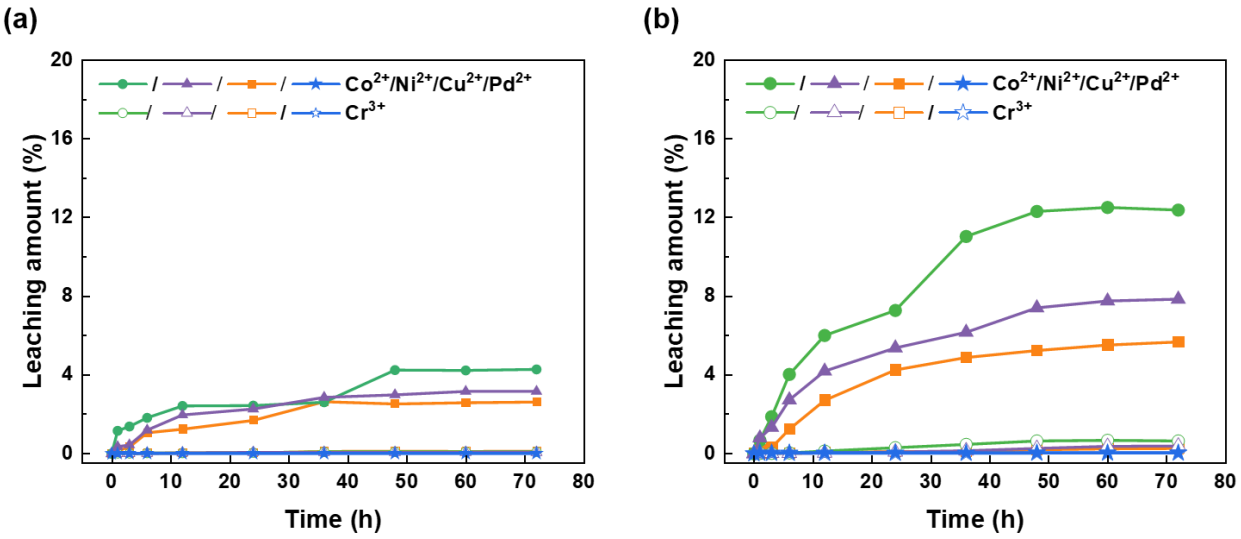

Figure S17. (a) The Cr^{3+}, Cu^{2+}, Co^{2+}, Ni^{2+}, and Pd^{2+} concentration of Cr-L2-Cu, Cr-L2-Co, Cr-L2-Ni, and Cr-L2-Pd after soaking in Tris-HCl buffer at different times. (b) The Cr^{3+}, Cu^{2+}, Co^{2+}, Ni^{2+}, and Pd^{2+} concentrations of Cr-L3-Cu, Cr-L3-Co, Cr-L3-Ni, and Cr-L3-Pd after soaking in Tris-HCl buffer at different times.

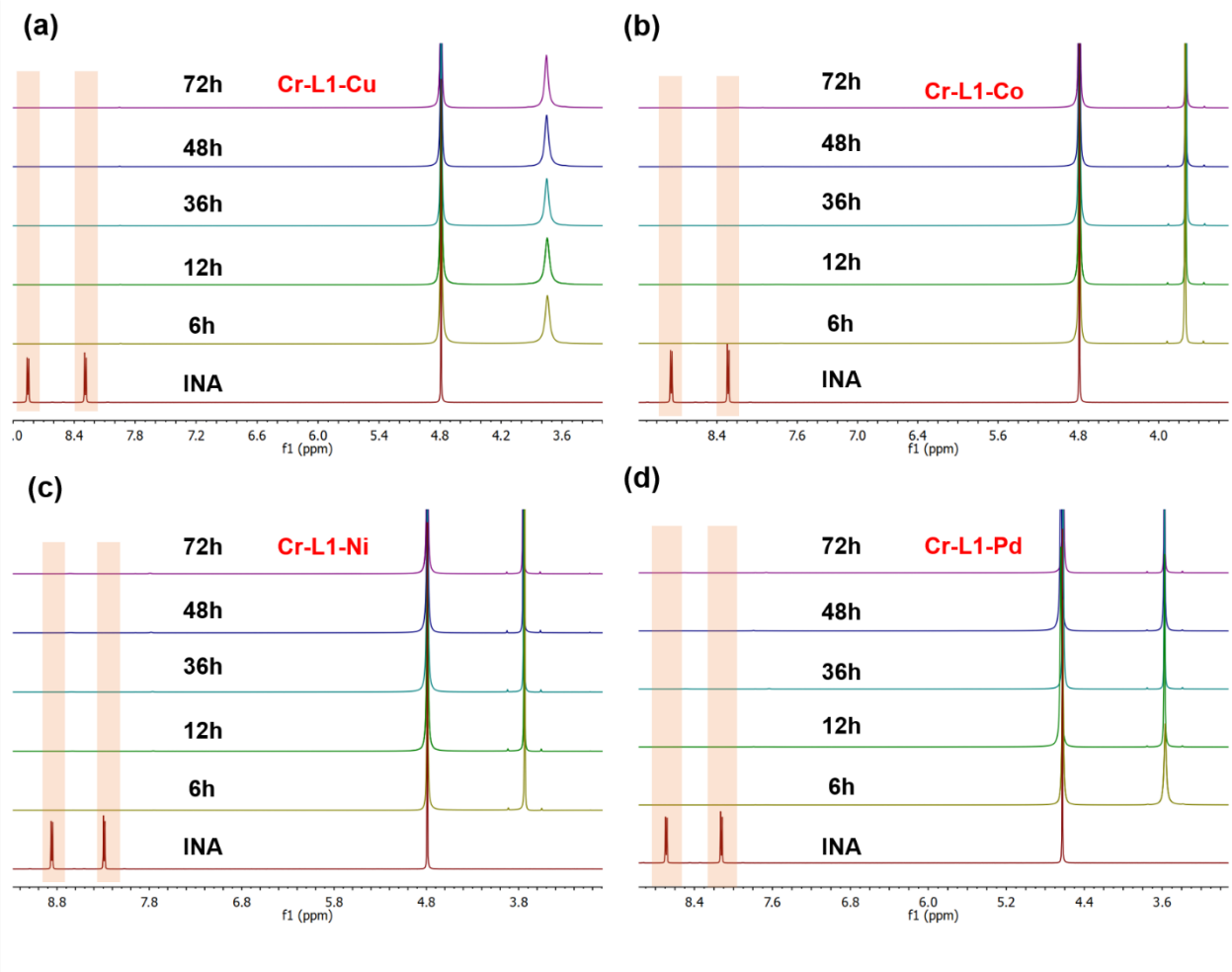

Figure S18. The ^{1}H NMR spectra of Cr-L1-Cu (a), Cr-L1-Co (b), Cr-L1-Ni (c), and Cr-L1-Pd (d) after soaking in Tris-HCl buffer at room temperature for 6, 12, 24, 36, 48, and 72 h.

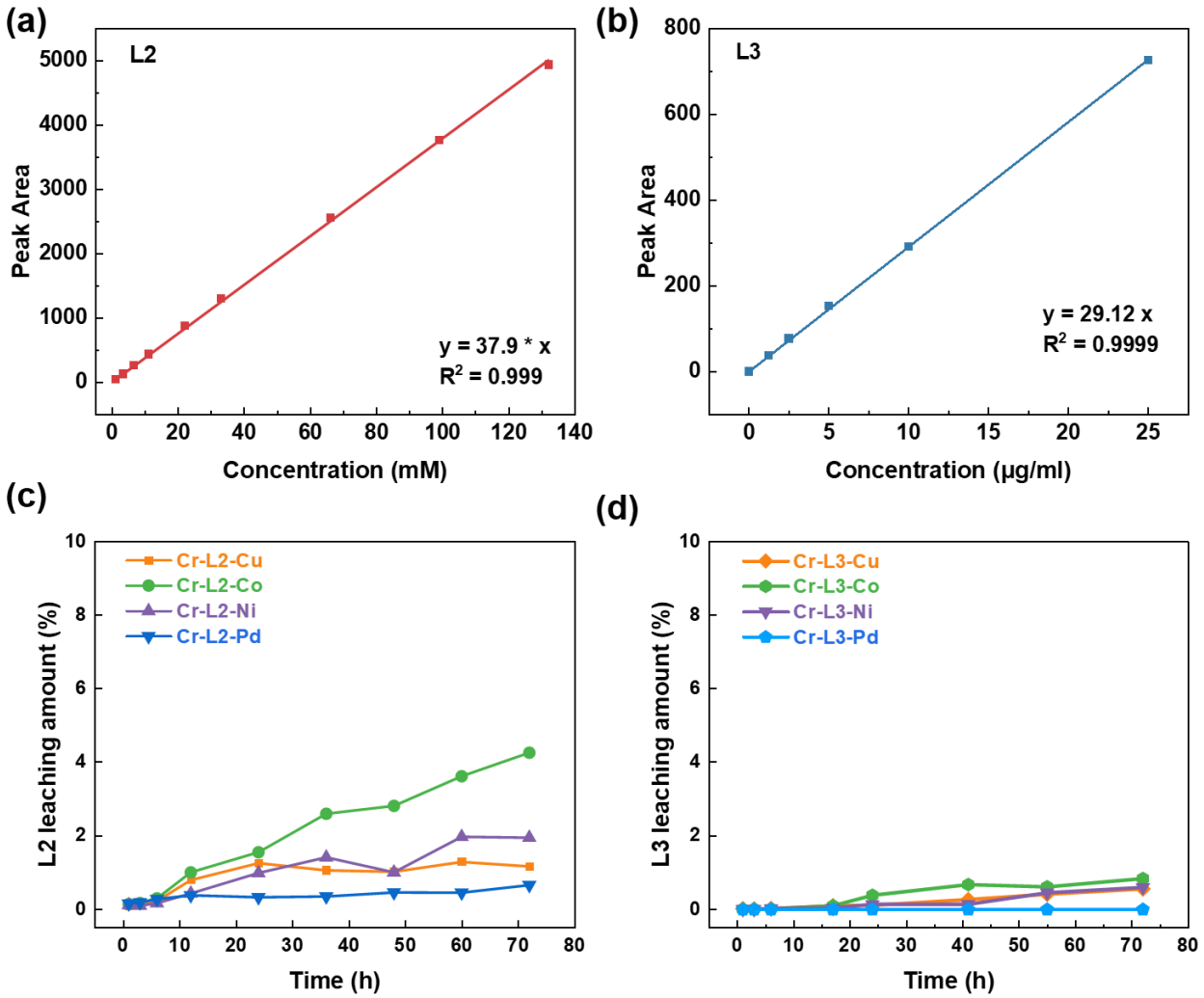

Figure S19. Standard curves for varying concentrations of L2 potassium salts (a) and L3 potassium salts (b); (c) The L2 leaching concentration of Cr-L2-Cu, Cr-L2-Co, Cr-L2-Ni, and Cr-L2-Pd after soaking in Tris-HCl buffer at different times; (d) The L3 leaching concentrations of Cr-L3-Cu, Cr-L3-Co, Cr-L3-Ni, and Cr-L3-Pd after soaking in Tris-HCl buffer at different times.

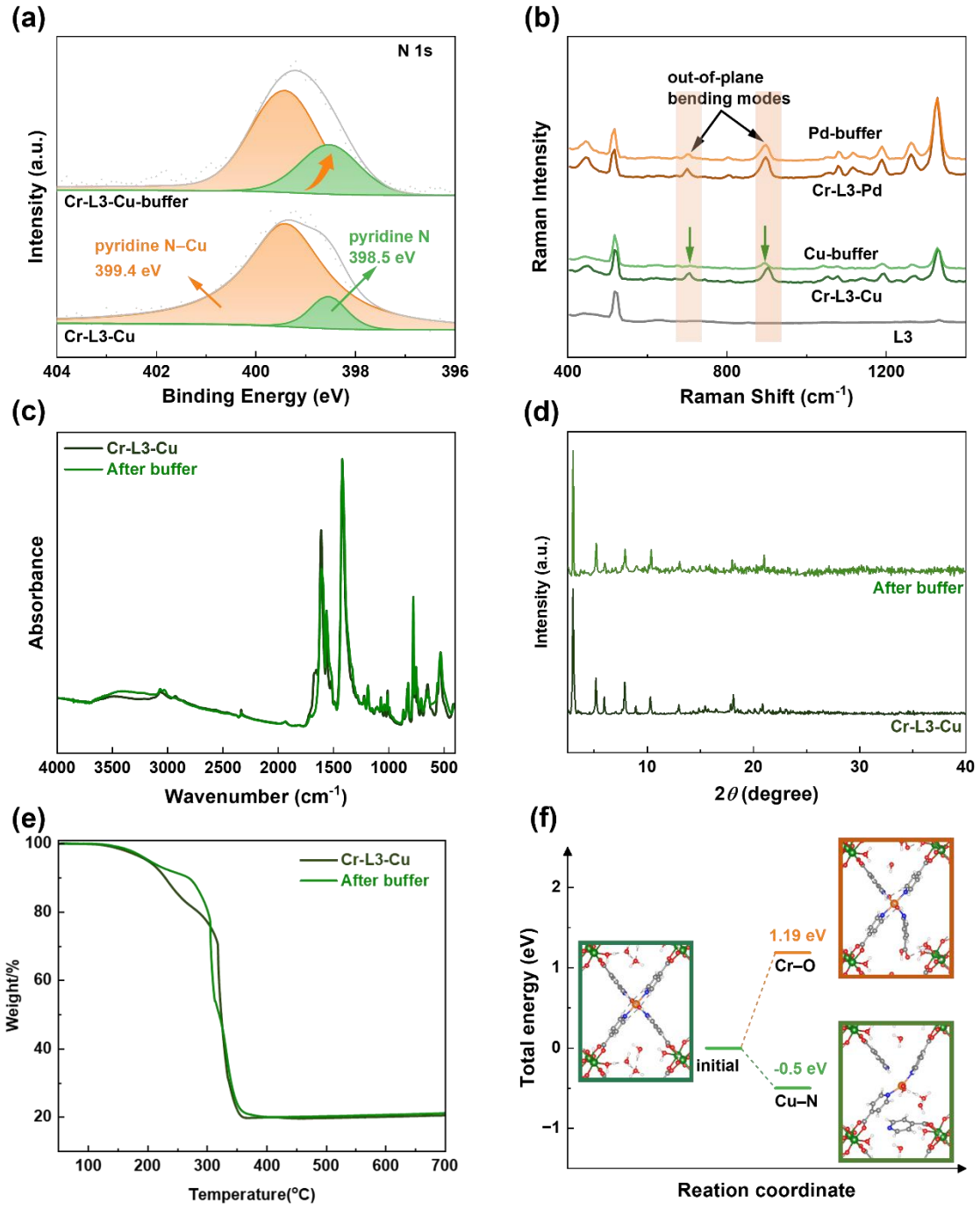

Figure S20. (a) N 1s XPS spectra of Cr-L3-Cu and Cr-L3-Cu-buffer. (b) Raman spectra of L3, Cr-L3-Cu, Cr-L3-Cu-buffer, Cr-L3-Pd, and Cr-L3-Pd-buffer. (c) In situ FT-IR spectra for Cr-L3-Cu and Cr-L3-Cu after soaking in Tris-HCl buffe. (d) PXRD patterns for Cr-L3-Cu and Cr-L3-Cu after soaking in Tris-HCl buffe. (e) TGA curve of Cr-L3-Cu and Cr-L3-Cu after soaking in Tris-HCl buffer. (f)DFT-calculated reaction energy profile of Cr-L1-Cu systems.

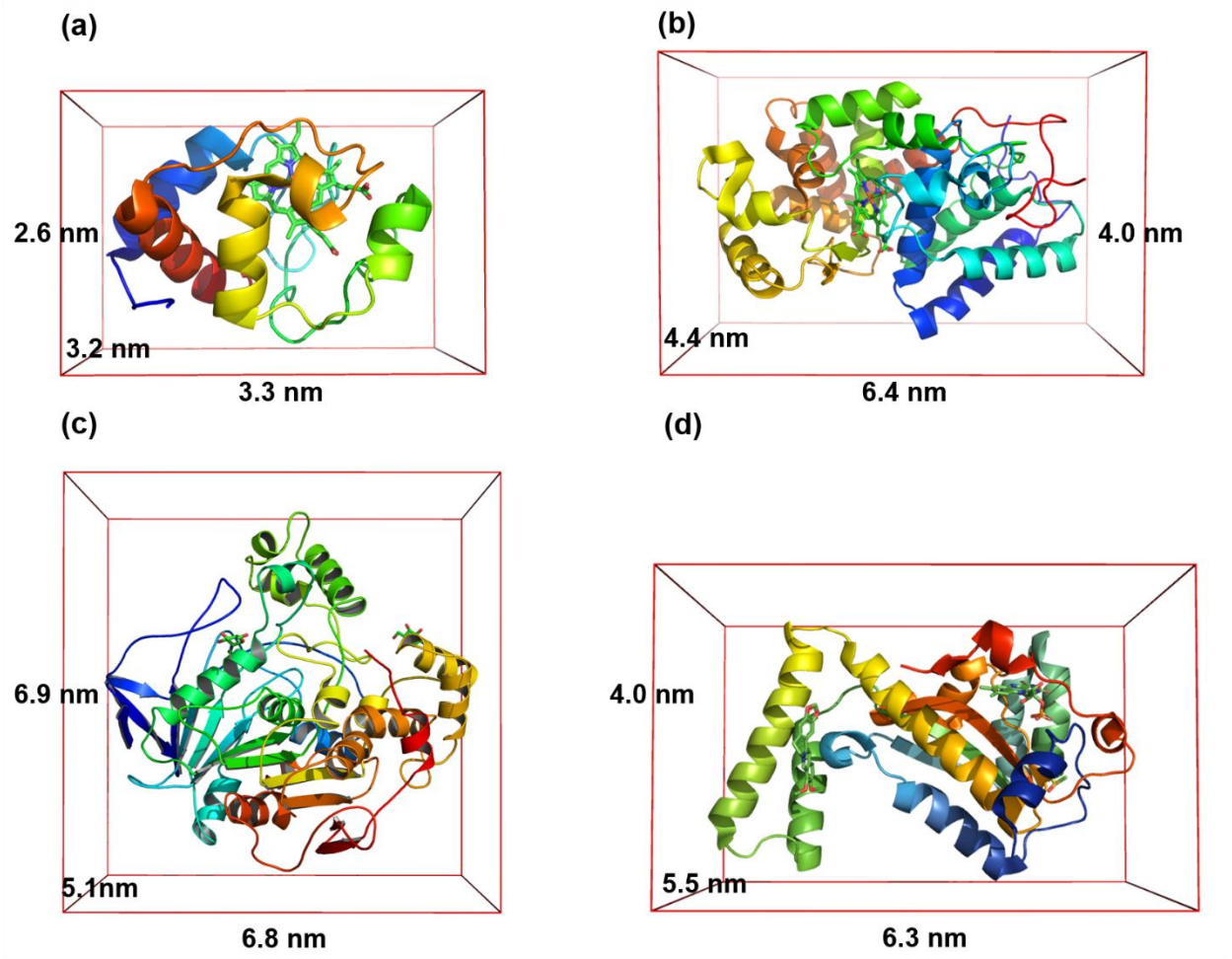

Figure S21. Structural analysis of Cyt C (a), HRP (b), lipase (c), and NTR (d) by PyMol.

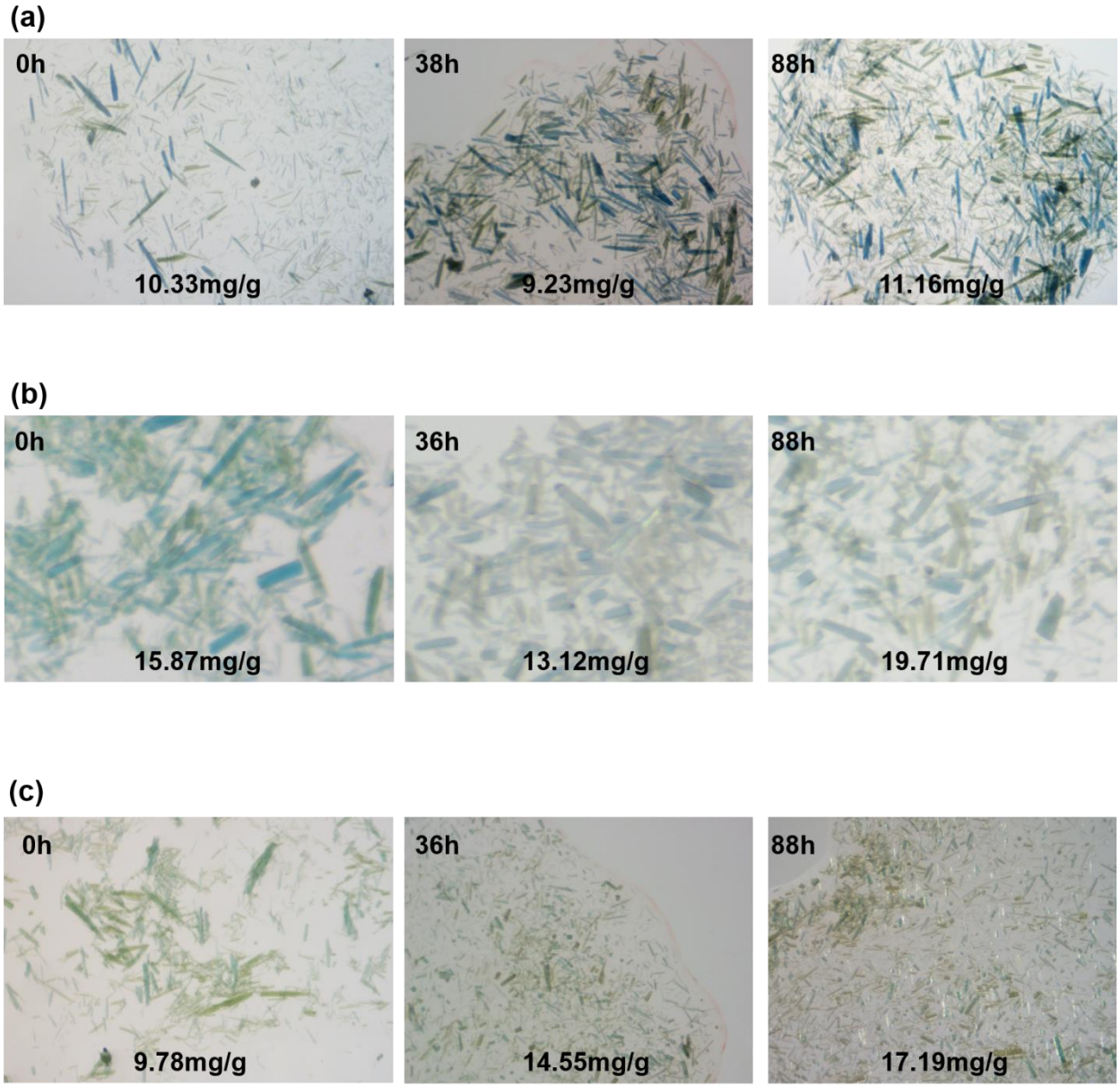

Figure S22. (a) The crystals of Cr-L1-Cu after soaking in Cyt C solution at room temperature for 0, 38, and 88 h; (b) Cr-L1-Co after soaking in Cyt C solution at room temperature for 0, 36, and 88 h; (c) Cr-L1-Ni after soaking in Cyt C solution at room temperature for 0, 36, and 88 h.

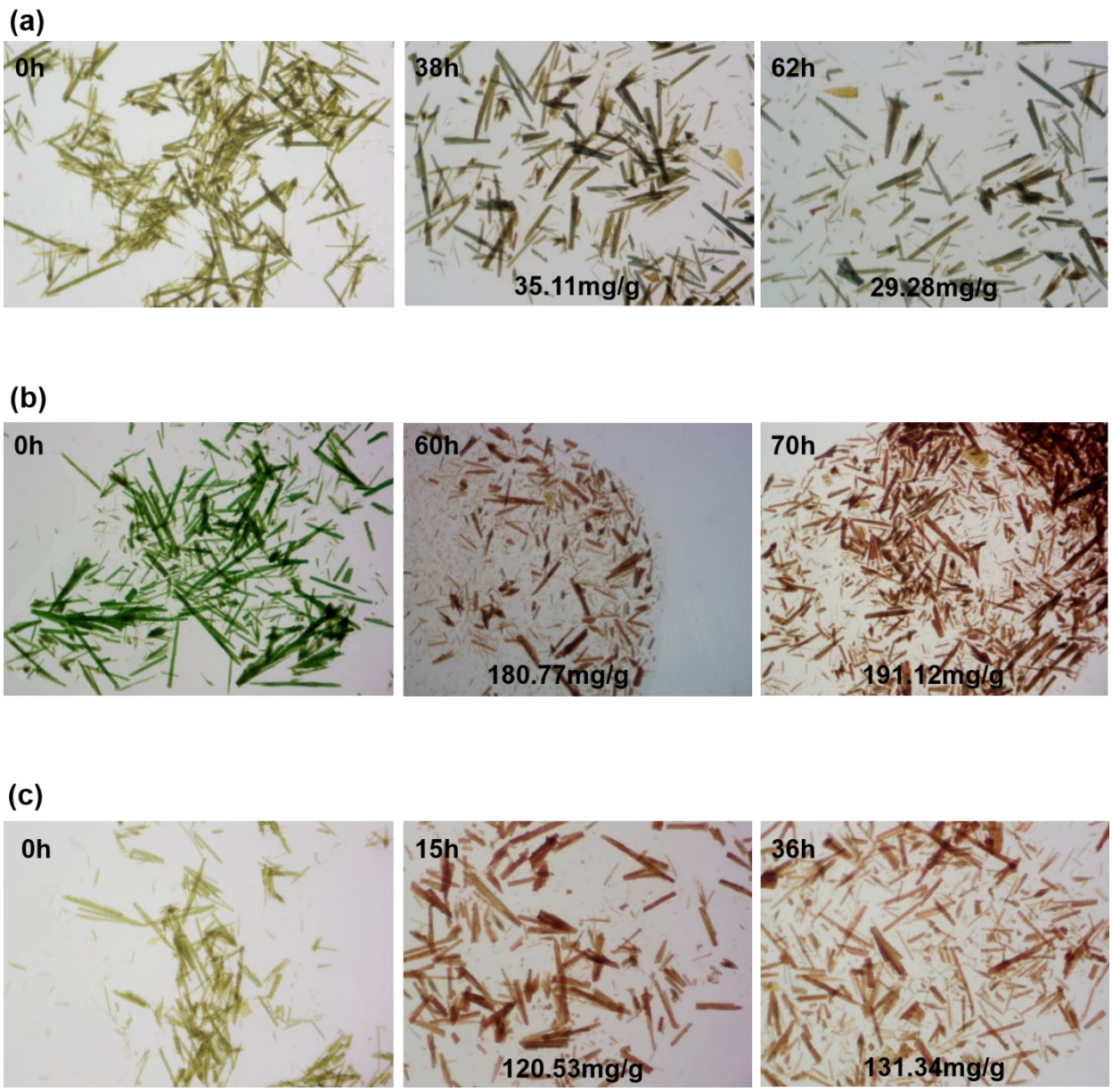

Figure S23. (a) The crystals of Cr-L2-Cu after soaking in Cyt C solution at room temperature for 0, 38, and 62 h; (b) Cr-L2-Co after soaking in Cyt C solution at room temperature for 0, 60, and 70 h; (c) Cr-L2-Ni after soaking in Cyt C solution at room temperature for 0, 15, and 36 h.

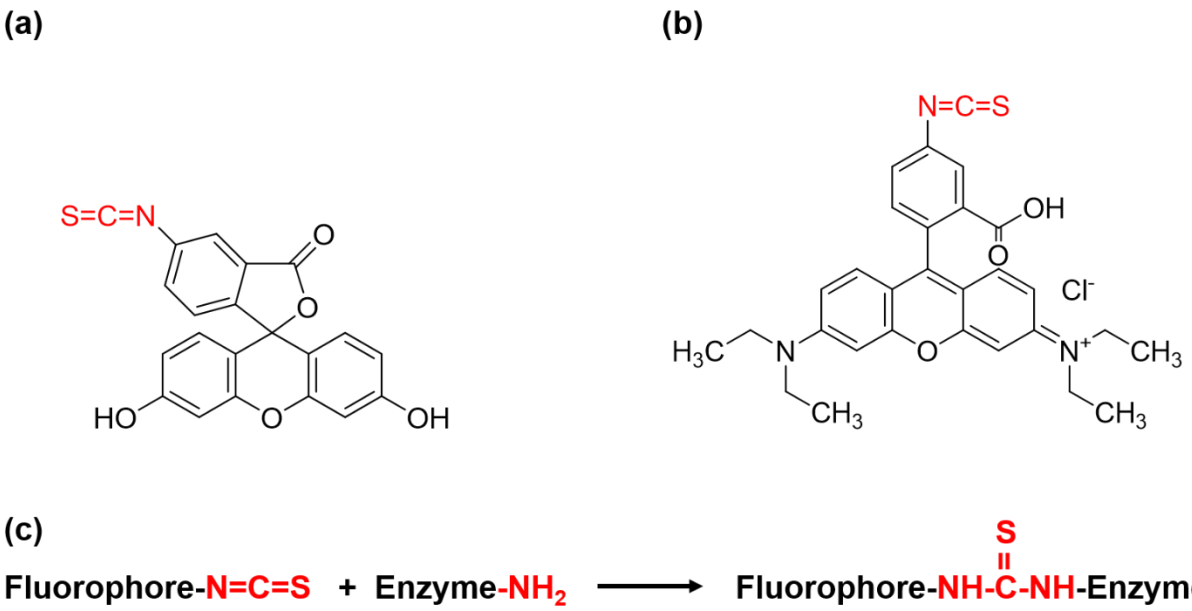

Figure S24. Reaction of a primary amine with the isothiocyanate group in rhodamine B isothiocyanate (RhB, a), fluorescein isothiocyanate (FITC, b), and a generic isothiocyanate-containing linker (c).

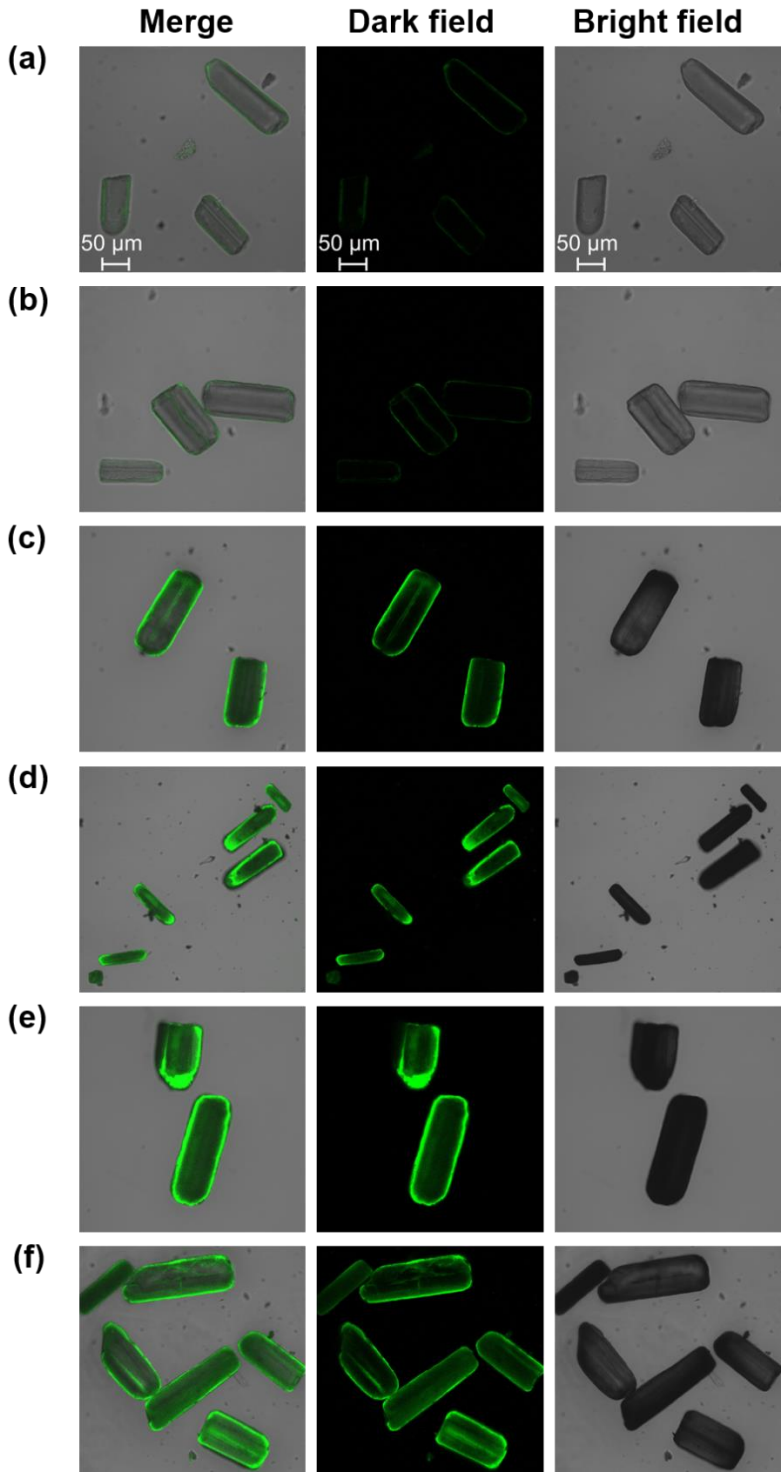

Figure S25. The CLSM images of FITC-labeled Cyt C@Cr-L3-Cu at various time points, including 3 hours (a), 8 hours (b), 12 hours (c), 24 hours (d), 48 hours (e), and 60 hours (f).

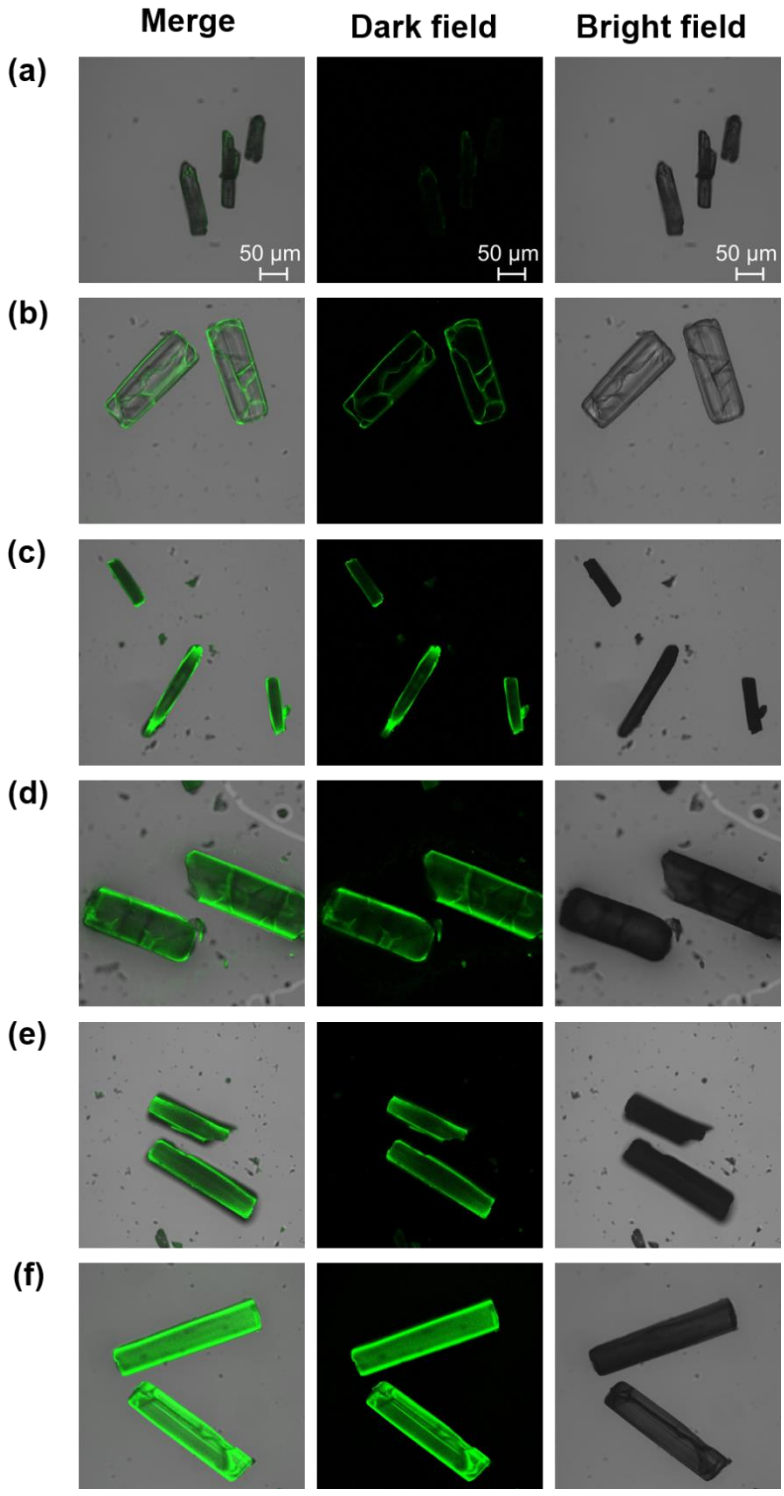

Figure S26. The CLSM images of FITC-labeled Cyt C@Cr-L3-Co at various time points, including 3 hours (a), 8 hours (b), 12 hours (c), 24 hours (d), 48 hours (e), and 60 hours (f).

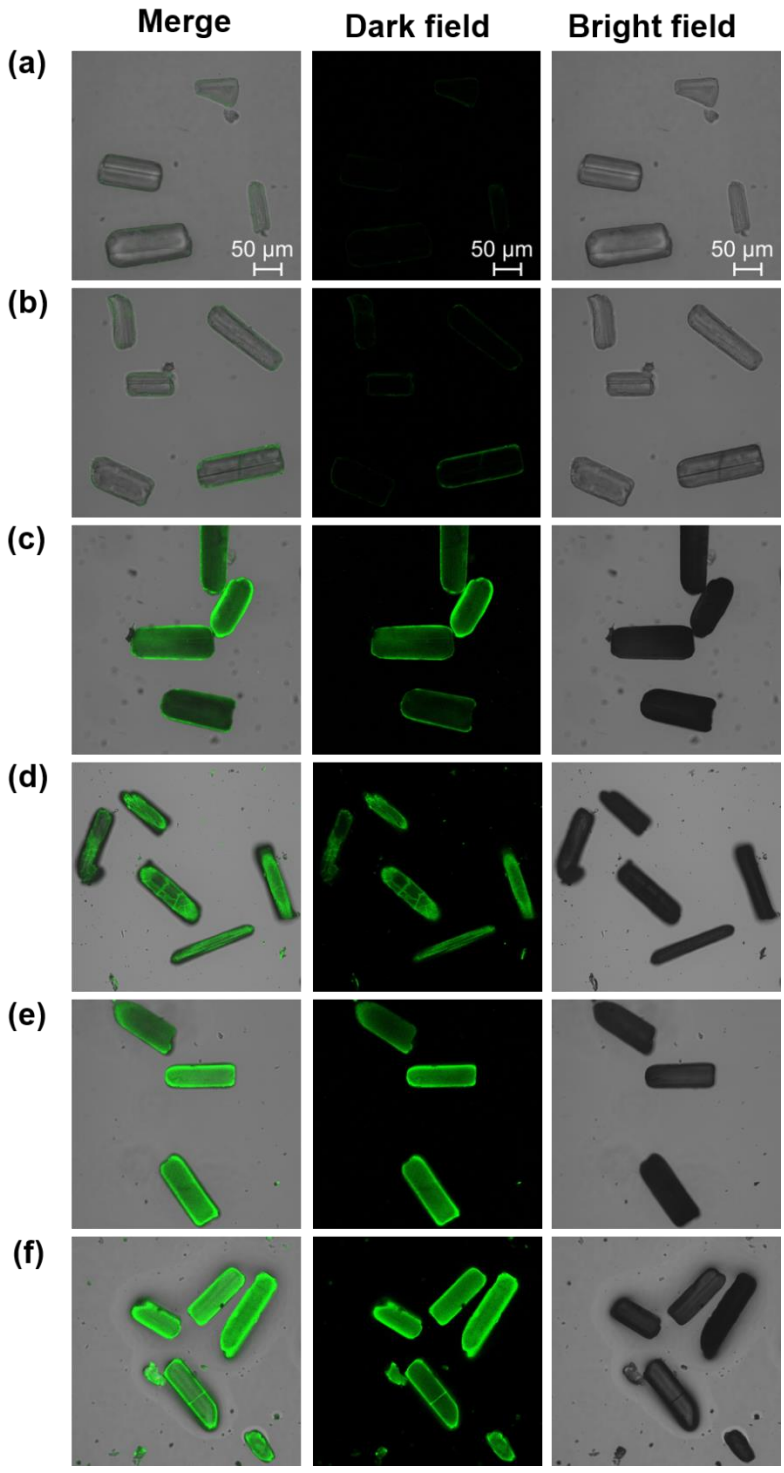

Figure S27. The CLSM images of FITC-labeled Cyt C@Cr-L3-Ni at various time points, including 3 hours (a), 8 hours (b), 12 hours (c), 24 hours (d), 48 hours (e), and 60 hours (f).

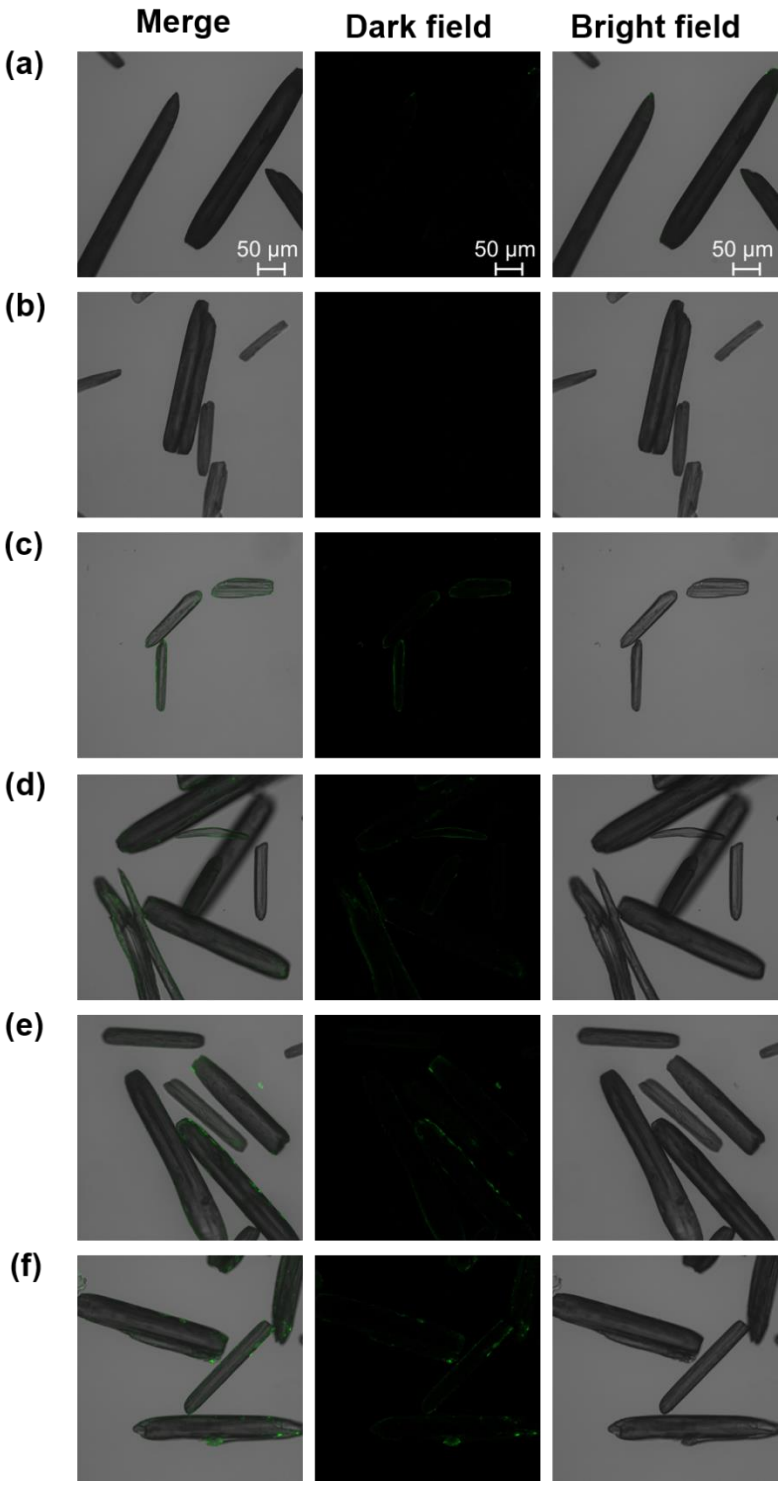

Figure S28. The CLSM images of FITC-labeled Cyt C@Cr-L3-Pd at various time points, including 3 hours (a), 8 hours (b), 12 hours (c), 24 hours (d), 48 hours (e), and 60 hours (f).

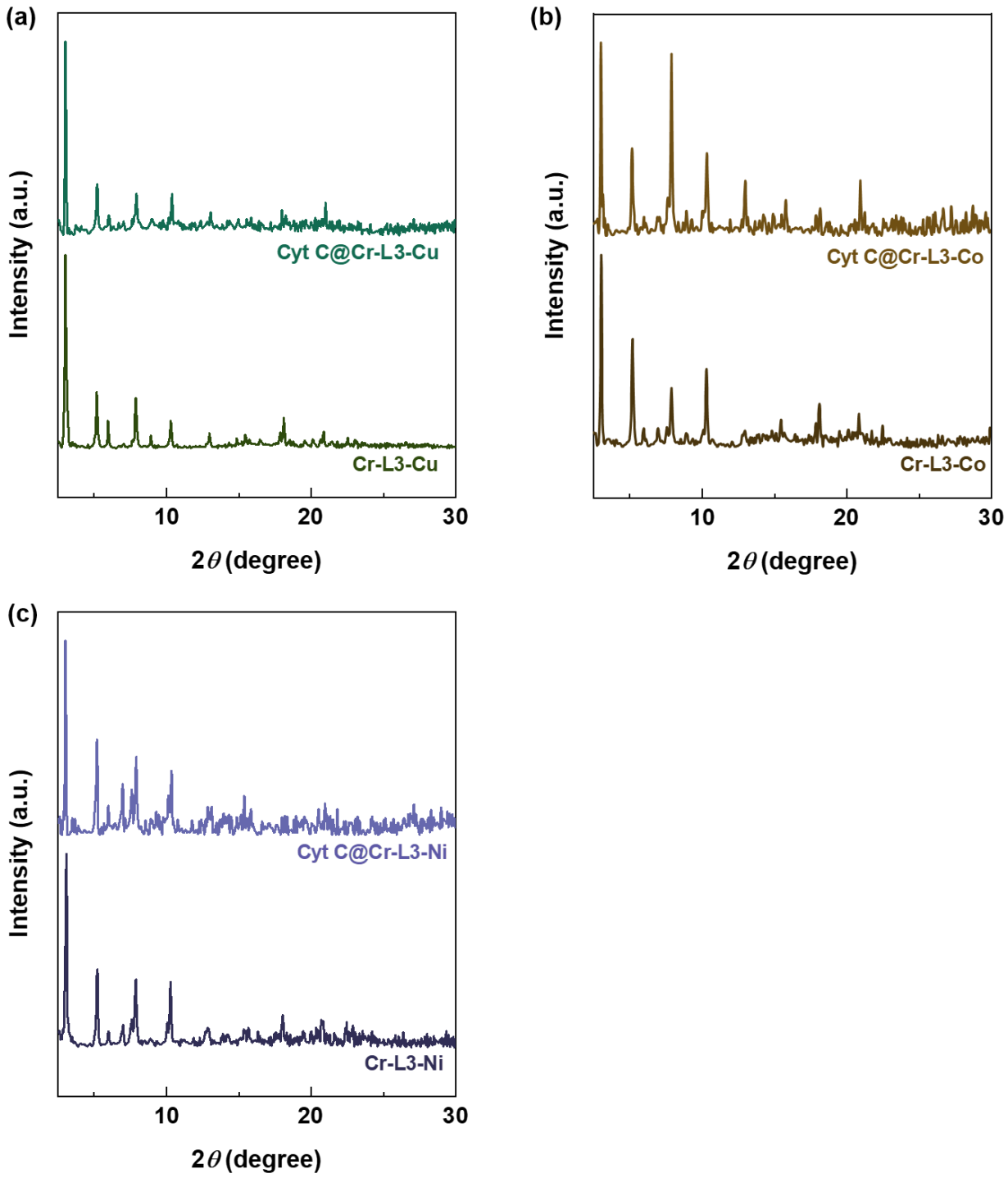

Figure S29. PXRD patterns before and after Cyt C enzyme loading for Cr-L3-Cu (a), Cr-L3-Co (b), and Cr-L3-Ni (c).

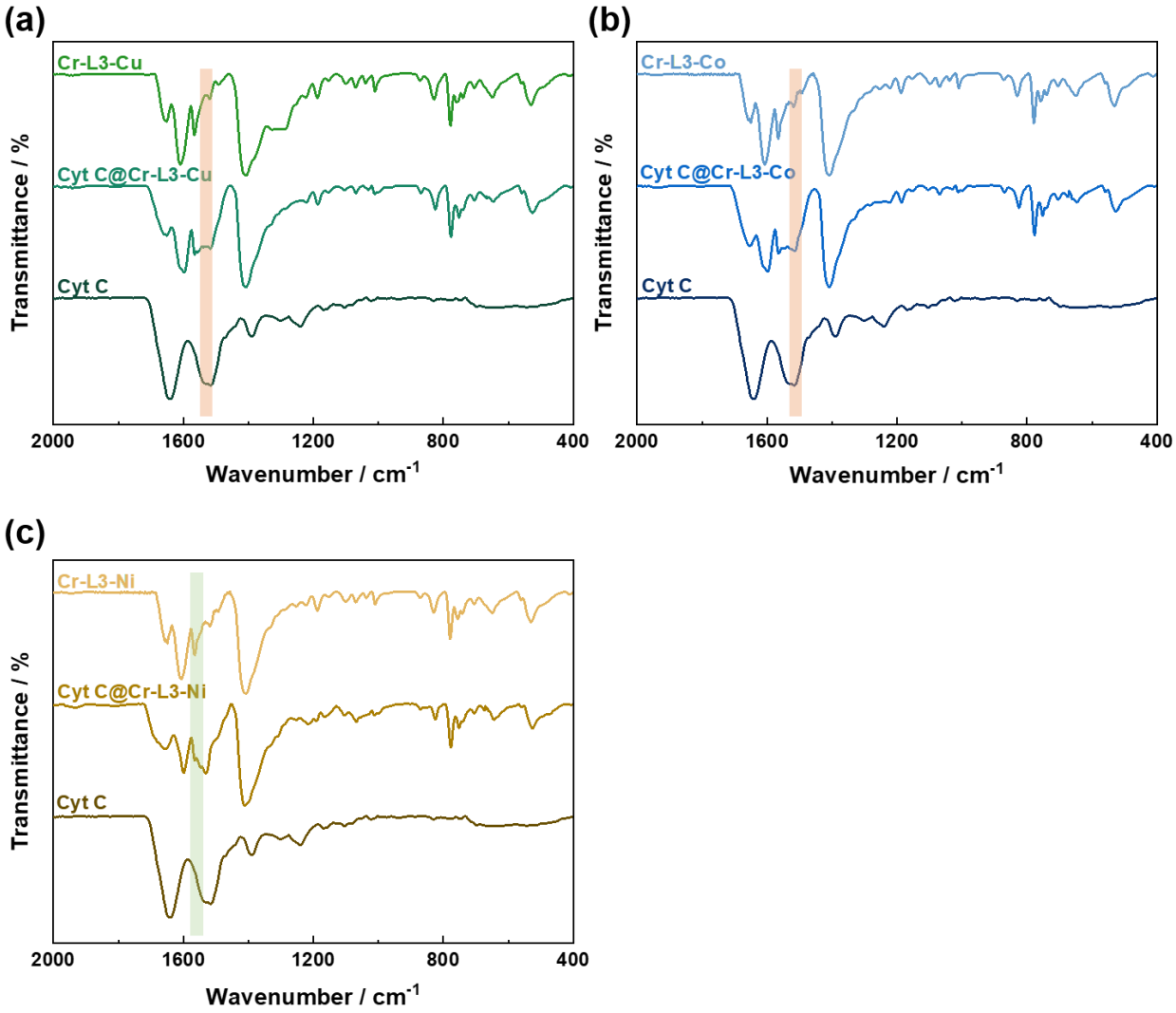

Figure S30. FI-IR spectra for Cyt C, Cyt C@Cr-L3-Cu, and Cr-L3-Cu (a); Cyt C, Cyt C@Cr-L3-Co, and Cr-L3-Co (b); Cyt C, Cyt C@Cr-L3-Ni, and Cr-L3-Ni (c).

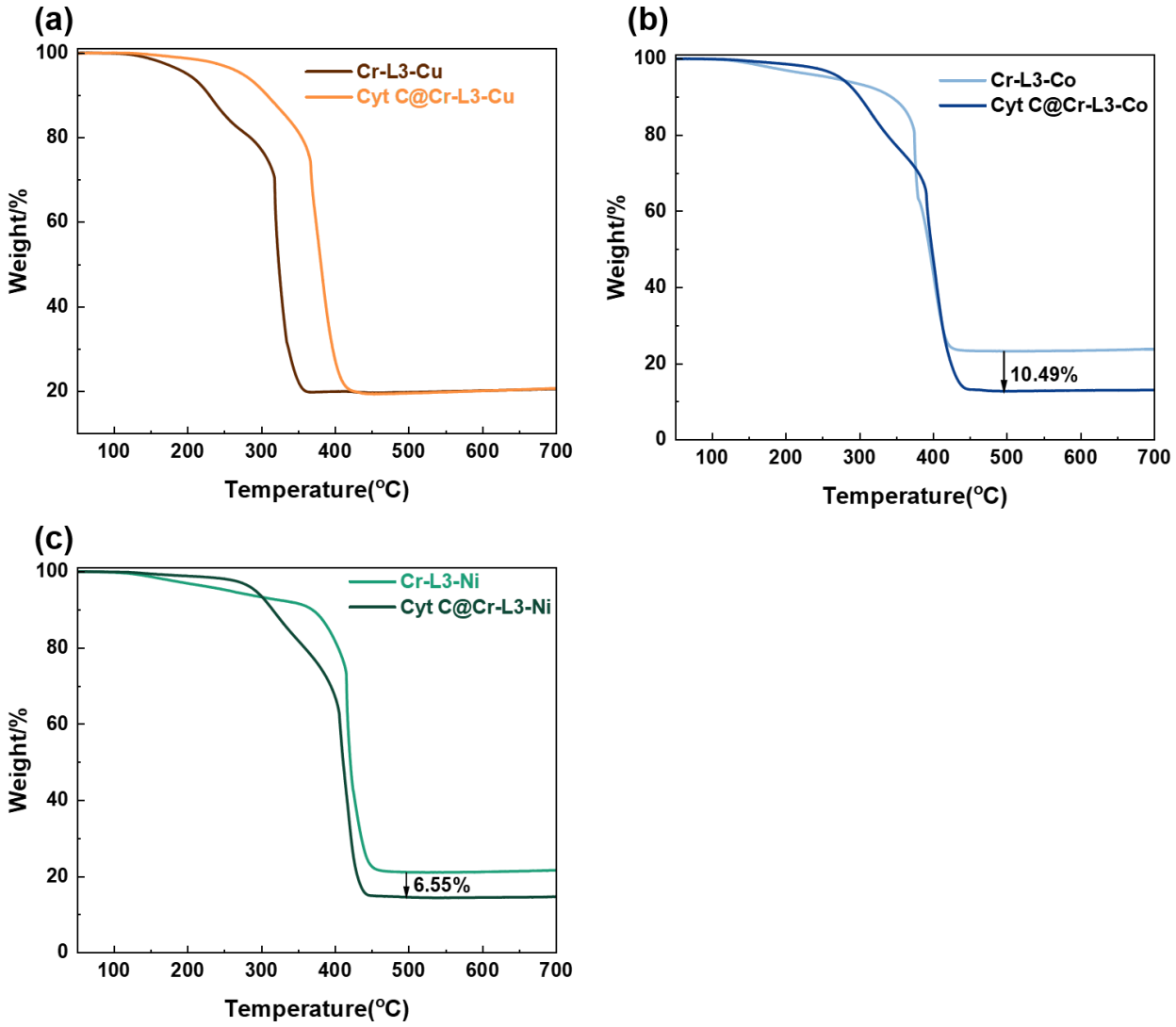

Figure S31. TGA curve of Cyt C@Cr-L3-Cu compared to Cr-L3-Cu (a); Cyt C@Cr-L3-Co compared to Cr-L3-Co (b); Cyt C@Cr-L3-Ni compared to Cr-L3-Ni (c).

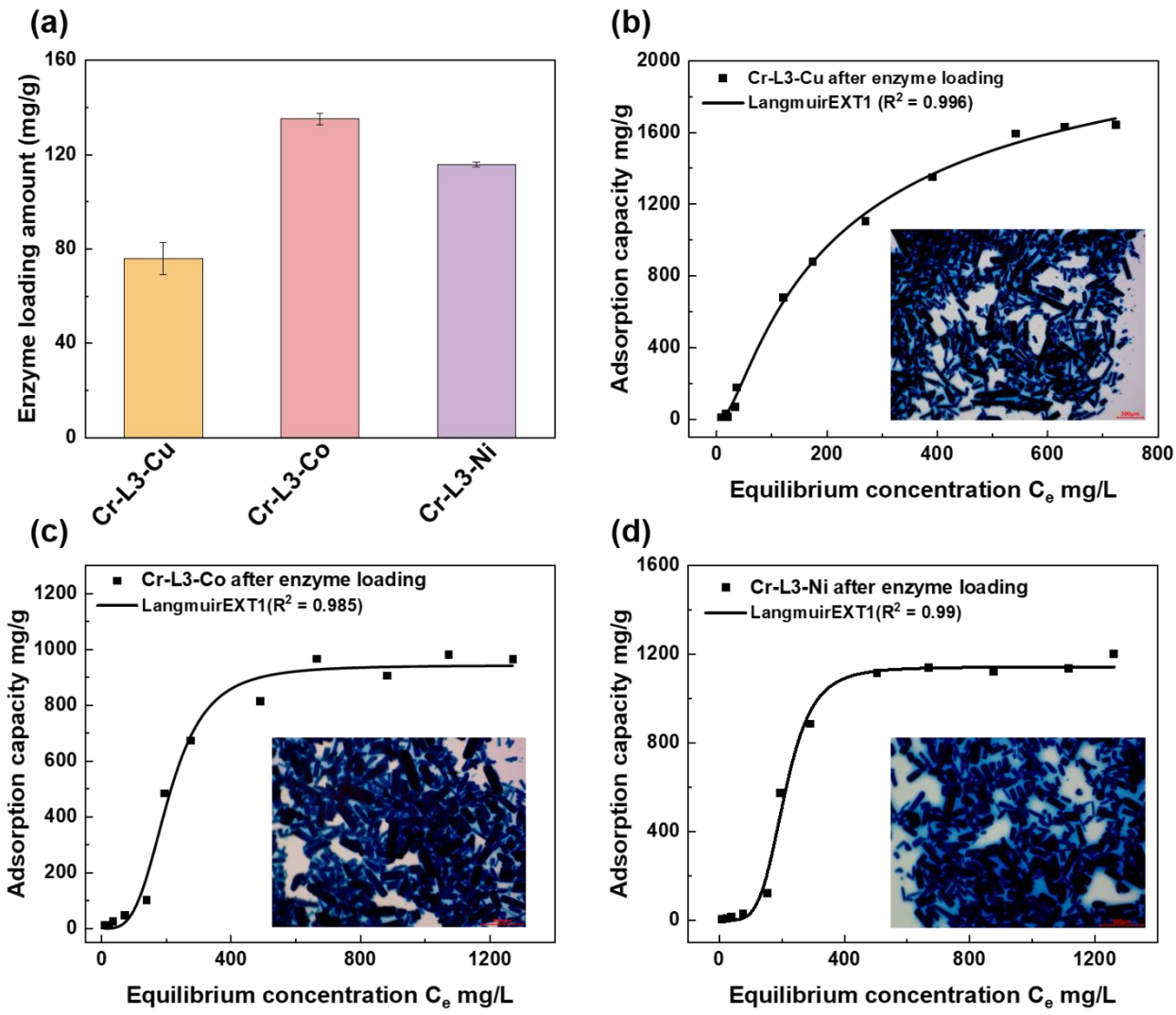

Figure S32. (a) Loading capacities of the enzyme on Cr-L3-M (M = Cu, Co, Ni). Adsorption isotherms of methylene blue on enzyme-loaded Cr-L3-Cu (b), Cr-L3-Co (c), and Cr-L3-Ni (d), respectively. Fitted with the Langmuir models. Error bars represent standard deviations from three independent measurements.

(a)

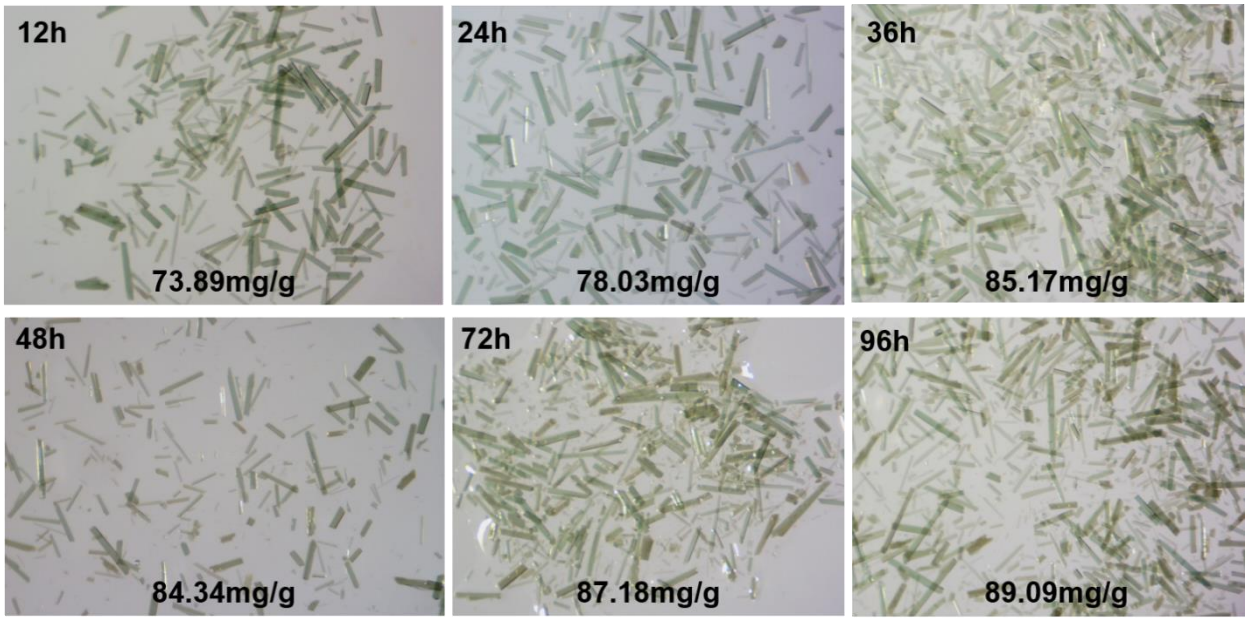
12h
73.89mg/g
24h
78.03mg/g
36h
85.17mg/g
48h
84.34mg/g
72h
87.18mg/g
96h
89.09mg/g

(b)

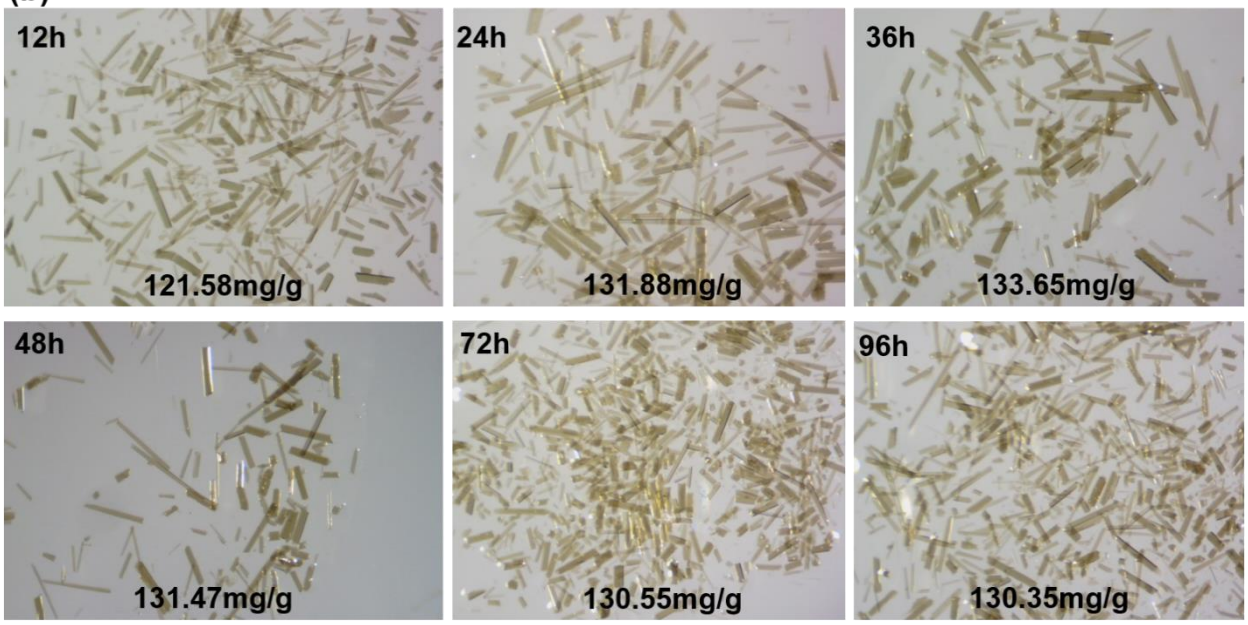
12h
121.58mg/g
24h
131.88mg/g
36h
133.65mg/g
48h
131.47mg/g
72h
130.55mg/g
96h
130.35mg/g

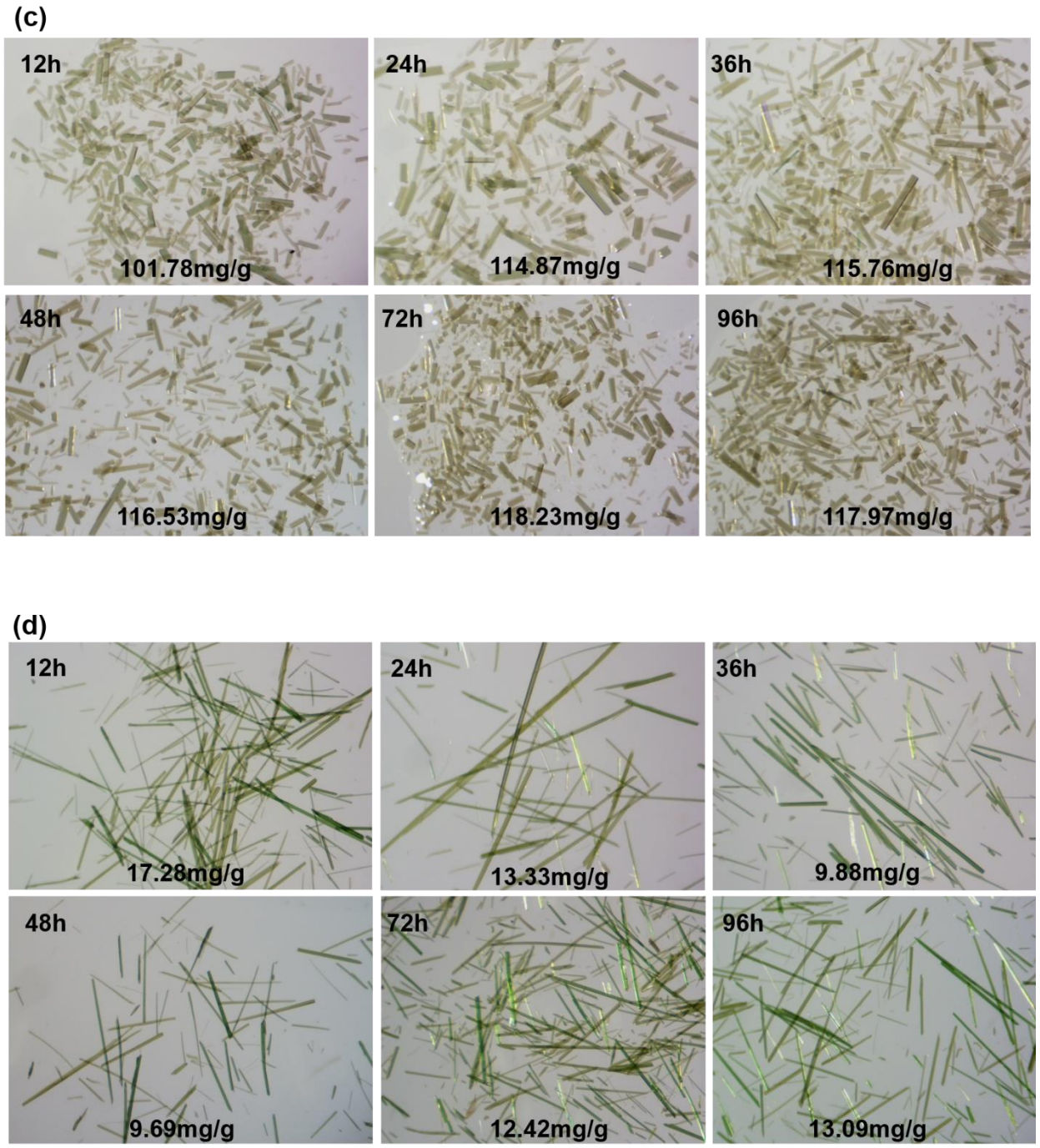

Figure S33. The crystals of Cr-L3-Cu (a), Cr-L3-Co (b), Cr-L3-Ni (c), and Cr-L3-Pd (d) after soaking in HRP solution at room temperature for 12, 24, 36, 48, 72, and 96 h.

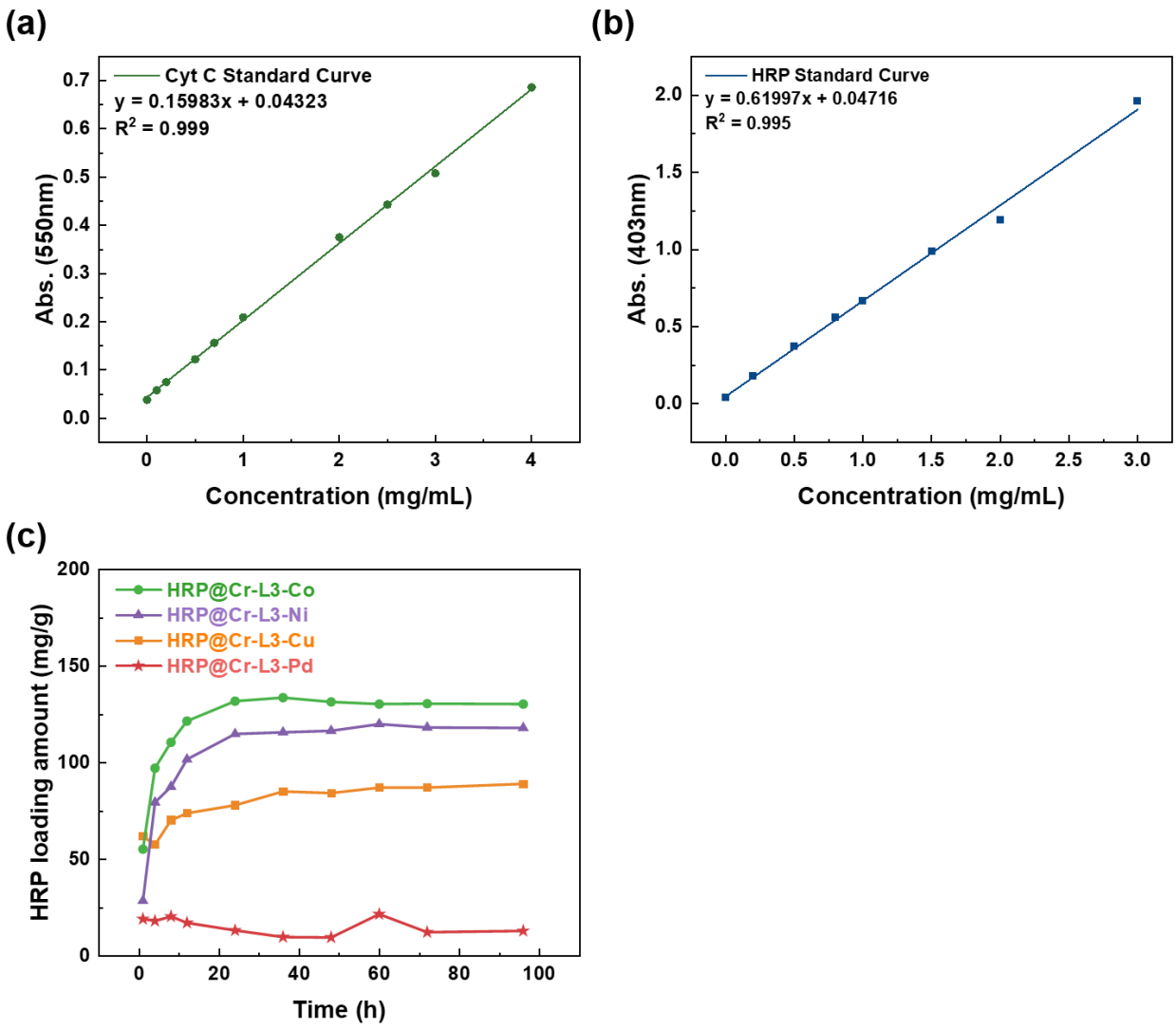

Figure S34. (a) Standard curves of Cyt C; (b) Standard curves of HRP; (c) Plots of the loading capacities of HRP in Cr-L3-M′ (M = Cu, Co, Ni, Pd).

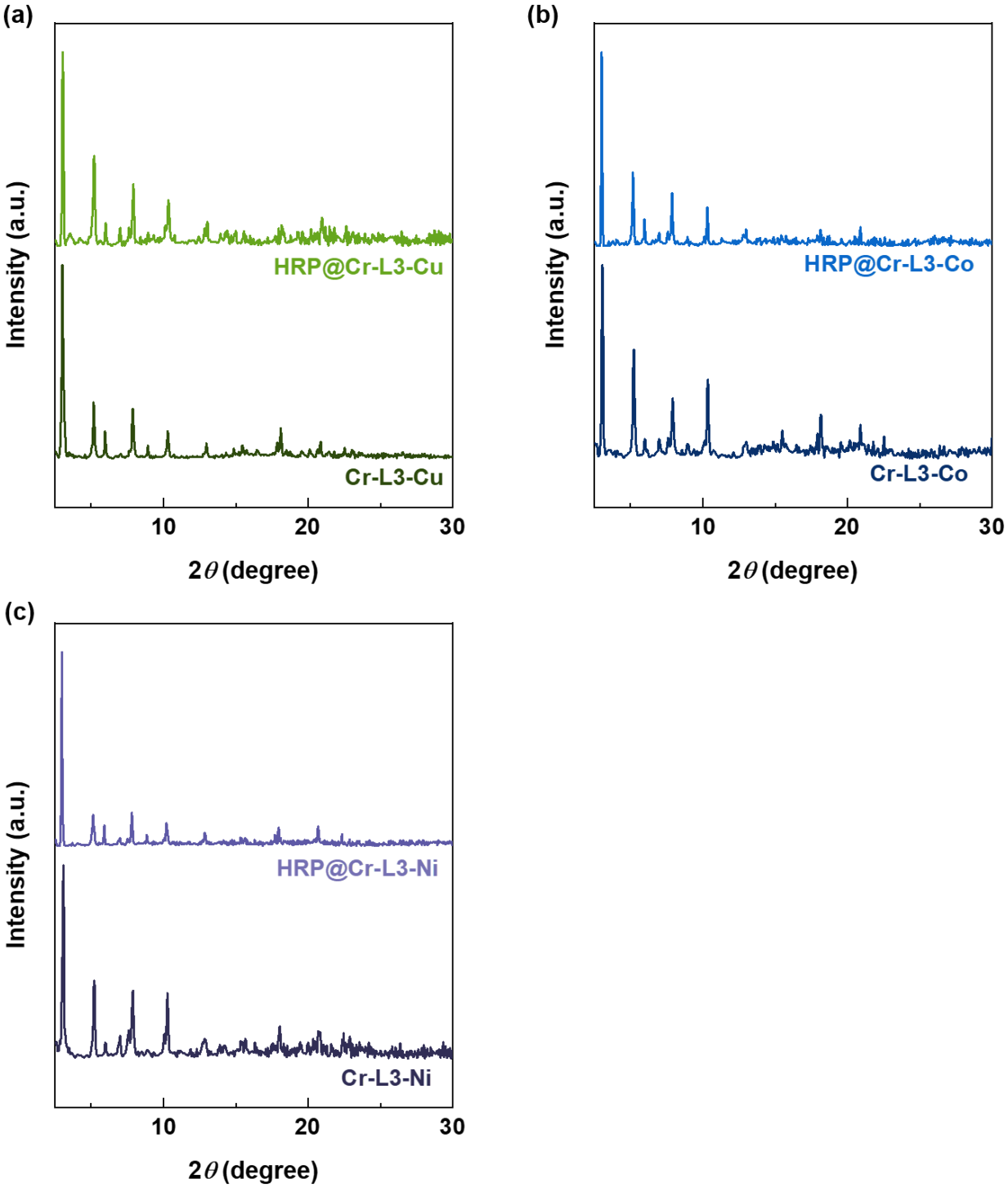

Figure S35. PXRD patterns before and after HRP loading for Cr-L3-Cu (a), Cr-L3-Co (b), and Cr-L3-Ni (c).

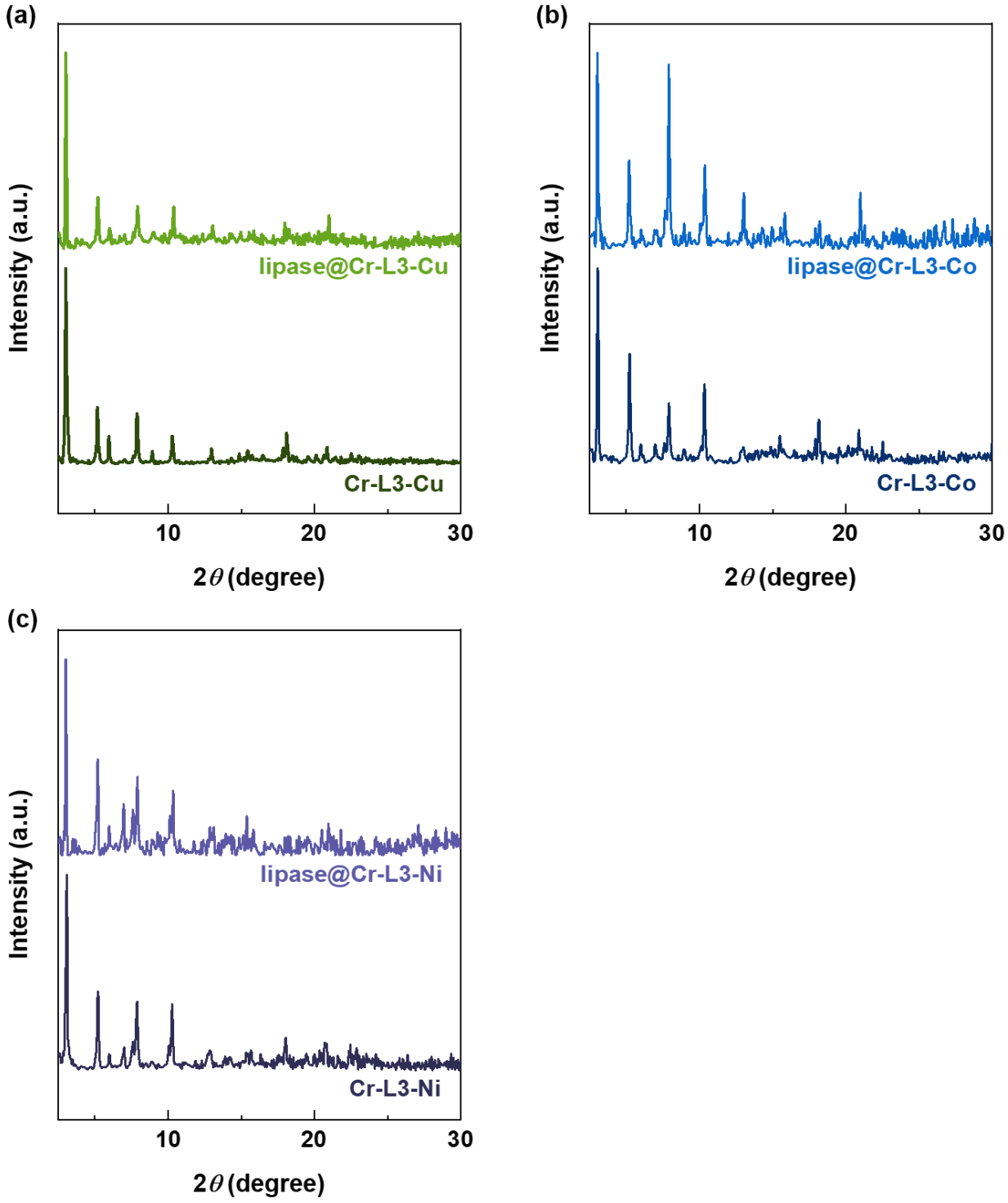

Figure S36. PXRD patterns before and after lipase loading for Cr-L3-Cu (a), Cr-L3-Co (b), and Cr-L3-Ni (c).

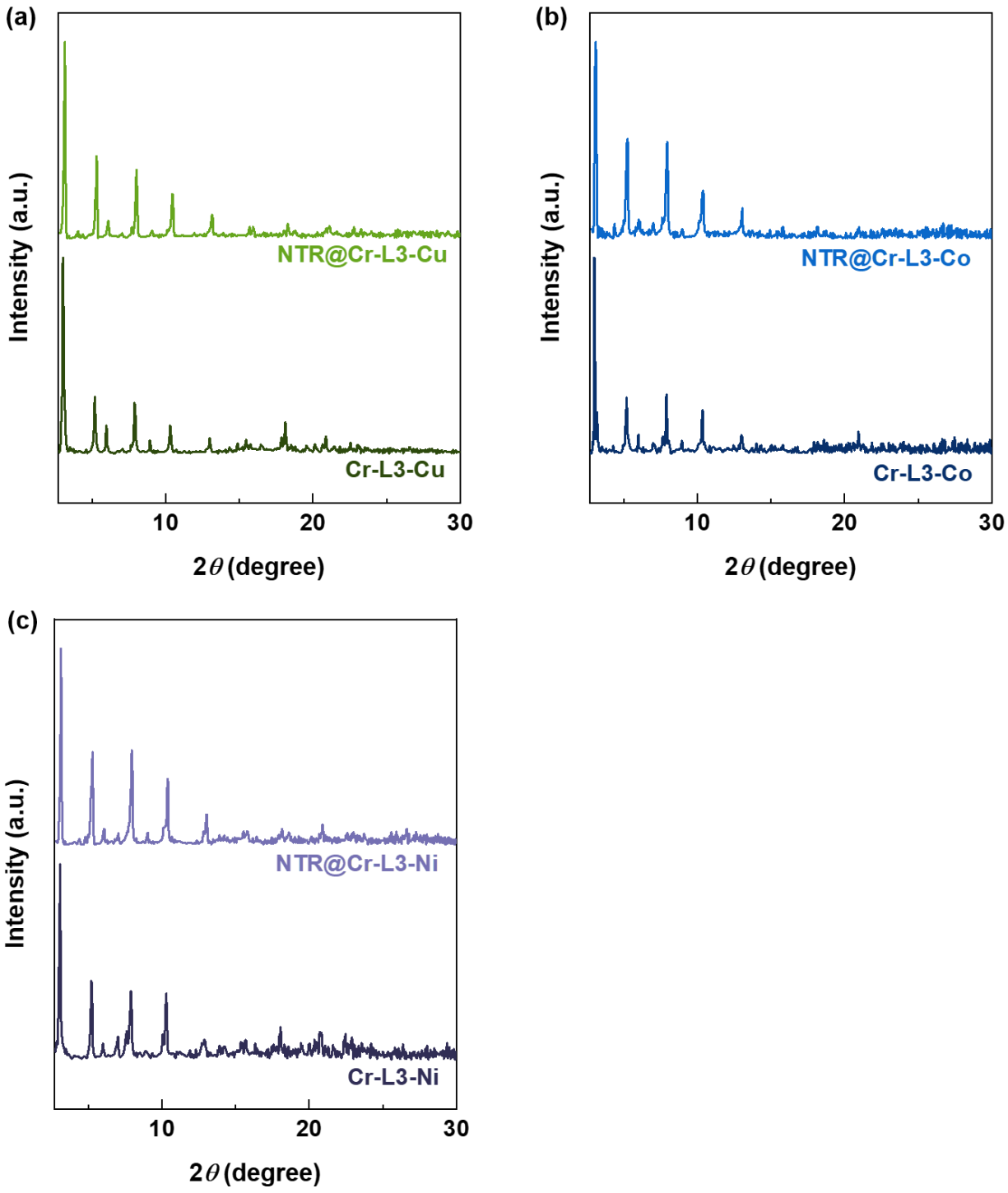

Figure S37. PXRD patterns before and after NTR loading for Cr-L3-Cu (a), Cr-L3-Co (b), and Cr-L3-Ni (c).

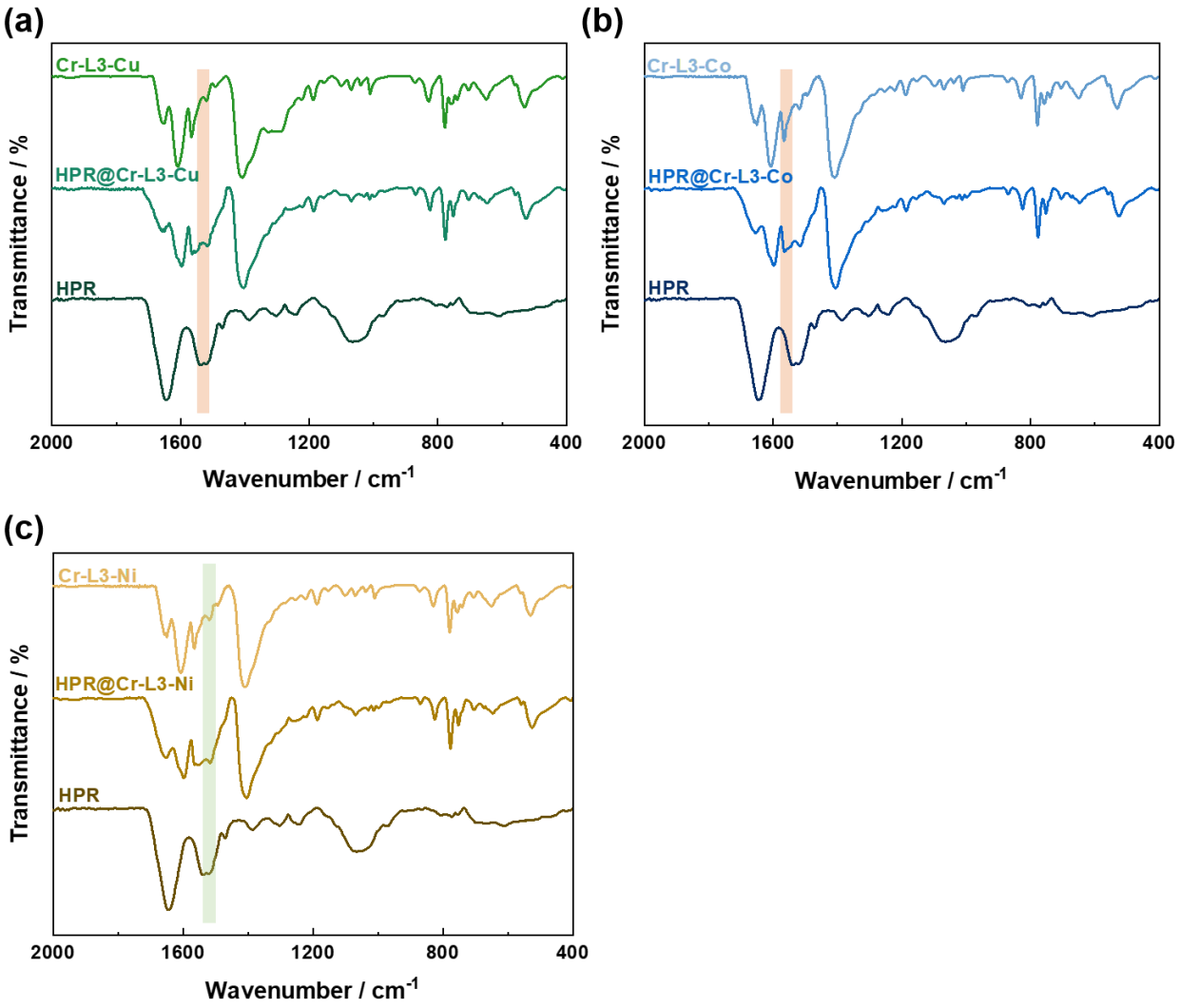

Figure S38. FI-IR spectra for HRP, HRP@Cr-L3-Cu, and Cr-L3-Cu (a); HRP, HRP@Cr-L3-Co, and Cr-L3-Co (b); HRP, HRP@Cr-L3-Ni, and Cr-L3-Ni (c).

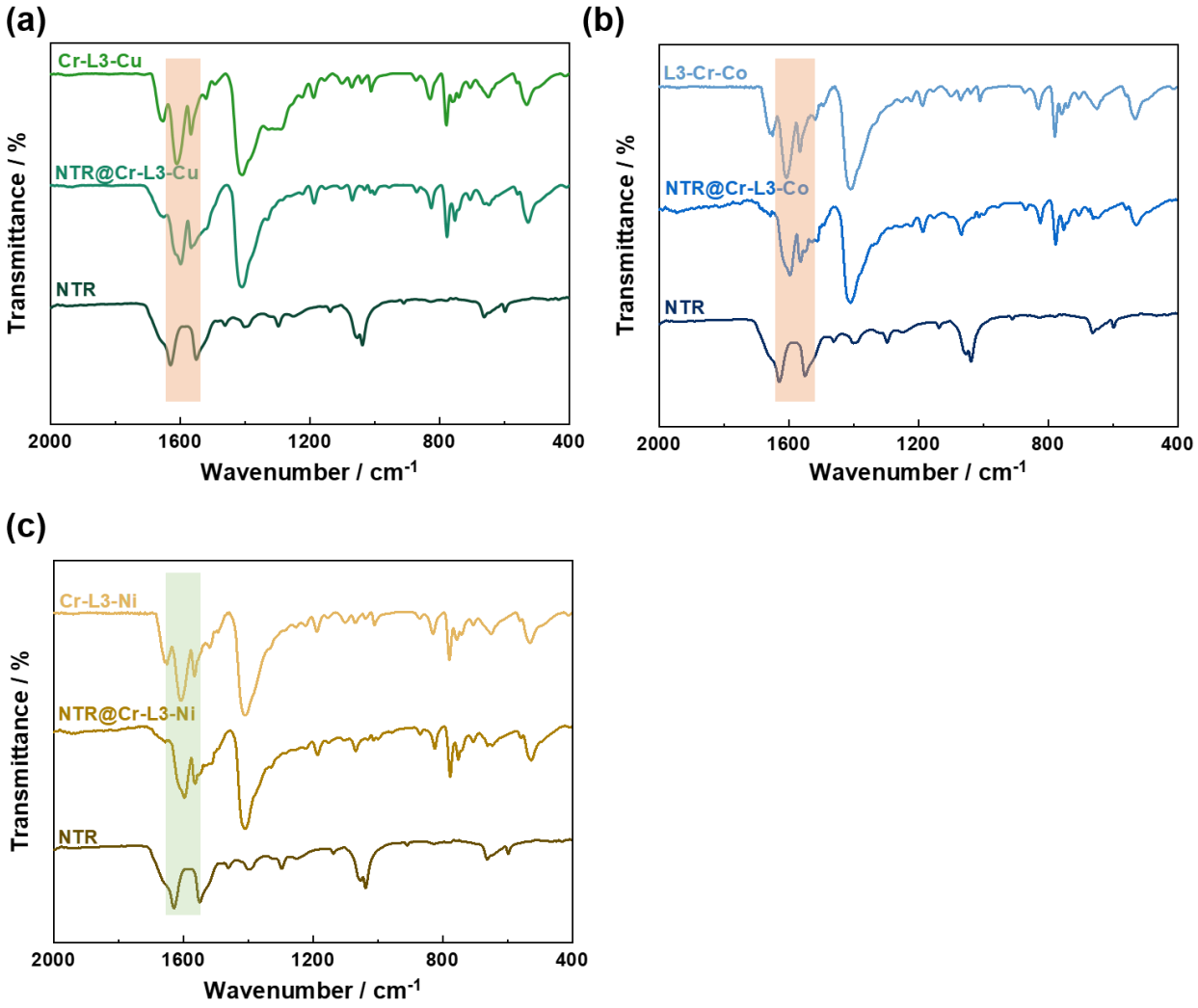

Figure S39. FI-IR spectra for NTR, NTR@Cr-L3-Cu, and Cr-L3-Cu (a); NTR, NTR@Cr-L3-Co, and Cr-L3-Co (b); NTR, NTR@Cr-L3-Ni, and Cr-L3-Ni (c).

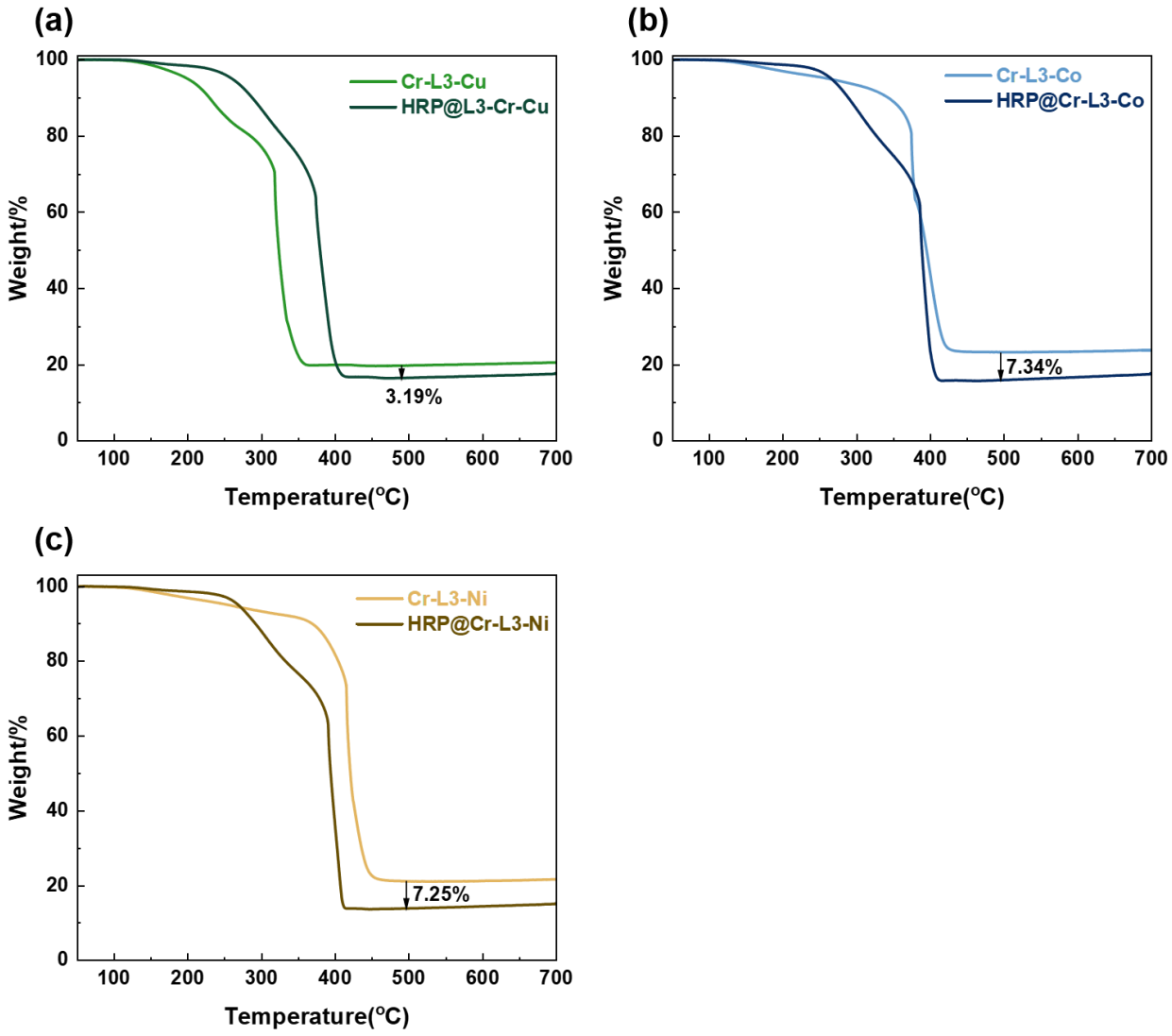

Figure S40. TGA curve of HRP@Cr-L3-Cu compared to Cr-L3-Cu (a); HRP@Cr-L3-Co compared to L3-Cr-Co (b); HRP@Cr-L3-Ni compared to Cr-L3-Ni (c).

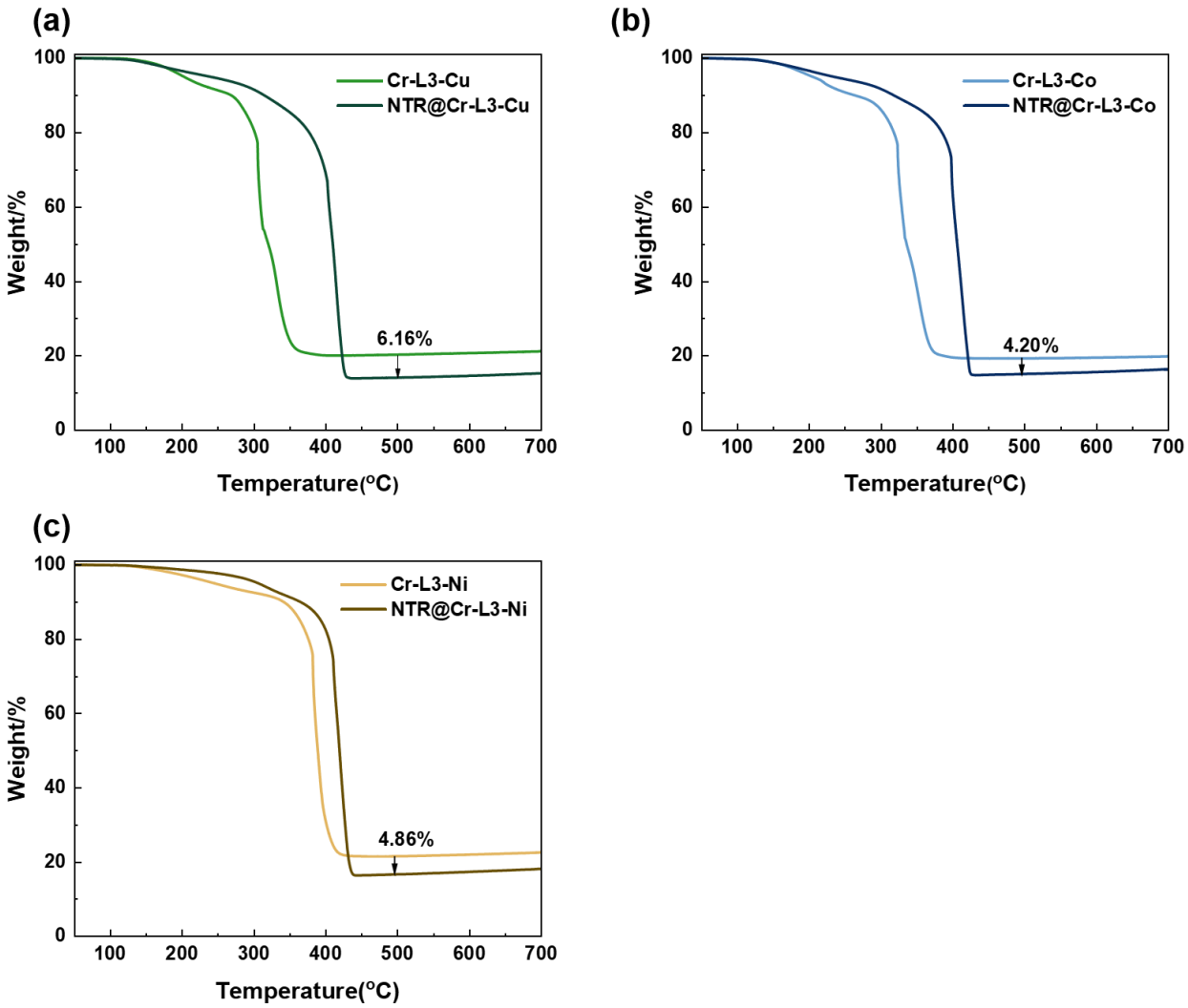

Figure S41. TGA curve of NTR@Cr-L3-Cu compared to Cr-L3-Cu (a); NTR@Cr-L3-Co compared to L3-Cr-Co (b); NTR@Cr-L3-Ni compared to Cr-L3-Ni (c).

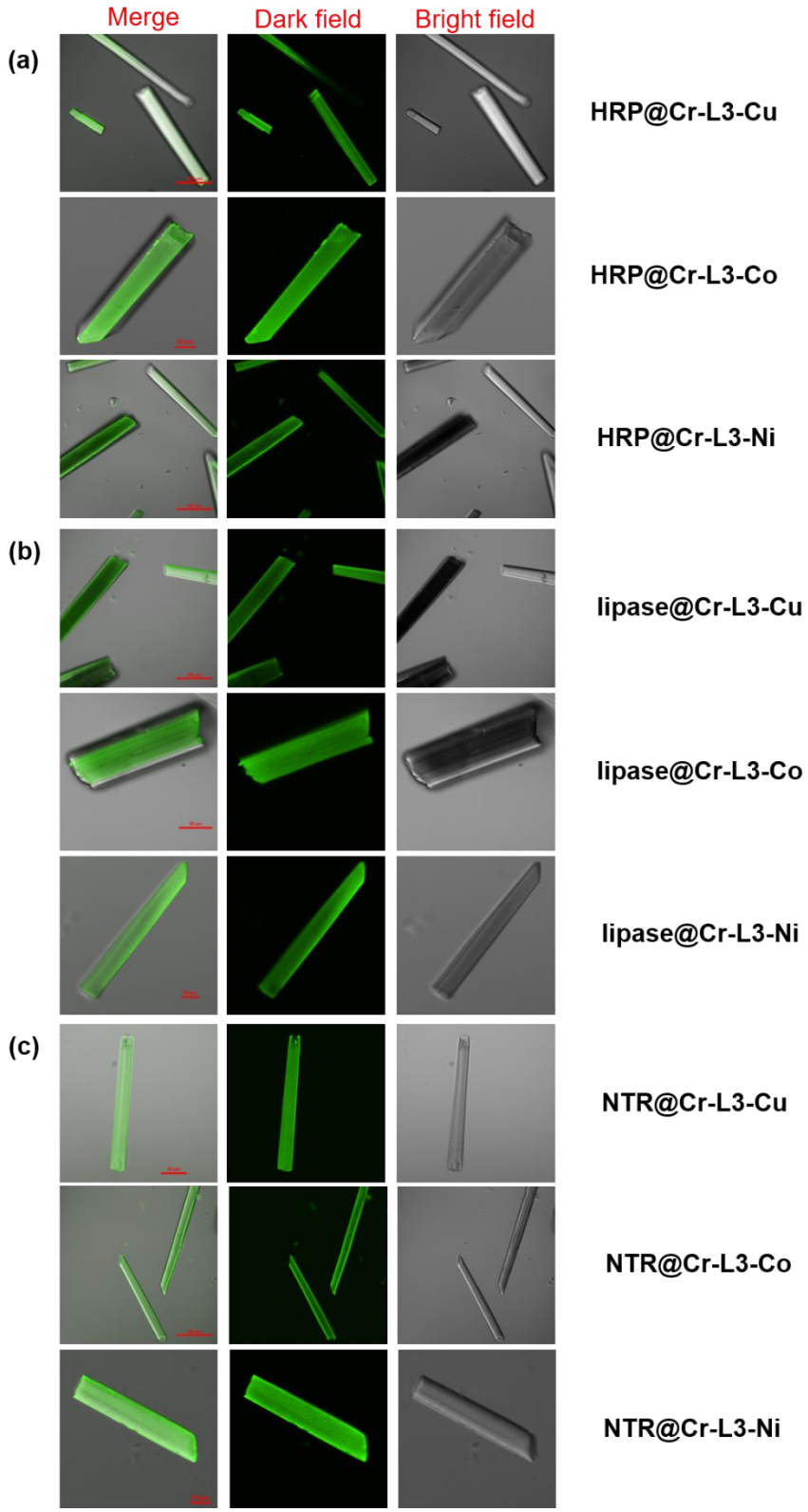

Figure S42. CLSM of FITC-labeled HRP@Cr-L3-Cu/Co/Ni (a); lipase@Cr-L3-Cu/Co/Ni (b); NTR@Cr-L3-Cu/Co/Ni (c).

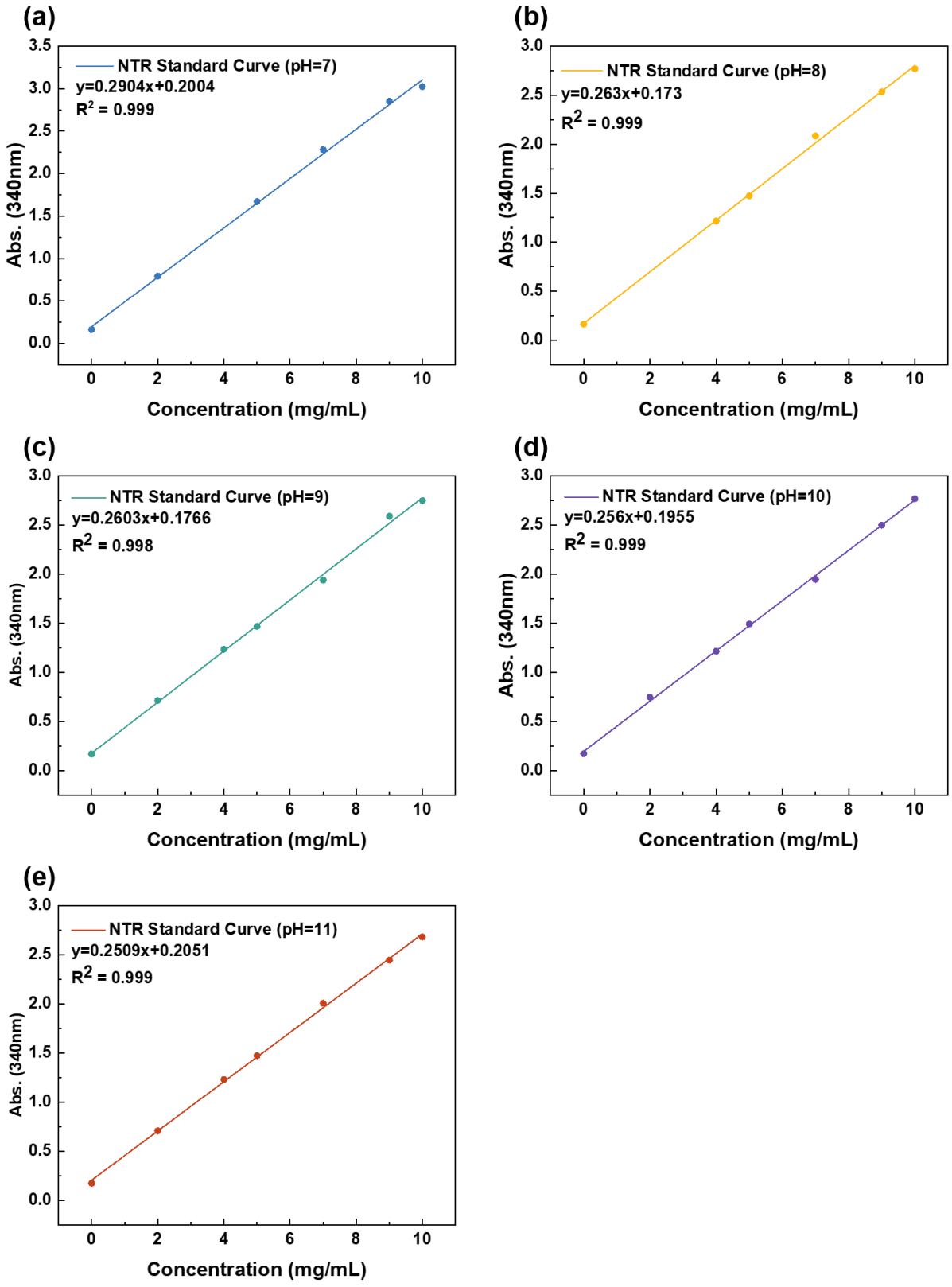

Figure S43. The standard curve of NTR at various pH levels: (a) pH = 7, (b) pH = 8, (c) pH = 9, (d) pH = 10, (e) pH = 11.

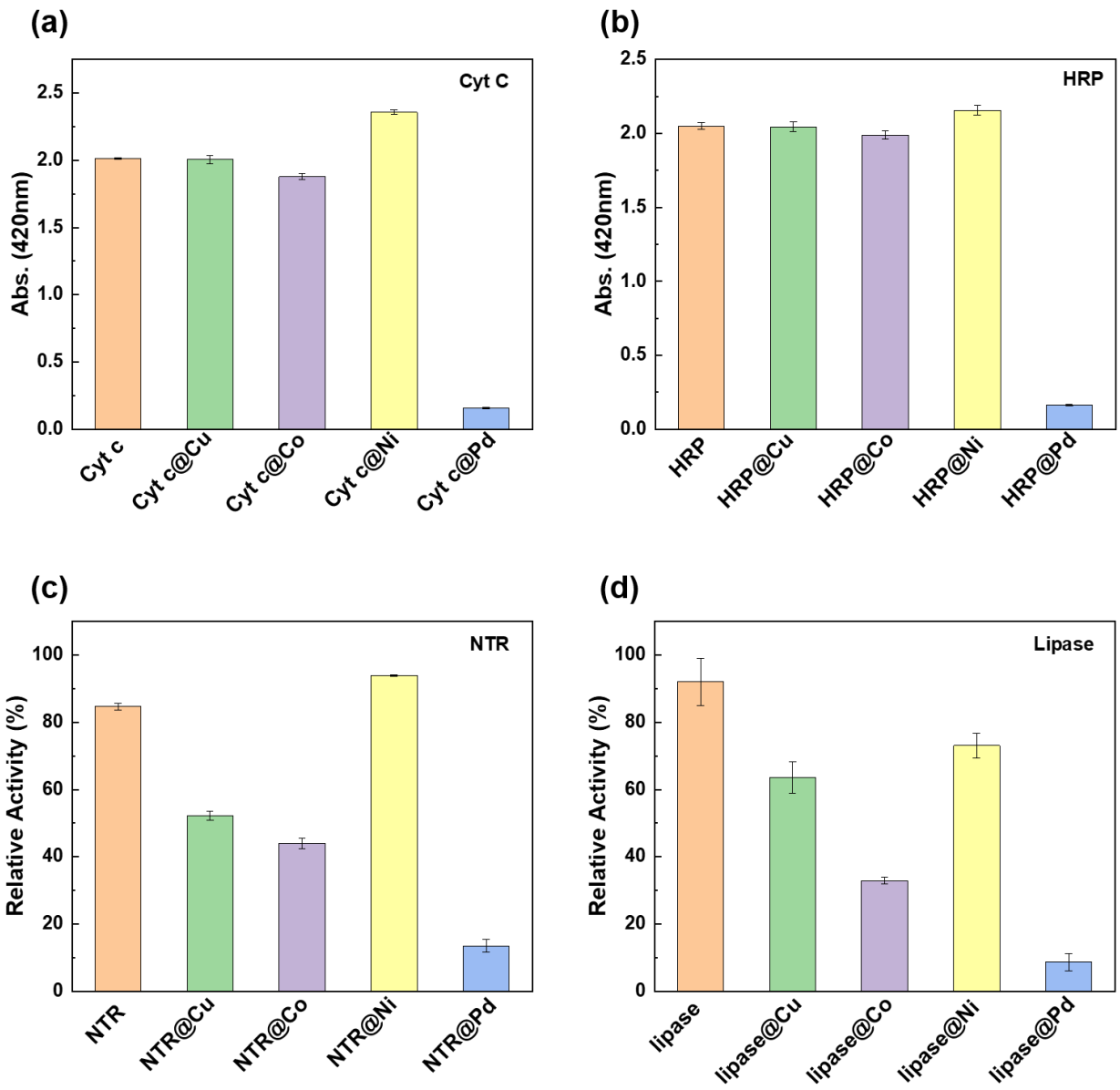

Figure S44. (a) The specific activities for Cr-L3-M (M = Cu, Co, Ni, Pd) immobilized Cyt C and free Cyt C were measured with 1 mM ABTS, 2 mM H_2O_2, 1 μg enzyme in 200 μL NaOAc/HOAc (50 mM, pH 4) at 25 °C for 10 min. The catalytic efficiency was evaluated by UV-vis measurement at 420 nm. (b) The specific activities for Cr-L3-M (M = Cu, Co, Ni, Pd) immobilized HRP and free HRP were measured with 1 mM ABTS, 2 mM H_2O_2, 1 μg enzyme in 200 μL NaOAc/HOAc (50 mM, pH 4) at 25 °C for 10 min. The catalytic efficiency was evaluated by UV-vis measurement at 420 nm. (c) The relative activities for Cr-L3-M (M = Cu, Co, Ni, Pd) immobilized NTR and free NTR were measured with 5 mM p-nitrophenyl, 5mM NADH, and 1 μg enzyme in 200 μL Tris-HCl buffer (200 mM, pH 7.4) at 37 °C for 1 h. The catalytic efficiency was evaluated by UV-

vis measurement at 340 nm. (d) The relative activity of for Cr-L3-M (M = Cu, Co, Ni, Pd) immobilized lipase and free lipase was measured with 1.5 mM p-nitrophenyl palmitate (p-NPP) mixed milky solution, 1 mg MOF in 2 mL PBS buffer (50 mM, pH 7.5) at 37 °C for 1 h. The catalytic efficiency was evaluated by UV-vis measurement at 405 nm.

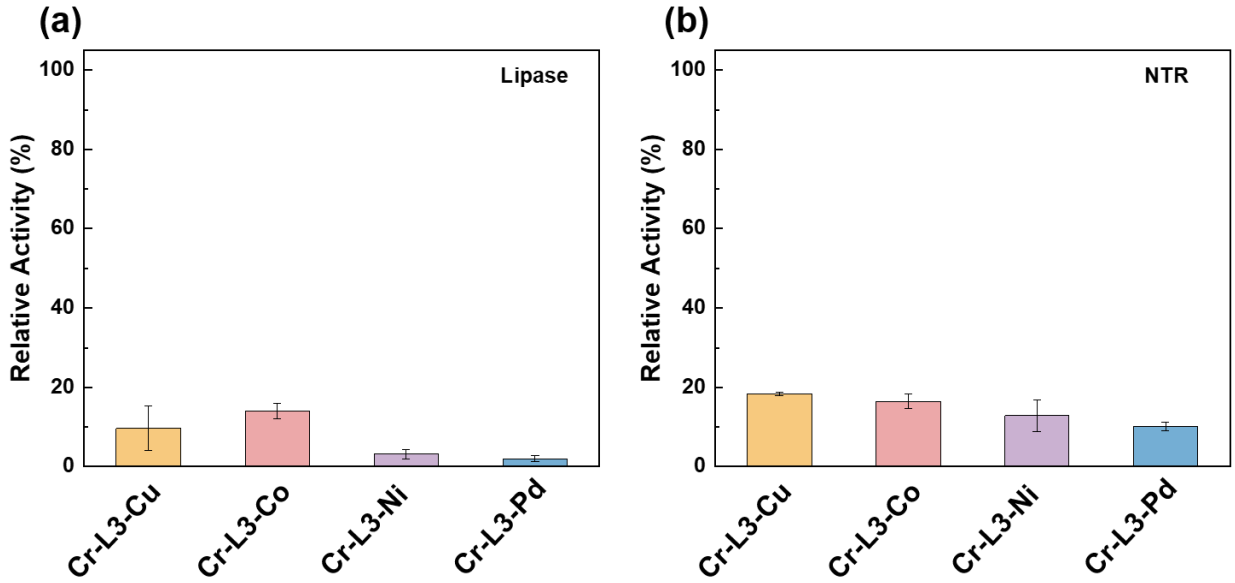

Figure S45. (a)The relative activity of blank control Cr-L3-Cu, Cr-L3-Co, Cr-L3-Ni, and Cr-L3-Pd in lipase catalysis was measured with 1.5 mM p-nitrophenyl palmitate (p-NPP) mixed milky solution, 1 mg MOF in 2 mL PBS buffer (50 mM, pH 7.5) at 37 °C for 1 h. The catalytic efficiency was evaluated by UV-vis measurement at 405 nm. (b) The relative activity of blank control Cr-L3-Cu, Cr-L3-Co, Cr-L3-Ni, and Cr-L3-Pd in NTR catalysis was measured with 5 mM p-nitrophenyl, 5mM NADH, and 1 μg enzyme in 200 μL Tris-HCl buffer (200 mM, pH 7.4) at 37 °C for 1 h. The catalytic efficiency was evaluated by UV-vis measurement at 340 nm.

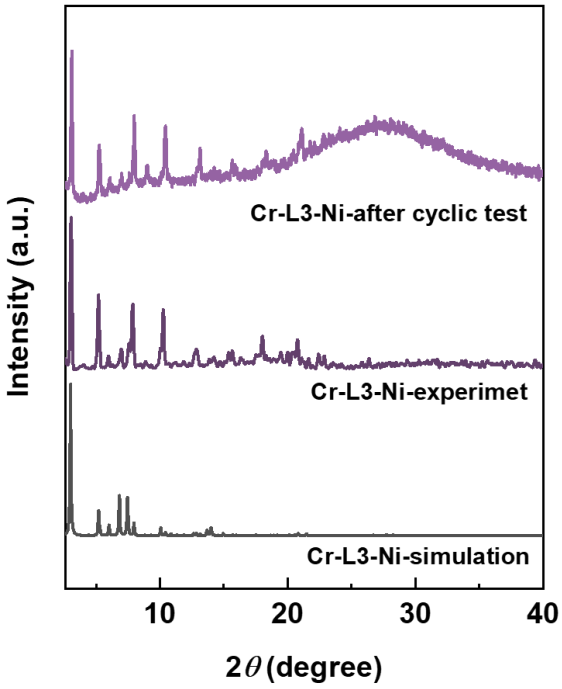

Figure S46. PXRD patterns of NTR@Cr-L3-Ni before and after catalysis cycles.

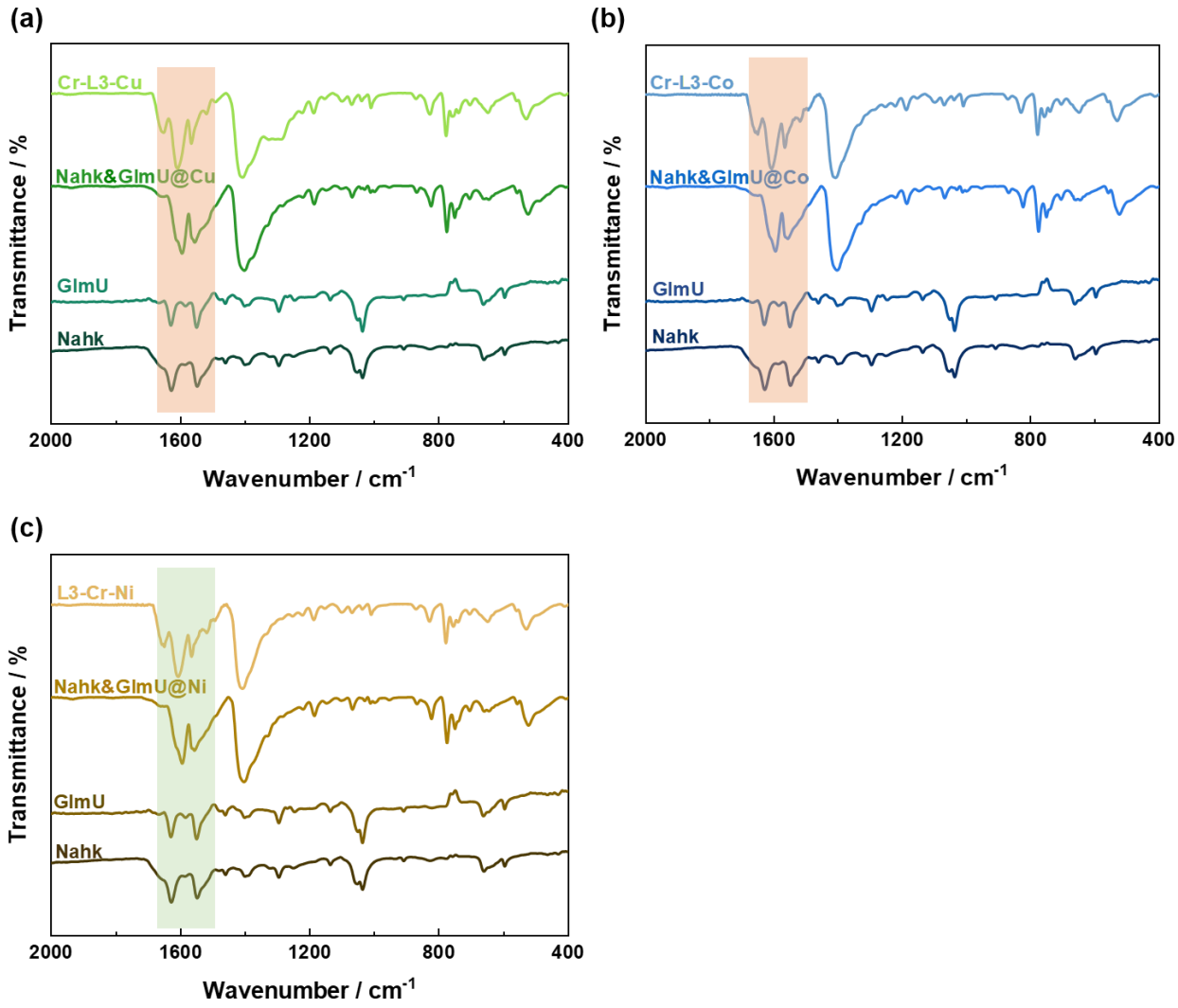

Figure S47. FI-IR spectra for NahK, GlmU, NahK&GlmU@Cr-L3-Cu, and Cr-L3-Cu (a); NahK, GlmU, NahK&GlmU@Cr-L3-Co, and Cr-L3-Co (b); NahK, GlmU, NahK&GlmU@Cr-L3-Ni, and Cr-L3-Ni (c).

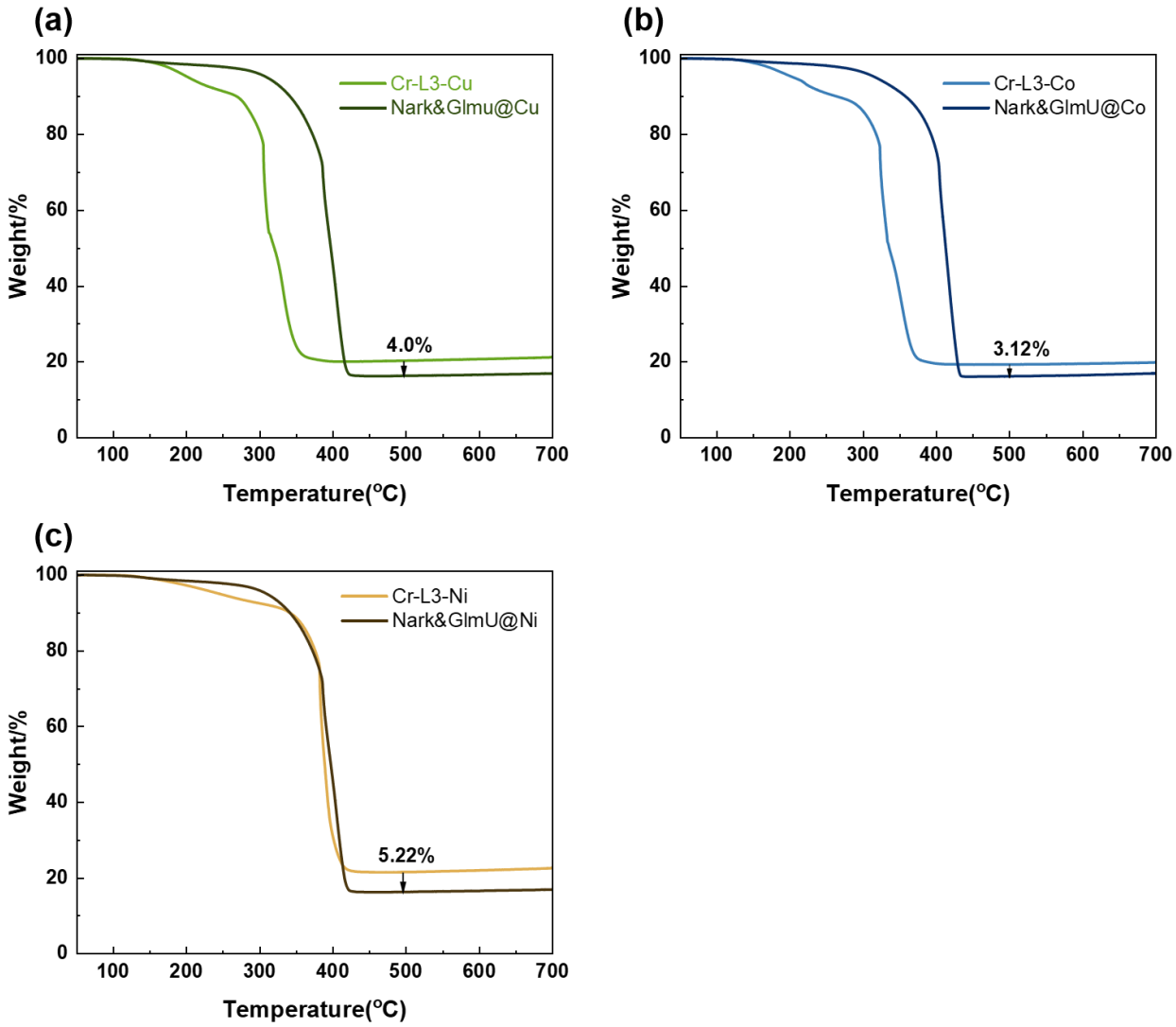

Figure S48. TGA curve of NarK&GlmU@Cr-L3-Cu compared to Cr-L3-Cu (a); NarK&GlmU@ Cr-L3-Co compared to Cr-L3-Co (b); NarK&GlmU@Cr-L3-Ni compared to Cr-L3-Ni (c).

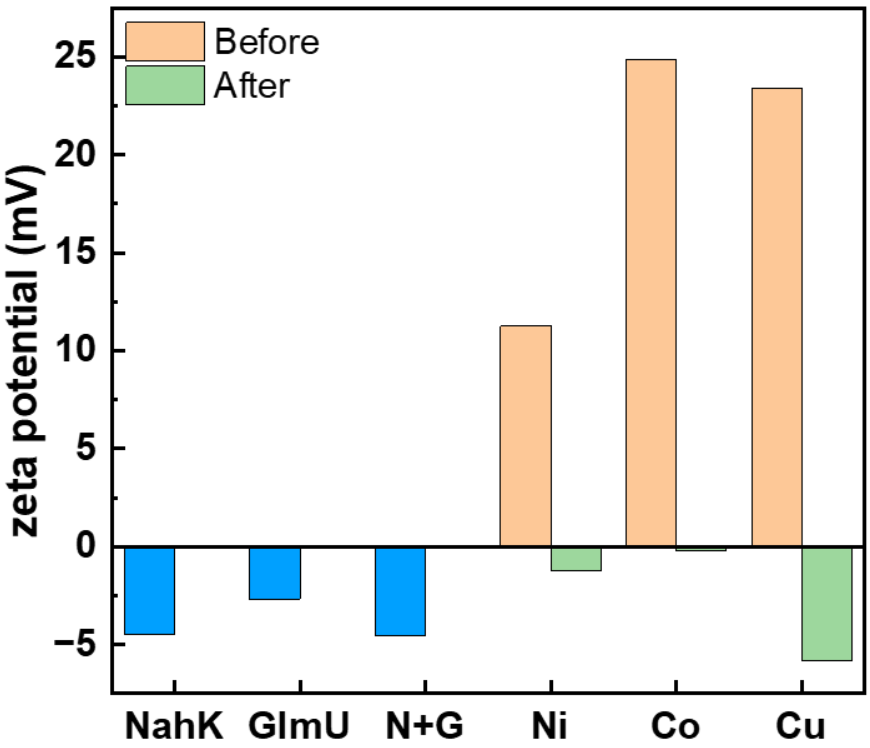

Figure S49. Zeta potential for NahK, GlmU, NahK&GlmU, Cr-L3-M (M′ = Cu, Co, Ni), and NahK&GlmU@Cr-L3-M.

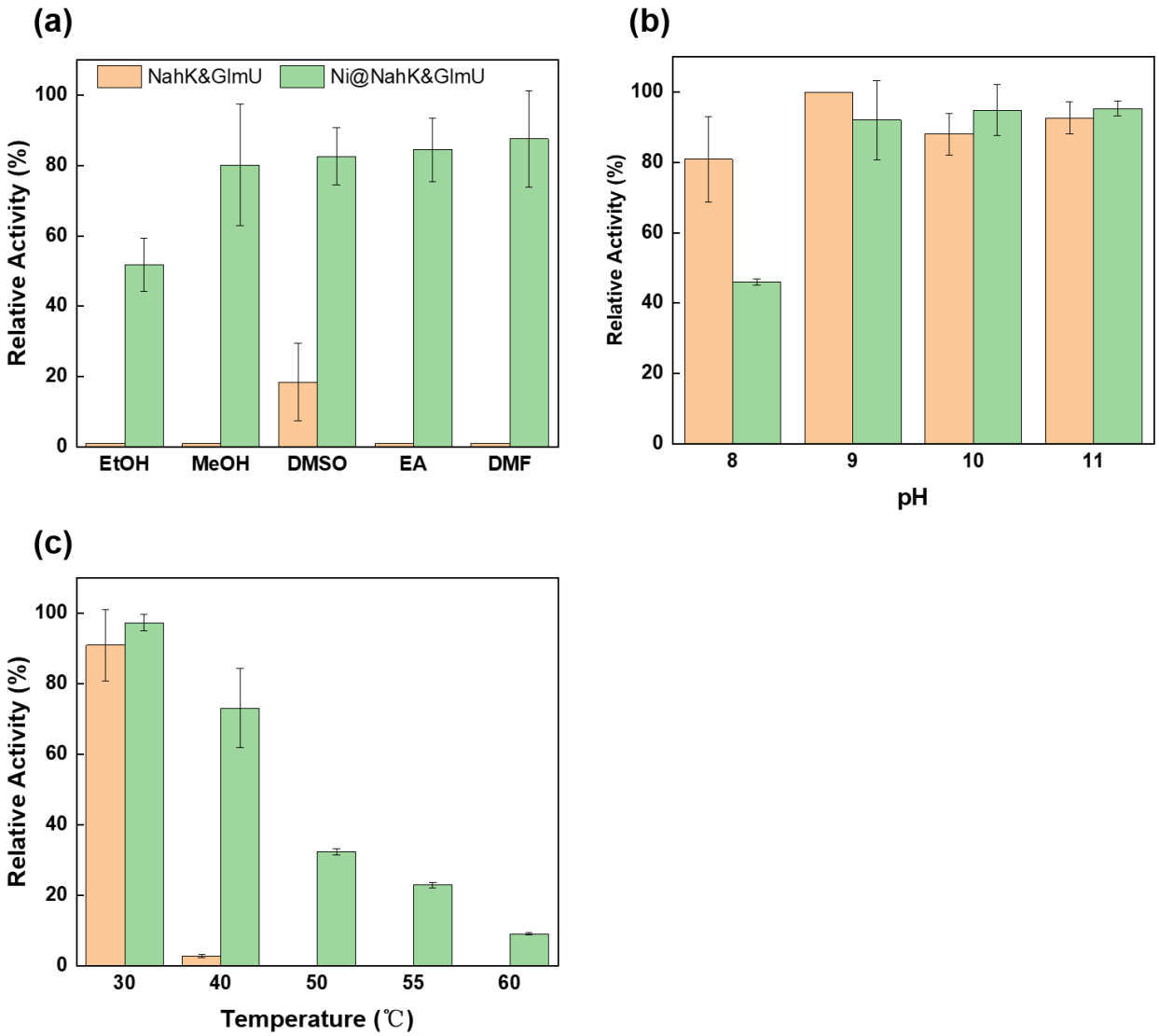

Figure S50. Stability of free NahK&GlmU and NahK&GlmU@Cr-L3-Ni under organic solvent (a), alkalinity (b), or heat (c) conditions.

Single Crystal X-Ray Crystallography

Table S1. Crystal data and structure refinement parameters of Cr-L1-Cu and Fe-L1-Cu.

Name	Cr-L1-Cu	Fe-L1-Cu
CCDC	2489486	2489488
Empirical formula	$C_{36}H_{33}Cr_3Cu_3N_6O_{19}$	$C_{36}H_{39}Fe_3Cu_{1.5}N_6O_{19}$
Formula weight	1104.99	1122.59
Temperature/K	296.15	253
Crystal system	hexagonal	hexagonal
Space group	*P6/mmm*	*P6/mmm*
a/Å	22.2970(15)	22.648(3)
b/Å	22.2970(15)	22.648
c/Å	13.4962(8)	13.4843(16)
α/°	90	90
β/°	90	90
γ/°	120	120
V/Å^3	5810.8(9)	5990.0 (18)
Z	2	2
ρ_{calc}/cm^{-3}	0.632	0.622
μ/mm^{-1}	0.574	0.648
F(000)	1117	1141
Crystal size/mm^3	0.3 × 0.03 × 0.02	0.15 × 0.12 × 0.1
Radiation	MoK_α (λ = 0.71073)	MoK_α (λ = 0.71073)
2Θ range for data collection/°	2.109 to 27.495	1.798 to 27.732
Index ranges	$-27 \le h \le 28$, $-28 \le k \le 28$, $-17 \le l \le 17$	$-28 \le h \le 29$, $-29 \le k \le 29$, $-17 \le l \le 14$
Reflections collected	56122	43156
Independent reflections	2601 [R_{int} = 0.1252]	2698 [R_{int} = 0.1738]
Data/restraints/parameters	2601/68/83	2698/32/87
Goodness-of-fit on F^2	1.067	0.963
Final *R* indexes [I>=2σ(I)][a,b]	R_1 = 0.0698, wR_2 = 0.2356	R_1 = 0.0625, wR_2 = 0.1661
Final *R* indexes [all data][a,b]	R_1 = 0.0926, wR_2 = 0.2570	R_1 = 0.0910, wR_2 = 0.1814
Largest diff. peak/hole / e Å^{-3}	0.965/-0.464	0.758/-0.444

[a] $R_1 = \Sigma||F_o| - |F_c||/\Sigma|F_o|$.

[b] $wR_2 = |\Sigma w(|F_o|^2 - |F_c|^2)|/\Sigma|w(F_o^2)^2|^{1/2}$.

Table S2. Crystal data and structure refinement parameters of Cr-L1-Pd and Cr-L3-Pd.

Name	Cr-L1-Pd	Cr-L3-Pd
CCDC	2489487	2489489
Empirical formula	$C_{57.2}H_{33.2}Cr_6N_{12}O_{32}Pd_3$	$C_{144}H_{108}Pd_3N_{12}O_{32}Cr_6$
Formula weight	2032.16	3149.62
Temperature/K	223.00	193.15
Crystal system	hexagonal	hexagonal
Space group	*P6/mmm*	*P6/mmm*
a/Å	22.459(5)	32.617(7)
b/Å	22.459	32.617(7)
c/Å	13.291(3)	19.871(4)
α/°	90	90
β/°	90	90
γ/°	120	120
V/Å^3	5806(3)	18308(9)
Z	1	1
ρ_{calc}/gcm^{-3}	0.581	0.286
μ/mm^{-1}	2.951	0.963
F(000)	999	1594
Crystal size/mm^3	0.25 × 0.22 × 0.2	0.3 × 0.1 × 0.1
Radiation	GaK_α (λ = 1.34139)	MoK_α (λ = 0.71073)
2Θ range for data collection/°	1.976 to 53.978	1.934 to 43.824
Index ranges	$-26 \le h \le 27$, $-27 \le k \le 27$, $-15 \le l \le 16$	$-31 \le h \le 33$, $-28 \le k \le 33$, $-14 \le l \le 20$
Reflections collected	78809	82105
Independent reflections	2105 [R_{int} = 0.5256]	3978 [R_{int} = 0.0967]
Data/restraints/parameters	2105/113/72	3978/0/89
Goodness-of-fit on F^2	0.979	1.123
Final *R* indexes [I>=2σ(I)][a,b]	R_1 = 0.1418, wR_2 = 0.3866	R_1 = 0.1004, wR_2 = 0.2779
Final *R* indexes [all data][a,b]	R_1 = 0.2268, wR_2 = 0.4384	R_1 = 0.1270, wR_2 = 0.3164
Largest diff. peak/hole / e Å^{-3}	0.601/-0.645	0.986/-0.882

[a] $R_1 = \Sigma||F_o| - |F_c||/\Sigma|F_o|$.

[b] $wR_2 = |\Sigma w(|F_o|^2 - |F_c|^2)|/\Sigma|w(F_o^2)^2|^{1/2}$.

Table S3. Pawley fitting results and fractional atomic coordinates of Cr-L2-Cu.

Space group: *P6/M*			
Lattice type: hexagonal			
a (Å) = 29.00498			
b (Å) = 29.00498			
c (Å) = 16.04700			
$\alpha = \beta = 90°$, $\gamma = 120°$			
Pawley refinement: *R*p = 2.22 %, w*R*p = 2.98 %			
Atom	***X***	***Y***	***z***
Cu1	0	0.5	0
Cr2	0.2873	0.68982	0.5
O3	0.25092	0.64993	0.41109
O4	0.25441	0.57299	0.42941
O5	0.22449	0.69062	0.5
O6	0.33333	0.66667	0.5
N7	0.05814	0.53199	0.08963
C8	0.11695	0.5214	0.18732
C9	0.07755	0.50059	0.12331
C10	0.11596	0.60682	0.17995
C11	0.07652	0.58421	0.11629
C12	0.23595	0.60033	0.39121
C13	0.13674	0.57547	0.21721
C14	0.17576	0.59961	0.28254
C15	0.19819	0.57447	0.32597
H16	0.13089	0.49468	0.21191
H17	0.06203	0.4591	0.10064
H18	0.12974	0.64853	0.20032
H19	0.06019	0.60818	0.0883
H20	0.18801	0.64165	0.29931
H21	0.18727	0.5326	0.31234

Table S4. Pawley fitting results and fractional atomic coordinates of Al-L1-Ni.

Space group: *P6/M*			
Lattice type: hexagonal			
a (Å) = 23.79180			
b (Å) = 23.79180			
c (Å) = 12.97594			
$\alpha = \beta = 90°$, $\gamma = 120°$			
Pawley refinement: *R*p = 1.91 %, w*R*p = 3.03 %			
Atom	***X***	***Y***	***z***
Ni1	0.5	0.5	1
Al2	0.71459	0.42918	0.5
O3	0.66356	0.43453	0.59506
O4	0.7604	0.52079	0.5
O5	0.58116	0.58116	1
O6	0.66667	0.33333	0.5
N7	0.53679	0.46321	0.89588
C8	0.37498	0.5186	0.77129
C9	0.39684	0.4988	0.85764
C10	0.58161	0.41839	0.72374
C11	0.60467	0.41839	0.72374
H12	0.51474	0.6771	1.25599
H13	0.54546	0.64358	1.10516
H14	0.54823	0.77412	0.5621
H15	0.60566	0.60566	0.93942

Table S5. Pawley fitting results and fractional atomic coordinates of Al-L2-Cu.

Space group: *P6/M*			
Lattice type: hexagonal			
a (Å) = 28.89113			
b (Å) = 28.89113			
c (Å) = 14.72013			
$\alpha = \beta = 90°$, $\gamma = 120°$			
Pawley refinement: *R*p = 2.64 %, w*R*p = 4.23 %			
Atom	***X***	***Y***	***z***
Cu1	0	0.5	0
Al2	0.2858	0.6951	0.5
O3	0.2431	0.6488	0.4165
O4	0.6762	0.2558	0.5834
O5	0.2394	0.7229	0.5
O6	0.33333	0.66667	0.5
N7	0.0555	0.5333	0.0905
C8	0.1014	0.5224	0.2059
C9	0.0638	0.5013	0.1427
C10	0.511	0.1203	0.834
C11	0.4958	0.0825	0.8966
C12	0.2339	0.6044	0.3887
C13	0.1309	0.5773	0.2175
C14	0.3977	0.5683	0.2846
C15	0.4207	0.616	0.321
H16	0.10807	0.495	0.24795
H17	0.03938	0.45668	0.13391
H18	0.48865	0.1426	0.8248
H19	0.46081	0.0737	0.93803
H20	0.38924	0.53667	0.3329
H21	0.43051	0.64646	0.27009

Table S6. Pawley fitting results and fractional atomic coordinates of Cr-L2-Pd.

Space group: *P6/M*			
Lattice type: hexagonal			
a (Å) = 28.85876			
b (Å) = 28.85876			
c (Å) = 15.89929			
$\alpha = \beta = 90°$, $\gamma = 120°$			
Pawley refinement: *R*p = 2.10%, w*R*p = 2.91%			
Atom	***X***	***Y***	***z***
Cu1	0	0.5	0
Pd2	0.28352	0.69347	0.5
O3	0.24143	0.64611	0.41593
O4	0.67908	0.25659	0.58395
O5	0.23483	0.71958	0.5
O6	0.33333	0.66667	0.5
N7	0.05497	0.5312	0.08651
C8	0.12103	0.52735	0.17137
C9	0.08253	0.50626	0.1084
C10	0.50255	0.10188	0.81178
C11	0.48697	0.06391	0.87526
C12	0.23357	0.60174	0.38774
C13	0.13084	0.57443	0.21292
C14	0.40086	0.57128	0.28151
C15	0.42391	0.61941	0.31861
H16	0.14246	0.50666	0.18619
H17	0.0743	0.46969	0.07727
H18	0.4726	0.10828	0.78173
H19	0.44543	0.04124	0.89391
H20	0.36203	0.54046	0.30355
H21	0.46293	0.65094	0.29949

Table S7. ICP-OES data for Cr-L1-M (M=Cu, Co, Ni, Pd)**.** (mg/L)

	Cr	**Cu**	**Co**	**Ni**	**Pd**
Cr-L1-Cu	6.34	4.27			
Cr-L1-Co	5.4	0.15	3.12		
Cr-L1-Ni	6.15	0.21		4.08	
Cr-L1-Pd	4.12	0.15			5.52

Table S8. ICP-OES data for Cr-L2-M (M=Cu, Co, Ni, Pd)**.** (mg/L)

	Cr	**Cu**	**Co**	**Ni**	**Pd**
Cr-L2-Cu	4.46	3.56			
Cr-L2-Co	4.02	0.11	3.27		
Cr-L2-Ni	4.01	0.01		2.67	
Cr-L2-Pd	3.54	<0.01			5.43

Table S9. ICP-OES data for Cr-L3-M (M=Cu, Co, Ni, Pd)**.** (mg/L)

	Cr	**Cu**	**Co**	**Ni**	**Pd**
Cr-L3-Cu	4.65	3.06			
Cr-L3-Co	6.24	0.31	4.56		
Cr-L3-Ni	4.95	0.18		3.19	
Cr-L3-Pd	3.72	0.07			5.58

Table S10. DFT model used for dissociation energy calculation, with the initial structure shown.

Atom	*X*	*Y*	*z*
Cu1	0.501376283	0.501775934	0.999793359
Cr1	0.557369373	0.275669867	0.499613527
Cr2	0.715458428	0.285907016	0.499888403
Cr3	0.284346451	0.570963097	0.500893841
Cr4	0.440280743	0.721086332	0.500177608
Cr5	0.284339796	0.714173743	0.499559681
Cr6	0.712976755	0.427461004	0.501612734
O1	0.65448058	0.434891388	0.600674898
O2	0.555945516	0.214202406	0.603188997
O3	0.783718768	0.341080191	0.601229702
O4	0.342380737	0.560101726	0.600134369
O5	0.442909187	0.784005838	0.603356935
O6	0.217804509	0.659424734	0.601488385
O7	0.442790593	0.659528106	0.39945107
O8	0.217022462	0.55798363	0.399157071
O9	0.340074268	0.781536885	0.39935955
O10	0.553746114	0.336999049	0.398139556
O11	0.782229709	0.441581583	0.398994629
O12	0.659778251	0.218565093	0.399907141
O13	0.336993215	0.562010729	0.391951739
O14	0.440696128	0.778663971	0.388721068
O15	0.223155311	0.662715009	0.390475038
O16	0.65978113	0.434534452	0.392412258
O17	0.776738738	0.337188169	0.390013282
O18	0.558318411	0.219979114	0.388884764
O19	0.553920607	0.331893047	0.610015197
O20	0.77441549	0.437803893	0.610820104
O21	0.663175766	0.224649205	0.608390222
O22	0.441334735	0.664336969	0.609720223
O23	0.223485923	0.56059122	0.610020722
O24	0.337004057	0.77610734	0.608392771
O25	0.759079653	0.539858005	0.50376134
O26	0.463418069	0.228285783	0.496314677
O27	0.767967306	0.224453723	0.499487115
O28	0.237296464	0.457213702	0.504080724
O29	0.53428872	0.767918852	0.497044836
O30	0.233106261	0.776742661	0.497810001
O31	0.615085034	0.611624756	0.001342401
O32	0.383033168	0.386119625	0.001011278
O33	0.668103022	0.332840523	0.500332137
O34	0.329717439	0.665321326	0.499668235

O35	0.438333407	0.475426019	0.577363488
O36	0.654360854	0.56922083	0.513990993
O37	0.52646697	0.518937534	0.400661405
N1	0.534644959	0.464663694	0.893283252
N2	0.464766748	0.537647038	0.896494506
N3	0.53547232	0.463531113	0.105266307
N4	0.466472564	0.536680948	0.107761734
C1	0.39792	0.79584	0.6396
C2	0.20416	0.60208	0.6396
C3	0.20416	0.60208	0.3604
C4	0.39792	0.79584	0.3604
C5	0.60208	0.20416	0.6396
C6	0.79584	0.39792	0.6396
C7	0.79584	0.39792	0.3604
C8	0.60208	0.20416	0.3604
C9	0.508438425	0.377593916	0.770247183
C10	0.489898734	0.402399093	0.853242678
C11	0.487550748	0.623511839	0.773064076
C12	0.507698396	0.600202605	0.855891135
C13	0.377858016	0.515208954	0.225845863
C14	0.40176722	0.495415608	0.143110624
C15	0.622088865	0.482714159	0.225905257
C16	0.599793089	0.503840604	0.142750202
C17	0.489234507	0.621373318	0.233482827
C18	0.50973988	0.59848536	0.15026893
C19	0.509882438	0.377290951	0.229885028
C20	0.491074301	0.401436956	0.14618373
C21	0.620967083	0.482372162	0.772955789
C22	0.598998362	0.50422636	0.855744805
C23	0.376877507	0.516861061	0.777445425
C24	0.400295833	0.496576377	0.860143761
C25	0.57483158	0.418286312	0.728807906
C26	0.596156926	0.392558648	0.638672213
C27	0.421479552	0.580737379	0.732011401
C28	0.400009416	0.603726693	0.63952941
C29	0.42217258	0.578814074	0.27231852
C30	0.398770992	0.602313406	0.362514705
C31	0.576465047	0.418654676	0.270745724
C32	0.598399374	0.394249298	0.361877087
H1	0.472180483	0.32749957	0.738069003
H2	0.439348164	0.375399722	0.891446657
H3	0.522798918	0.673339873	0.739366697
H4	0.558518737	0.628178204	0.892568663
H5	0.325639482	0.481761248	0.253747717

H6	0.372380037	0.445976249	0.102485402
H7	0.673798328	0.515472338	0.256063362
H8	0.630044926	0.553692274	0.103675226
H9	0.523907868	0.671305329	0.267629805
H10	0.560764102	0.626509618	0.113817831
H11	0.654384226	0.658498925	0.997995027
H12	0.473922108	0.327574886	0.263469582
H13	0.440316185	0.374261755	0.108530286
H14	0.673117973	0.514023229	0.743484265
H15	0.340668332	0.341291351	0.001853749
H16	0.62994382	0.553792256	0.894993828
H17	0.325240681	0.483005758	0.747940839
H18	0.370812664	0.446737022	0.899336639
H19	0.719862804	0.549702351	0.505147357
H20	0.443917501	0.210378807	0.561626218
H21	0.753139108	0.198187845	0.561380372
H22	0.270903687	0.452913973	0.546029925
H23	0.553665684	0.790472747	0.560314508
H24	0.247583664	0.802965175	0.559804951
H25	0.245182226	0.444681031	0.437927345
H26	0.259046958	0.810805298	0.446146766
H27	0.78248917	0.558655497	0.440815608
H28	0.743242994	0.190308097	0.447394625
H29	0.587420629	0.171809015	0.707368661
H30	0.588834634	0.172182157	0.292418093
H31	0.830418403	0.415478624	0.704993508
H32	0.829562404	0.415491752	0.294117847
H33	0.170428999	0.585805193	0.705846309
H34	0.171087686	0.584977043	0.293489061
H35	0.413570533	0.829044141	0.706516809
H36	0.412127956	0.828895126	0.293408006
H37	0.465128898	0.483039463	0.516289105
H38	0.447685788	0.444019271	0.615893131
H39	0.637389979	0.568679828	0.580665401
H40	0.612808315	0.551532373	0.471887515
H41	0.523207202	0.555783738	0.366201068
H42	0.520350383	0.486060295	0.348289747

Table S11. DFT model for dissociation energy calculation, Cr–N dissociation.

Atom	***X***	***Y***	***z***
Cu1	0.505348116	0.537860415	0.961622041
Cr1	0.561179366	0.280181238	0.502033623
Cr2	0.716036847	0.286071811	0.499614668
Cr3	0.282692365	0.569841889	0.500098412
Cr4	0.439752174	0.721124447	0.499881318
Cr5	0.284616487	0.7136909	0.499897502
Cr6	0.715936738	0.429774823	0.500209132
O1	0.659282305	0.441726575	0.598129713
O2	0.557086339	0.216071241	0.603412233
O3	0.78253574	0.34067836	0.601524189
O4	0.442363165	0.782586618	0.604473682
O5	0.217860231	0.659292711	0.601000482
O6	0.441285262	0.660041842	0.399146223
O7	0.214493584	0.556893229	0.400838184
O8	0.340074854	0.781806132	0.39860041
O9	0.558268165	0.343477964	0.40616597
O10	0.781811705	0.441633728	0.3975271
O11	0.659868518	0.217940962	0.398946551
O12	0.334758566	0.564766114	0.382215159
O13	0.440472897	0.778508328	0.390126741
O14	0.224530196	0.663031338	0.389985797
O15	0.662698381	0.441990533	0.394782836
O16	0.777306849	0.337541928	0.391152448
O17	0.560348535	0.222891554	0.389074505
O18	0.561930766	0.337482788	0.620524227
O19	0.776924792	0.439602403	0.609502098
O20	0.663058372	0.224085245	0.608584882
O21	0.223887376	0.560613308	0.610720465
O22	0.33717902	0.776502997	0.608055618
O23	0.765712072	0.544054629	0.503310477
O24	0.467193764	0.236269592	0.502056465
O25	0.767726769	0.223771318	0.497677532
O26	0.232043454	0.456012532	0.492906637
O27	0.53393259	0.765384598	0.499829586
O28	0.231339787	0.774519841	0.495827802
O29	0.594112075	0.614577741	0.980314262
O30	0.414411633	0.479385548	0.911915069
O31	0.671085339	0.335410498	0.500333936
O32	0.329400407	0.664346439	0.500882646

O33	0.423259823	0.466168619	0.370990709
O34	0.398501214	0.578614308	0.830101061
O35	0.544230559	0.67448638	0.802120428
O36	0.342825621	0.552677162	0.583939767
O37	0.441664363	0.655069732	0.606294125
N1	0.54483382	0.488747488	0.881501845
N2	0.520207543	0.463859136	0.121849179
N3	0.466005014	0.566805528	0.076341453
N4	0.51575367	0.475570727	0.574117569
C1	0.39792	0.79584	0.6396
C2	0.20416	0.60208	0.6396
C3	0.20416	0.60208	0.3604
C4	0.39792	0.79584	0.3604
C5	0.60208	0.20416	0.6396
C6	0.79584	0.39792	0.6396
C7	0.79584	0.39792	0.3604
C8	0.60208	0.20416	0.3604
C9	0.525875529	0.388081793	0.789175178
C10	0.507549143	0.419921188	0.863176924
C11	0.374482149	0.53618587	0.194930257
C12	0.399691207	0.525494353	0.105548681
C13	0.614458277	0.48734997	0.232733434
C14	0.585976796	0.504572438	0.152259519
C15	0.488155388	0.635165979	0.224099412
C16	0.509322986	0.62083006	0.133963288
C17	0.503496374	0.382397046	0.252089377
C18	0.480219949	0.404459271	0.170797702
C19	0.627107344	0.499377556	0.757906914
C20	0.604557037	0.527488617	0.831598239
C21	0.585834091	0.429055786	0.73272404
C22	0.603368737	0.399443545	0.643322387
C23	0.419662741	0.591710961	0.256117197
C24	0.396404184	0.606427713	0.354391009
C25	0.57244275	0.424890367	0.283474751
C26	0.599922447	0.401480167	0.368940274
C27	0.515398086	0.584196165	0.572535065
C28	0.546807928	0.543981274	0.556289227
C29	0.414605909	0.479797482	0.630440176
C30	0.451239722	0.444827763	0.612417685
C31	0.446925669	0.550849135	0.608031391
C32	0.407634885	0.590165454	0.602944683

H1	0.493422504	0.333082205	0.77321874
H2	0.461248093	0.391044677	0.908504333
H3	0.321046266	0.501727789	0.217320254
H4	0.367931973	0.48307303	0.055043657
H5	0.668150976	0.521043505	0.254846156
H6	0.616204241	0.552378323	0.109814023
H7	0.524082412	0.678794871	0.269673699
H8	0.561944309	0.650327008	0.104711326
H9	0.594678222	0.649059448	0.934686433
H10	0.470035048	0.33388982	0.290483408
H11	0.42711591	0.373121349	0.143628952
H12	0.675065051	0.53249456	0.71837435
H13	0.416662937	0.45670339	0.851512903
H14	0.632542901	0.581826594	0.853905772
H15	0.735350781	0.5481997	0.551942809
H16	0.448224326	0.206291528	0.55983709
H17	0.752852911	0.196954845	0.559098924
H18	0.268208172	0.451056794	0.526960503
H19	0.552816441	0.797276825	0.555681081
H20	0.246601003	0.802600256	0.556110926
H21	0.237414234	0.447199025	0.42337551
H22	0.25600085	0.80721657	0.442088151
H23	0.751836264	0.554749427	0.439967869
H24	0.742283708	0.190188469	0.445224745
H25	0.586264385	0.170703692	0.706229056
H26	0.586680048	0.170558652	0.293956089
H27	0.829180441	0.414149323	0.706237406
H28	0.829392615	0.415039628	0.294007951
H29	0.170185571	0.585801306	0.705498916
H30	0.171826235	0.585712914	0.29273763
H31	0.413876408	0.829549756	0.705937391
H32	0.413041388	0.82861136	0.293094285
H33	0.439107065	0.471119075	0.302642449
H34	0.450729274	0.449563778	0.405154803
H35	0.400998981	0.539135541	0.863825181
H36	0.379879638	0.595966536	0.880558618
H37	0.543332568	0.692366144	0.736567791
H38	0.494247531	0.64288093	0.814923438
H39	0.541385169	0.639100042	0.553479102
H40	0.599212326	0.567903772	0.525624464
H41	0.361882475	0.452518086	0.659456909

Table S12. DFT model for dissociation energy calculation, Cr–O dissociation.

Atom	***X***	***Y***	***z***
Cu1	0.501197448	0.50199054	0.000391526
Cr1	0.560175826	0.279217131	0.499403857
Cr2	0.715572019	0.285866159	0.499605309
Cr3	0.287106308	0.569245838	0.506813207
Cr4	0.441655757	0.72491546	0.496669944
Cr5	0.285059638	0.711804863	0.500068557
Cr6	0.716515812	0.429777258	0.500336724
O1	0.658071063	0.4407681	0.599154364
O2	0.557203324	0.216267758	0.603409868
O3	0.781931108	0.340556993	0.601377903
O4	0.443714694	0.78510789	0.602368653
O5	0.218673774	0.659496129	0.600670768
O6	0.443972043	0.662905017	0.396511284
O7	0.217677028	0.557971208	0.394977901
O8	0.339720193	0.77957225	0.398019742
O9	0.558822836	0.341365151	0.398631171
O10	0.782896417	0.442163581	0.398373801
O11	0.659860957	0.21832848	0.39934603
O12	0.340611129	0.562077361	0.397537907
O13	0.442254714	0.780731778	0.389784202
O14	0.223379891	0.662582207	0.39294602
O15	0.663783092	0.439983718	0.39355105
O16	0.777031076	0.337464024	0.391113044
O17	0.559649465	0.221843002	0.388602498
O18	0.558992247	0.336400129	0.609124211
O19	0.777225449	0.439946396	0.609752944
O20	0.662896182	0.223638081	0.608371756
O21	0.223384122	0.560221621	0.612252373
O22	0.337132878	0.775443087	0.609012885
O23	0.765844313	0.544110295	0.503109264
O24	0.466287476	0.233329608	0.496084381
O25	0.766602453	0.222720157	0.499276537
O26	0.233350498	0.455058379	0.504256649
O27	0.537410728	0.770714664	0.5002773
O28	0.233052779	0.774107472	0.499669664
O29	0.615958621	0.60930942	0.996112202
O30	0.371882463	0.370154364	0.028546472
O31	0.670728231	0.335316404	0.4996513
O32	0.332910163	0.664870272	0.504324369

O33	0.344675352	0.362790014	0.317477459
O34	0.372830807	0.442799024	0.540528692
O35	0.46520596	0.549949142	0.510404934
O36	0.464021011	0.670980269	0.608338874
O37	0.338839326	0.552770544	0.598516337
N1	0.537400938	0.462609395	0.898945903
N2	0.534962171	0.465381034	0.108959086
N3	0.463311365	0.537074822	0.103073754
N4	0.459993044	0.525245218	0.883685086
C1	0.39792	0.79584	0.6396
C2	0.20416	0.60208	0.6396
C3	0.20416	0.60208	0.3604
C4	0.39792	0.79584	0.3604
C5	0.60208	0.20416	0.6396
C6	0.79584	0.39792	0.6396
C7	0.79584	0.39792	0.3604
C8	0.60208	0.20416	0.3604
C9	0.514077115	0.376416758	0.775163705
C10	0.495302317	0.399190726	0.86006154
C11	0.377466753	0.515772684	0.226274356
C12	0.399894608	0.495451952	0.142212463
C13	0.624180537	0.485666971	0.224914626
C14	0.600112026	0.505836428	0.142808745
C15	0.48728367	0.62318693	0.227558974
C16	0.506235431	0.599914297	0.143455036
C17	0.511646367	0.381148131	0.235113851
C18	0.491147149	0.403852138	0.151608646
C19	0.62253915	0.485269218	0.774001084
C20	0.600330732	0.504885328	0.858674631
C21	0.578652003	0.420448174	0.730555597
C22	0.600201008	0.39710263	0.638281676
C23	0.421843757	0.580255722	0.270565157
C24	0.400315421	0.603747857	0.362987692
C25	0.579085227	0.422890546	0.272703958
C26	0.602297182	0.399171667	0.362711435
C27	0.496567229	0.568838723	0.718767243
C28	0.506551239	0.573745542	0.821342805
C29	0.384721344	0.466677926	0.746116619
C30	0.398845663	0.474187513	0.847899249
C31	0.435445873	0.512994988	0.679776971
C32	0.426659963	0.505515682	0.568481803

H1	0.479275531	0.325950535	0.742864561
H2	0.445880426	0.368793258	0.898939621
H3	0.326683255	0.48092219	0.257590917
H4	0.369518896	0.44460897	0.105627761
H5	0.677043916	0.518226923	0.251098627
H6	0.629930363	0.554744544	0.101299761
H7	0.522651204	0.673331307	0.260403285
H8	0.556382625	0.628466363	0.105845288
H9	0.648823386	0.65872435	0.000331711
H10	0.47633358	0.332038673	0.270885446
H11	0.439364402	0.375069912	0.115308669
H12	0.673048925	0.52022938	0.741960732
H13	0.338692705	0.326781511	0.996962597
H14	0.629357084	0.555457612	0.896878103
H15	0.739061261	0.551102363	0.554752403
H16	0.446146758	0.207334779	0.556896087
H17	0.752294222	0.197054752	0.561730513
H18	0.264510098	0.45333501	0.55449726
H19	0.556225734	0.81652872	0.529972804
H20	0.248832171	0.801072832	0.560910931
H21	0.246373792	0.441581486	0.442535712
H22	0.256737994	0.807764527	0.446647458
H23	0.750310541	0.555172473	0.441524321
H24	0.740818494	0.187949036	0.448364696
H25	0.586371022	0.170990234	0.706559147
H26	0.587462368	0.170998478	0.29350773
H27	0.829242045	0.413764225	0.706183696
H28	0.828950334	0.414778742	0.293520053
H29	0.16915574	0.586414991	0.704439322
H30	0.170290176	0.586872304	0.294130315
H31	0.413548281	0.828521712	0.707065098
H32	0.412313642	0.829127584	0.293688729
H33	0.32981366	0.345564908	0.250008018
H34	0.394844439	0.384333045	0.31152917
H35	0.536424419	0.60660101	0.669851202
H36	0.55402038	0.613254002	0.857322054
H37	0.335681074	0.424703935	0.719021879
H38	0.364596909	0.436648091	0.903144801
H39	0.371939657	0.441987274	0.467547367
H40	0.513123571	0.70359255	0.589318519
H41	0.452011248	0.626082284	0.578568233

Table S13. Enzymes used in this work.

Enzyme		**Source**	**Ref**
NTR	Nitroreductase	*E. coli BL21 (DE3)*	[10]
NahK	*N*-acetyl hexosamine 1-kinase	*Bifidobacterium infantis*	[11]
GlmU	UDP-*N*-acetylgalactosamine pyrophosphorylase	*Escherichia coli*	[12]

REFERENCES

1 Gorbitz, C. What is the best crystal size for collection of X-ray data? Refinement of the structure of glycyl-l-serine based on data from a very large crystal. *Acta Crystallographica Section B* **55**, 1090-1098 (1999).

2 Sheldrick, G. A short history of SHELX. *Acta Crystallographica Section A* **64**, 112-122 (2008).

3 Perdew, J. P., Burke, K. & Ernzerhof, M. Generalized gradient approximation made simple. *Phys. Rev. Lett.* **77**, 3865-3868 (1996).

4 Giannozzi, P. *et al.* Advanced capabilities for materials modelling with Quantum ESPRESSO. *J. Phys.: Condens. Matter* **29**, 465901 (2017).

5 Giannozzi, P. *et al.* Quantum ESPRESSO: a modular and open-source software project for quantum simulations of materials. *J. Phys.: Condens. Matter* **21**, 395502 (2009).

6 Giannozzi, P. *et al.* Quantum ESPRESSO toward the exascale. *J. Chem. Phys.* **152**, 154105 (2020).

7 Schlipf, M. & Gygi, F. Optimization algorithm for the generation of ONCV pseudopotentials. *Comput. Phys. Commun.* **196**, 36-44 (2015).

8 van Setten, M. J. *et al.* The PseudoDojo: training and grading a 85 element optimized norm-conserving pseudopotential table. *Comput. Phys. Commun.* **226**, 39-54 (2018).

9 Grimme, S., Antony, J., Ehrlich, S. & Krieg, H. A consistent and accurate ab initio parametrization of density functional dispersion correction (DFT-D) for the 94 elements H-Pu. *J. Chem. Phys.* **132**, 154104 (2010).

10 Dai, R. *et al.* Reduction of nitro phenols using nitroreductase from E. coli in the presence of NADH. *J. Hazard. Mater.* **170**, 141-143 (2009).

11 Wang, K.-C. *et al.* Insights into the binding specificity and catalytic mechanism of N-acetylhexosamine 1-phosphate kinases through multiple reaction complexes. *Acta Crystallographica Section D* **70**, 1401-1410 (2014).

12 Olsen, L. R. & Roderick, S. L. Structure of the escherichia coli GlmU pyrophosphorylase and acetyltransferase active sites. *Biochem.* **40**, 1913-1921 (2001).